Investigation of Fe(III) Reduction in Geobacter Sulfurreducens Characterization of Outer Surface Associated Electron Transfer Components

INVESTIGATION OF FE(III) REDUCTION IN *GEOBACTER SULFURREDUCENS*

CHARACTERIZATION OF OUTER SURFACE ASSOCIATED ELECTRON TRANSFER COMPONENTS

A Dissertation Presented

by

XINLEI QIAN

Submitted to the Graduate School of

the University of Massachusetts Amherst

in partial fulfillment of the requirements for the degree of

DOCTOR OF PHILOSOPHY

September 2009

Microbiology

INVESTIGATION OF FE(III) REDUCTION IN *GEOBACTER*

SULFURREDUCENS

CHARACTERIZATION OF OUTER SURFACE ASSOCIATED ELECTRON TRANSFER COMPONENTS

A Dissertation Presented

by

XINLEI QIAN

Approved as to style and content by:

_____
Derek R. Lovely, Chair

_____
Tünde Mester，Member

_____
Michael J. Maroney, Member

_____
Wilmore Webley, Member

_____
John M. Lopes, Department Head
Microbiology

DEDICATION

To my parents, Mrs. Qi Sun and Mr. Longsheng Qian.

ACKNOWLEDGMENTS

I would like to thank my advisors, Tünde Mester and Derek R. Lovley for their thoughtful, patient guidance and support. I am especially indebted to Tünde Mester for her years of tireless and selfless contribution to my professional development. Thanks to my committee members, Michael J. Maroney and Wilmore Webley, for their helpful comments and suggestions to this project.

I would like to thank Manju L. Sharma for her technical support and friendship when things got tough. Thanks to Ching Leang for her valuable help at all stages. Thanks are also due to Betsy L. Blunt and Joy Ward for their technical support.

I wish to express my appreciation to all the individuals who have contributed to this project and to all the previous and current lab members for their technical help and friendship.

Last but not least, I want to thank my loving husband, my family and my friends for their support and encouragement.

ABSTRACT

INVESTIGATION OF FE(III) REDUCTION IN *GEOBACTER SULFURREDUCENS*

CHARACTERIZATION OF OUTER SURFACE ASSOCIATED ELECTRON TRANSFER COMPONENTS

SEPTEMBER 2009

XINLEI QIAN, B.E., SOUTHERN YANGTZE UNIVERSITY

M.E., SOUTHERN YANGTZE UNIVERSITY

Ph.D., UNIVERSITY OF MASSACHUSETTS AMHERST

Directed by: Professor Derek R. Lovley

Outer membrane cytochromes OmcB and OmcS of *Geobacter sulfurreducens* are two important components of the respiratory chain for extracellular Fe(III) reduction. OmcS is a loosely bound cell surface protein involved in the reduction of insoluble Fe(III). OmcB is an outer membrane protein and required for insoluble and soluble Fe(III) reduction. The objective of this study was to understand better the mechanism of dissimilatory Fe(III) reduction, focusing on the cell surface proteins by further localization, identification of protein-protein interactions, and biochemical characterization of OmcB and OmcS. OmcB was found to be surface-exposed but

embedded in the outer membrane because mild protease treatment of cells resulted in partial degradation of OmcB. Removal of surface-exposed proteins inhibited Fe(III) reduction, which is at least partially due to the degradation of OmcB. Co-immunoprecipitation studies with outer surface proteins using an antibody against OmcS revealed that OmcS interacts with several proteins, of which some are implicated in Fe(III) reduction, such as PilA, OmpJ, and OmpB, and in electricity production, such as OmcZ. Other OmcS-associated proteins, which have not been studied, include a cytochrome (GSU2887), a hypothetical and a conserved hypothetical protein, and a putative protease with a PDZ domain. The results suggest that co-immunoprecipitation with other antibodies would help to identify more elements of electron transport pathways related to extracellular Fe(III) reduction. OmcB was purified via preparative sodium dodecylsulfate polyacrylamide gel electrophoresis (SDSPAGE) and anion-exchange chromatography. The molecular mass was determined as 82 kDa, and 11.5 hemes per molecule were found. OmcB was able to transfer electrons to either soluble or insoluble Fe(III). OmcS was purified by detergent extraction. The molecular mass was 47 kDa and it contains 6 heme groups. UV-visible, EPR, and NMR spectroscopies determined that all hemes are *bis*-histidyl hexacoordinated and low-spin in both oxidized and reduced forms. OmcS has a –212 mV midpoint redox potential, and donates electrons to soluble and insoluble metals and quinones. Transient state kinetics showed that OmcS reduces anthroquinone-2, 6-disulfonate 10 times faster than it reduces Fe(III) citrate. This study revealed valuable further details about the mechanism of Fe(III) reduction by *G. sulfurreducens* by identifying the localization, protein-protein interactions and biochemical characteristics of the components of extracellular electron transport.

CONTENTS

LIST OF TABLES

LIST OF FIGURES

CHAPTER 1

INTRODUCTION

Iron cycle and Fe(III) reduction

Microbial reduction of ferric iron [Fe(III)] to ferrous iron [Fe(II)] is an essential part of the global iron cycle (Schroder, 2003). Fe(II) also can be released from corrosion of iron containing minerals. In the environment, wherever the pH is higher than 5, Fe(II) is chemically oxidized to Fe(III) in the presence of oxygen. Aerobic lithotrophic Fe(II)-oxidizing bacteria are also capable of oxidizing Fe(II) to Fe(III) (Druschel, 2008; Straub, 1996). In most environments, Fe(III) forms minerals such as oxide, hydroxide, phosphate and sulfate salts with very low solubility. Although, iron is the fourth most abundant element in the Earth's crust, the low solubility of Fe(III) minerals in the subsurface limits its availability to microorganisms.

There are two physiologically distinct types of microbial Fe(III) reduction: assimilatory and dissimilatory. The purpose of assimilatory Fe(III) reduction is to incorporate reduced iron into proteins with important catalytic activities, while that of dissimilatory Fe(III) reduction or Fe(III) respiration is to generate energy to support cell growth. Dissimilatory Fe(III) reduction is the most significant Fe(III)-reducing process under anoxic conditions (White, 2000). Despite its importance, little is known about the biochemical basis of dissimilatory Fe(III) reduction or the mechanism of energy generation coupled to Fe(III) reduction. This is in contrast to assimilatory Fe(III) reduction, which has been extensively characterized (Schroder, 2003).

Geobacteraceae* and *Geobacter sulfurreducens

Microorganisms in the family *Geobacteraceae* are predominant in a wide variety of subsurface environments in which respiratory Fe(III) reduction plays an important role in the degradation of organic matter and the bioremediation of organic compounds (Lloyd, 2001; Lovley, 1991a; Rooney-Varga, 1999; Sung, 2006; Thamdrup, 2000), as well as the immobilization of metal contaminants such as U (uranium), Tc (technetium) and Cr (chromium) (Coates, 1996; Holmes, 2002; Lovley, 1995; Snoeyenbos-West, 2000). Therefore, Fe(III) reduction is an environmentally significant process and an understanding of this process would contribute to the potential application of *Geobacter* species to clean up contaminated subsurface sites.

Current research has also demonstrated that *Geobacter* species can use a graphite electrode instead of Fe(III) as an extracellular electron acceptor and produce electricity (Bond, 2002), which greatly extends the potential application of Fe(III) reducers to power small and/or remote electric devices (Lovley, 2006a; Tendera, 2008), to bioremediation of organic contaminants (Bond, 2002), and to waste treatment (Lovley, 2006a)

The most studied member of the *Geobacteraceae* family, *G. sulfurreducens*, was isolated from the sediment of a hydrocarbon-contaminated site in Oklahoma (Caccavo, 1994). *G. sulfurreducens* became the model organism for studying the mechanism of Fe(III) respiration of *Geobacter* species because its genome sequence was available first (Methe, 2003) and a system for genetic manipulation (Coppi, 2001) and an *in silico* genome-based metabolic model (Mahadevan, 2006) were developed. Furthermore, *G. sulfurreducens* can readily be cultured with soluble Fe(III) in the form

of Fe(III) citrate, or with fumarate as the electron acceptor.

Mechanisms of dissimilatory Fe(III) reduction

Bacterial respiration of Fe(III) can be defined as the use of Fe(III) as a terminal electron acceptor in an energy-conserving electron transport pathway that results in the extracellular accumulation of Fe(II). The process plays an important role in the degradation of natural and contaminant organic matter in aquatic sediments and the subsurface and influences the mobility of a variety of trace metals in these environments (Lovley, 2000; Lovley, 2001).

Insoluble Fe(III) oxides are the primary form of Fe(III) in most soils and sediments (Murad, 1998; Schroder, 2003); therefore, the reduction of extracellular Fe(III) is likely to proceed via mechanisms significantly different from those for the reduction of soluble electron acceptors such as oxygen, nitrate, fumarate, or sulfate. Dissimilatory metal reducers have to transfer electrons derived from central metabolism in the cytoplasm and inner membrane onto an insoluble, extracellular electron acceptor via the periplasm and outer membrane (Lovley, 2004). The inner membrane components of this electron transport also generate a proton motive force, but the periplasmic and outer membrane processes are thought only to transport electrons to the terminal oxidant. *C*-type cytochromes were found to be involved in the latter process (Butler, 2004; Leang, 2003; Lloyd, 2003; Mehta, 2005). At present, two strategies have been described to access insoluble Fe(III) in dissimilatory Fe(III) oxide reduction. *Geothrix fermentans* and *Shewanella oneidensis* produce soluble compounds which can serve as electron shuttles between microorganisms and insoluble Fe(III) substrates (Nevin, 2000; Nevin, 2002). *G. fermentans* and *Shewanella alga* also secrete

iron-chelating compounds that significantly solubilize Fe(III) oxides(Nevin, 2002). Other species, such as *Geobacter metallireducens*, do not produce electron shuttles or Fe(III) chelators (Nevin, 2000), or solubilize Fe(III) before reduction (Nevin, 2000), but require direct contact with insoluble Fe(III) (Childers, 2002).

Fe(III) reduction in *Geobacter* species

G. sulfurreducens was initially proposed to reduce Fe(III) by releasing an electron shuttle, a small (9.6 kDa) *c*-type cytochrome (Seeliger, 1998). However, further studies revealed that *G. sulfurreducens* did not secrete this cytochrome into the extracellular environment and this cytochrome could not function as an electron shuttle even when it was added into cultures (Lloyd, 2000). At present *G. sulfurreducens* cells are believed to reduce insoluble Fe(III) by direct contact (Nevin, 2000).

Biochemical analysis showed that Fe(III) reductase activity in Fe(III)-reducing bacteria was predominantly found in the membrane fraction (Gorby, 1991; Lloyd, 2000; Magnuson, 2000; Myers, 1993). In *S. oneidensis*, 54 to 56% of this activity was localized in the outer membrane (Myers, 1993). The same was subsequently confirmed in studies with *G. sulfurreducens*; 75 to 79% of the Fe(III) reductase activity of the membrane fraction was present in the outer membrane (Gaspard, 1998).

Several studies suggested that the Fe(III) reductase activity is cytochrome-associated in *S. oneidensis* (Myers, 1997; Myers, 1992). In *G. sulfurreducens*, a genome study revealed that there are 103 genes encoding putative *c*-type cytochromes, many of which were predicted to be outer membrane-associated (Methe, 2003) or found to be outer membrane proteins by a global proteomics approach (Ding, 2006). The apparent abundance of *c*-type cytochromes in the outer membrane

implies the importance of electron transport from cytoplasm to outer membrane. It may also indicate a flexible electron transfer network for the reduction of diverse electron acceptors in the environment (Methe, 2003).

Current research on *c*-type cytochromes and other proteins involved in Fe(III) reduction in *G. sulfurreducens*

To understand the mechanism of Fe(III) reduction, the expression patterns and functions of several proteins that are predicted to be either in the periplasmic fraction or in the outer membrane fraction have been studied. The most significant findings about proteins related to Fe(III) reduction are summarized below.

MacA and PpcA

Genetic analysis indicated that two periplasmic *c*-type cytochromes, MacA and PpcA, were involved in Fe(III) reduction (Butler, 2004; DiDonato, 2004; Lloyd, 2003). MacA and PpcA were suggested to be the links between the cytoplasmic membrane and the outer membrane in the flow of electrons from the cytoplasm to the extracellular insoluble Fe(III).

The *macA* gene encodes a diheme *c*-type cytochrome with a putative signal peptide but no transmembrane regions, suggesting a periplasmic location. It was found to be highly expressed during growth on soluble Fe(III) (Butler, 2004). Analysis of a *macA*-deficient mutant revealed that its capability to reduce soluble Fe(III) was greatly diminished compared to that of the wild type (Butler, 2004). However, subsequent studies showed that the *macA* deficient mutant did not produce OmcB, an outer membrane *c*-type cytochrome that is critical for Fe(III) reduction (Kim, 2008). When the *macA* mutant was complemented with *omcB in trans*, Fe(III) reduction capability

was partially restored, which suggests that instead of serving as a member of the electron transfer chain, *macA* is involved in Fe(III) reduction through regulation of *omcB* expression (Kim, 2008).

PpcA is a 9.6 kDa triheme *c*-type cytochrome with a hydrophobic signal peptide (Lloyd, 2003). It was purified from the soluble fraction of *G. sulfurreducens* after lysozyme treatment, and the absence of the signal peptide in the hydrophilic mature protein was in agreement with its predicted periplasmic location (Lloyd, 2003). The growth rate and cell yield of a *ppcA*-deficient mutant were lower than those of the wild type during growth with Fe(III) as the electron acceptor (Lloyd, 2003). Four paralogs of PpcA: PpcB, PpcC, PpcD, and PpcE with 77%, 62%, 57%, and 65% amino acid sequence identity to PpcA, respectively, were identified in *G. sulfurreducens* (DiDonato, 2004). When *ppcA* was deleted, of *ppcB-E* was upregulated and could partially compensate for the loss of PpcA (DiDonato, 2004). When any of its paralogs was deleted, *ppcA* was upregulated and the rate of soluble Fe(III) reduction increased above that of the wild type, indicating that PpcA is the most efficient periplasmic electron carrier (DiDonato, 2004).

OmcB

OmcB was the first cytochrome shown to be involved in the reduction of both soluble and insoluble Fe(III) (Leang, 2005; Leang, 2003). This high-molecular-mass cytochrome is predicted to have 12 heme-binding sites and to be localized to the outer membrane due to the presence of a 10 amino acid lipoprotein signal peptide at its N-terminus. The ability of an OmcB-deficient mutant to reduce soluble Fe(III) and insoluble Fe(III) was greatly impaired (Leang, 2003). OmcB was not homologous to

any other protein found in the databases except a paralog, OmcC, which is 73% identical and does not appear to be involved in Fe(III) reduction (Leang, 2003).

OmcS and OmcE

Two *c*-type cytochromes, OmcS and OmcE, have been implicated in the reduction of insoluble Fe(III). The deletion of either *omcS* or *omcE* severely reduced the capability of *G. sulfurreducens* to grow on Fe(III) oxide as electron acceptor, but had no effect on the reduction of soluble Fe(III) forms (Mehta, 2005). These cytochromes were found to be loosely attached to the cell surface and could be isolated from intact cells by treating cells with gentle shearing force (Mehta, 2005). A paralog of *omcS*, *omcT*, is located directly downstream of the *omcS* gene. The amino acid sequences of OmcS and OmcT are 62.6% identical. Although RT-PCR showed that *omcS* and *omcT* are both expressed (Mehta, 2005), in proteomic studies only OmcS was detected under the same growth conditions (Ding, 2008). OmcE is less abundant than OmcS in cells grown on Fe(III) oxide (Ding, 2008). Moreover, the abundance of OmcE relative to total protein is statistically the same in cultures supplemented with either Fe(III) oxide or Fe(III) citrate (Ding 2008) indicating its lesser importance in Fe(III) oxide reduction.

OmcF

OmcF, a 10 kDa monoheme cytochrome *c* with an N-terminal lipoprotein signal peptide sequence, was detected in outer membrane-enriched fractions. Its structure greatly resembles that of a cytochrome c_6 from the photosynthetic alga *Monoraphidium braunii,* which is involved in electron transport in the photosynthetic system (Pokkuluri, 2009). An *omcF*-deficient mutant was greatly impaired in Fe(III) reduction (Kim, 2005), and it was later found that OmcB was not expressed in this mutant, as was also found in

the case of the *macA* deletion mutant (Kim, 2005). This result suggested that OmcF may be involved in regulation of *omcB* expression directly or indirectly, and that the phenotype of the *omcF*-deficient mutant maybe due to the lack of *omcB* expression (Kim, 2005).

OmcZ

OmcZ, an extracellular matrix-associated *c*-type cytochrome, exists in two different forms, a larger $OmcZ_L$ (50kDa) and a smaller $OmcZ_S$ (30kDa), but both forms retain all 7 heme-binding motifs, resulting in the same number of hemes (Inoue, manuscript in preparation). Most probably, OmcZ goes through a posttranslational modification process originating in the periplasm, because most of the large form of OmcZ is found in the periplasm and the outer membrane, while the majority of the small form is present in the extracellular matrix. OmcZ is the most significant *c*-type cytochrome that is involved in electricity production when a graphite electrode is the only electron acceptor, but it is not required for reduction of fumarate, Fe(III) citrate or Fe(III) oxide (Nevin, 2009). Immunogold labeling using an OmcZ specific antibody revealed that OmcZ is localized in a biofilm structure, consistent with the involvement of OmcZ in electricity production (K. Inoue, unpublished data), and is part of a "conductive network of bound electron transfer mediators" with OmcB and PilA (Richter, 2009).

OmpB

OmpB is a putative multicopper protein with highest homology to the manganese oxidase, MofA, from *Leptothrix discophora* (Mehta, 2006). The failure to export OmpB to the outer membrane upon deletion of *oxpG*, a member of an atypical type II secretion

system, disabled the cells to reduce Fe(III) oxide. The *ompB* disruption mutant showed the same phenotype when insoluble Fe(III) was provided as electron acceptor, providing further evidence that OmpB is involved in the reduction of insoluble Fe(III) (Mehta, 2006). However, the role of this protein in Fe(III) reduction is still unclear.

Pili

Pili in *Geobacter* were proposed to aid in establishing contact between the cell and insoluble Fe(III) oxide (Childers, 2002). Further studies showed that pili in *G. sulfurreducens* are highly conductive and not required for cells to contact insoluble Fe(III) oxide directly; rather, they have the potential role of serving as biological nanowires to transfer electrons from the cell to insoluble Fe(III) oxide or an anode (Reguera, 2005). More recent studies showed that the *pilA* gene may not be responsible for pilus production because a filament structure composed of PilA monomers has not been identified by trasmission electron microscopy using PilA-specific antibodies (C. Leang, personal communication). However, PilA antigens were found on the surface of the cell (C. Leang, unpublished data). It was also recently discovered that PilA may not play a direct role in the reduction of Fe(III) oxide because the *pilA* disruption mutant failed to localize outer membrane-associated *c*-type cytochromes correctly, indicating an additional role of PilA in protein transport (Izallalen, 2008; Klimes, 2008). Further studies are required to understand the role of PilA in Fe(III) reduction.

In this study an attempt was made to characterize further the mechanism of extracellular Fe(III) reduction, mainly focusing on the outer surface of the cell and the proteins suggested to be outer surface-localized and in direct contact with insoluble Fe(III). This study concentrates on two cytochromes, OmcB and OmcS, because their

importance in Fe(III) reduction has been identified by genetic, microarray and proteomic studies. A biochemical approach was chosen to identify their exact localization and their interactions with other surface proteins, and to determine their physical, (electro)chemical and redox characteristics in order to understand better their roles in extracellular electron transport and/or Fe(III) reduction.

CHAPTER 2

EVIDENCE THAT OMCB AND OMPB OF *GEOBACTER SULFURREDUCENS* ARE OUTER MEMBRANE SURFACE PROTEINS

Abstract

The *c*-type cytochrome (OmcB) and the multicopper protein (OmpB) required for Fe(III) oxide reduction by *G. sulfurreducens* were previously predicted to be outer membrane proteins, but it is not clear whether they are positioned in a manner that permits interaction with Fe(III). Treatment of whole cells with proteinase K inhibited Fe(III) reduction, but had no impact on inner membrane-associated fumarate reduction. OmcB was digested by the protease, resulting in a smaller peptide. However, immunogold labeling coupled with transmission electron microscopy (TEM) did not detect OmcB, suggesting that is only partially exposed on the cell surface. In contrast, OmpB was completely digested by the protease. OmpB was loosely associated with the cell surface, as a substantial portion of it was recovered in the culture supernatant. Immunogold labeling demonstrated that OmpB associated with the cell was evenly distributed on the cell surface rather than localized to one side of the cell like the conductive pili. Although several proteins required for Fe(III) oxide reduction are shown to be exposed on the outer surface of *G. sulfurreducens*, the finding that OmcB is also surface-exposed is the first report that a protein required for optimal Fe(III) citrate reduction is at least partially accessible on the cell surface.

Introduction

It is important to understand the mechanisms of electron transfer to Fe(III) in *Geobacter* species because they are the most abundant Fe(III)-reducing microorganisms in a diversity of subsurface environments in which Fe(III) reduction is an important process (Anderson, 2003; Holmes, 2005; Holmes, 2002; North, 2004; Ortiz-Bernad, 2004; Röling, 2001; Rooney-Varga, 1999; Snoeyenbos-West, 2000; Vrionis, 2005). The insoluble nature of Fe(III) oxides requires that *Geobacter* species transfer electrons outside the cell in order to reduce Fe(III) (Lovley, 2004). In addition to Fe(III) oxides, *Geobacter* species are capable of reducing a variety of other extracellular electron acceptors, including Mn(IV) oxides (Lovley, 1988), other metals (Caccavo, 1994; Lovley, 1991b; Lovley, 1993; Ortiz-Bernad, 2004), humic substances (Lovley, 1996), and electrodes (Bond, 2003 ; Bond, 2002; Lovley, 2006b).

Most studies of extracellular electron transfer in *Geobacter* species have focused on *G. sulfurreducens* because the complete genome sequence (Methe, 2003), a genetic system (Coppi, 2001), and an *in silico* genome-based metabolic model (Mahadevan, 2006) are available. Furthermore, *G. sulfurreducens* can readily be cultured with soluble Fe(III) in the form of Fe(III) citrate, or with fumarate as the electron acceptor.

Previous studies have identified various electron transfer components required for Fe(III) reduction by *G. sulfurreducens*. Several *c*-type cytochromes are required for optimal reduction of Fe(III) citrate as well as Fe(III) oxide. They are localized in the inner membrane (Butler, 2004) or periplasm (Lloyd, 2003), as well as in the outer membrane, the last group including the *c*-type cytochrome, OmcB (Kim, 2006; Leang, 2005; Leang, 2003). However, other components are exclusively required for Fe(III) oxide reduction, but not the reduction of Fe(III) citrate. These include the *c*-type

cytochromes OmcS and OmcE (Mehta, 2005), the multicopper protein, OmpB (Mehta, 2006), and the electrically conductive pili, known as 'microbial nanowires' (Reguera, 2005). The pili are clearly displayed outside the cell (Reguera, 2005) as are OmcS and OmcE (Mehta, 2006). OmpB and OmcB are both considered to be located in the outer membrane, but whether these proteins are exposed to the outer surface has not been previously determined.

The purpose of this study was to localize OmpB and OmcB further in order to understand better their roles in Fe(III) reduction. The results suggest that whereas OmpB is highly exposed on the outer surface and is only loosely associated with the outer membrane, OmcB appears to be tightly associated with the outer membrane, with only a portion of the protein exposed to the extracellular environment.

Materials and methods

Bacterial strains and culture conditions

Wild type (DL1) as well as *omcB* (DL6, *ΔomcB::cam*) (Leang, 2003) and *ompB* (*ΔompB::spec*) (Mehta, 2006) mutant strains of *G. sulfurreducens* are routinely maintained in our laboratory. These pure cultures were grown under strict anaerobic conditions as previously described (Coppi, 2001). Briefly, the growth medium consisted of a carbonate buffered minimal medium with 20 mM acetate as the electron donor and 40 mM fumarate as the electron acceptor. Cell growth was monitored by measuring the optical density at 600 nm (Genesys 2, Spectronic Instruments, Rochester, NY).

For OmcB peptide overexpression, *Escherichia coli* strain Rosetta 2 (DE3) (Novagen, WI) was used, which contains the pRARE plasmid expressing tRNAs for

rarely used codons in *E. coli*, which was essential for the successful overexpression of OmcB peptide. Cells also containing plasmid pET15b-omcBpep were grown in Luria-Bertani medium at 37 °C, supplemented with 12.5 mg/L chloramphenicol and 100 mg/L ampicillin. Expression of OmcB peptide was induced by adding 1 mM IPTG in exponential growth phase (OD 600 nm = 0.6).

Cell fractionation

Wild type and mutant *G. sulfurreducens* cells in their late exponential growth phase were harvested by centrifugation (4000 x *g* for 15 min at 4°C). The supernatants were concentrated 10-fold with a centrifugal filtration system equipped with a 10 kDa-cutoff membrane (Millipore, MA). Cells from the cultures were disrupted by sonication (Sonic dismembrator F550; Fisher Scientific, PA) and cell debris was separated from cell lysate by centrifugation (8000 x *g* for 15 min at 4°C). The membrane proteins were separated from cytoplasmic and periplasmic fractions by ultracentrifugation at 257000 x *g* for 60 min at 4°C. Membrane proteins were further fractionated into cytoplasmic membrane and outer membrane proteins by solubilizing the former in 1% (w/v) sodium laurylsarcosine, as described elsewhere (Kaufmann, 2001; Nikaido, 1994).

Antibody production and purification

In order to generate an OmcB-specific antiserum, an 846-bp fragment of the *omcB* gene(A116 to N397) (Fig. 2.1) was amplified using primers OmcbpepnotI and Omcbpephindiii (Table 2.1), digested with *Not* I and *Hind* III, and inserted into the *Not* I and *Hind* III sites of the expression vector pET15b (Novagen, WI). Sequencing

confirmed the accuracy of the PCR amplification. Competent *E. coli* strain Rosetta 2 (DE3) (Novagen, WI) was transformed with the resulting plasmid, pET15b-omcBpep. The His-tagged OmcB peptide was successfully overexpressed and purified by Ni-nitrilotriacetic acid affinity chromatography as recommended by Novagen. The correct amino acid sequence was confirmed by matrix-assisted laser desorption ionization mass spectrometry (MALDI/MS). A total amount of 3 mg OmcB peptide was used to immunize two rabbits to generate polyclonal OmcB antibodies at UMass Antibody Production Service.

OmpB polyclonal antibodies were raised against a peptide of OmpB (KPDKTPIGPGDTPDC) in rabbits (Sigma Genosys) (Mehta, 2006).

Cross-reacting antibodies were removed by immunoabsorption using proteins extracted with acetone from an OmcB-deficient or OmpB-deficient mutant as described by Sambrook *et al*. (Sambrook, 1989), except that cells were disrupted by sonication and cell debris and unbroken cells were removed by centrifugation at 10000 x *g* for 10 min.

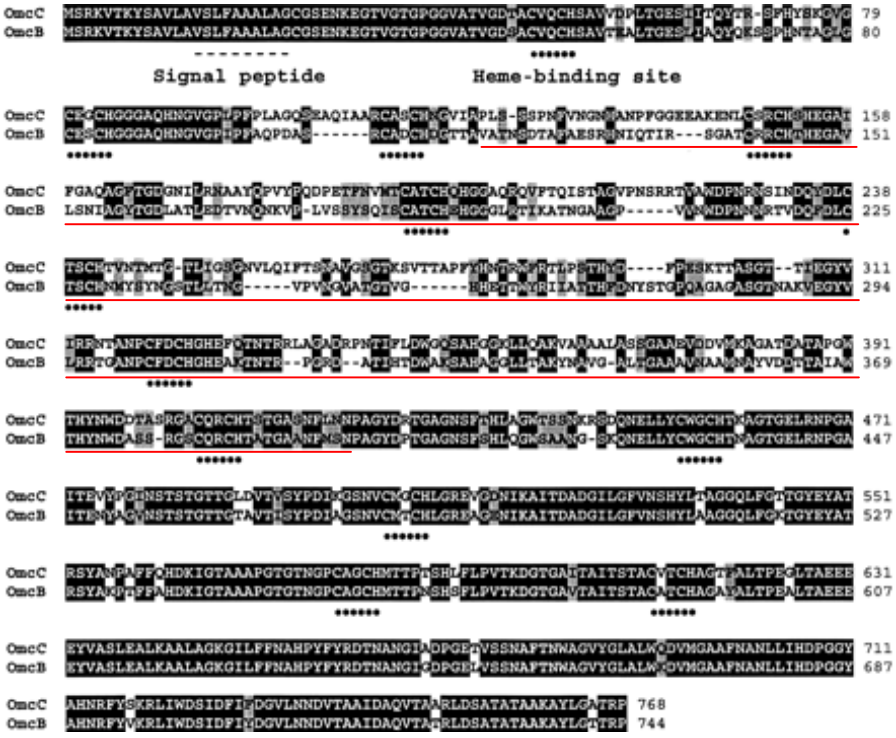

Fig. 2.1. Selection of peptide for production of OmcB specific antibody with the least homology to OmcC. Modified from *Leang et al, J. Bacteriol. 185*. The peptide selected for overexpression in *E. coli* for antibody production is underlined. Heme-binding domains (CXXCH) are indicated with dotted lines. The signal peptide (dashed line) is indicated for both proteins.

Table 2.1. Primers used for expression of OmcB peptide fragment

Primer name	Primer sequence (5' to 3')	Position
OmcBpepnoti	GGGGCGGCCGCCGTGGCAACCAACTCGGAC[a]	+349 to +368 of *omcB*
OmcBpephindiii	GGGAAGCTTTTAGTTGCTCATGAAATTAGCG[b]	+1173 to +1191 of *omcB*

Not I (*a*) and *Hind* III (*b*) sites are underlined.

Western blot analysis

Proteins were separated by SDSPAGE in 10% acrylamide gels. Western blot

analysis was performed by transferring the proteins to Immunoblot polyvinylidene difluoride (PVDF) membranes (BioRad, CA). The membranes were probed with polyclonal antibodies raised against a peptide of OmcB or OmpB (Kim, 2006; Mehta, 2006). Polyclonal alkaline phosphatase-conjugated anti-rabbit antibody (Sigma, MO) was used as a secondary antibody. OmcB and OmpB were visualized by staining with SigmaFast^{TM} 5-bromo-4-chloro-3-indolyl phosphatase/nitroblue tetrazolium (Sigma, MO).

Proteinase K digestion analysis of cell surface proteins

Cells were grown on acetate and fumarate as electron donor and acceptor, respectively, and were harvested in the mid-exponential phase by centrifugation at 6000 x *g* for 10 min at 4°C. The cells were washed twice, and resuspended in 10 mM HEPES (pH 7.5) containing 500 mM $MgCl_2$. The final cell density was 38.7 mg wet cells mL^{-1}. Washed cells were incubated with or without 1 U mL^{-1} proteinase K at 37°C, for different lengths of time (i.e. 10, 20, and 30 min). A protease inhibitor (Roche, NJ) was then added to stop the proteolytic reaction. Cells were recovered by centrifugation at 6000 x *g* for 1 min and washed twice in HEPES buffer containing protease inhibitor.

The washed cells were subjected to protein analyses by SDSPAGE followed by Coomassie Brilliant Blue (CBB) staining. The *c*-type cytochromes in the protein preparations were separated by Tricine-SDSPAGE, and visualized by heme-specific staining (Francis, 1984; Thomas, 1976). The effect of proteinase K treatment on OmcB and OmpB was monitored by Western blot analysis with OmcB and OmpB antibodies.

Cell suspension assay

The preparation of resting cell suspensions was carried out as previously described (Shelobolina, 2007). Briefly, cells from late-exponential phase cultures were harvested by centrifugation as described above and washed twice in an osmotically balanced wash buffer ($NaHCO_3$, 2.5 g L^{-1}; NH_4Cl, 0.25 g L^{-1}; NaH_2PO_4 - H_2O, 0.006 g L^{-1}; KCl, 0.1 g L^{-1}; NaCl, 1.75 g L^{-1}). Cells were resuspended in the wash buffer and a portion was subjected to proteinase K (Sigma, MO) treatment for 30 min, as described below. The other untreated portion served as a control. The proteinase K reaction was stopped by adding a protease inhibitor (Roche, NJ) to the sample. The cells were then washed twice and resuspended in wash buffer. Untreated and proteinase K-treated cell suspensions were incubated in a minimal buffer ($NaHCO_3$, 2.5 g L^{-1}, NH_4Cl, 0.25 g L^{-1}, and NaH_2PO_4 - H_2O, 0.006 g L^{-1}) with 5 mM acetate as the electron donor and 20 mM Fe(III) citrate or 10 mM fumarate as the electron acceptors to assay Fe(III)- and fumarate-reducing activities, respectively. The rate of fumarate reduction by resting cell suspensions was monitored by measuring the concentration of fumarate over time by HPLC (Shimadzu LC-6A, Kyoto, Japan). Samples were eluted from an Aminex HPX-87H column (300 mm-7.8 mm, Bio-Rad Laboratories, CA) at a rate of 1 mL min^{-1} for 20 min using 8 mM H_2SO_4 as an eluent. The fumarate concentration of the samples was monitored at a wavelength of 210 nm using matching retention times of fumarate standards of known concentration as controls. Fe(III) reduction was determined as the amount of HCl-extractable Fe(II) using a ferrozine assay, as previously described (Lovley, 1988). Protein concentration was determined with the bicinchoninic acid method using bovine serum albumin as a standard (Smith, 1985).

Transmission electron microscopy localization

For immunolocalization of the OmcB and OmpB proteins, mid-exponential phase cultures of the wild type and the *omcB* and *ompB* disruption mutant strains were adsorbed onto carbon-coated copper grids and fixed with 1% glutaraldehyde. Immunolabeling was performed at room temperature using primary antibodies raised against the OmcB and OmpB proteins [1:100 in phosphate buffered saline–bovine serum albumin (PBS–BSA) buffer for 1 h] and NanoGolds- conjugated secondary antibodies (Nanoprobes; 1:50 in PBS–BSA buffer for 30 min) following the manufacturer's recommendations. After immunolabeling, cells were treated with the Goldenhance^{TM}-EM reagent (Nanoprobes, Yaphank, NY) for 5 min to increase the size of the gold particles, and were negatively stained with the vanadium-based Nanovan^{TM} stain (Nanoprobes, Yaphank, NY), also following the manufacturer's recommendations. Immunolabeling was also performed in cell suspensions following the manufacturer's recommendations. Briefly, cells were harvested by centrifugation (300 x *g* for 5 min) and washed with PBS buffer containing 0.02 M glycine. Cells were incubated for 3 min with the primary antibody in a PBS–BSA buffer with gentle agitation and with the NanoGolds-conjugated secondary antibodies before treatment with the Goldenhance^{TM}-EM reagent (Nanoprobes, Yaphank, NY). The immunolabeled cells were washed twice in PBS–BSA and fixed with glutaraldehyde before being immobilized on the copper grid. Immunolabeled samples were examined with a JEOL 100S transmission electron microscope operated at 80 V. Samples containing strains in which the gene for OmcB (Leang, 2003) or OmpB (Mehta, 2006) was deleted were labeled, respectively, with the OmcB and OmpB anti-sera and used as controls for

nonspecific binding of the primary antibody and background noise.

Results and discussion

Protease digestion of whole cells removes the capability to reduce Fe(III)

Information on the localization of proteins required for Fe(III) reduction in *Geobacter* species can aid in understanding the mechanisms of this process. One strategy to evaluate whether proteins are exposed on the outer surface of the cell is to determine whether these proteins are susceptible to protease digestion in whole cell preparations.

Microscopic examination revealed that cells of *G. sulfurreducens* treated with proteinase K (1 U mL^{-1}) for up to 30 minutes remained intact (Fig. 2.2B). The protease-treated cells reduced fumarate as well as controls, which were not treated with protease (Fig 2.2A). Fumarate is reduced at the inner membrane (Butler., 2006). Thus, these results demonstrated that the protease treatment did not disrupt electron transfer processes within the cell. However, the rate of Fe(III) citrate reduction in protease-treated cells was only 21% of that in untreated controls (Fig. 2.3B). These results suggested that protease treatment removed outer surface proteins that were required for Fe(III) citrate reduction.

When the proteins in the proteinase K-treated cells and untreated cells were separated with SDSPAGE, the total protein profile of the treated cell samples did not differ significantly (Fig. 2.4A), suggesting that proteinase K did not have access to the majority of the most abundant cell proteins. However, when the proteins were stained for heme there were notable differences in the composition and intensity of the bands

(Fig. 2.4B). The intensity of the heme-containing proteins in the high-molecular-mass range decreased with increasing duration of proteinase K treatment, with a corresponding increase in the intensity of lower-molecular-mass bands. The 9.6 kDa periplasmic *c*-type cytochrome PpcA (Ding, 2004; Lloyd, 2003) remained intact throughout the proteinase K treatment (Fig. 2.4B), providing further evidence that the outer membrane was not disrupted during proteolysis.

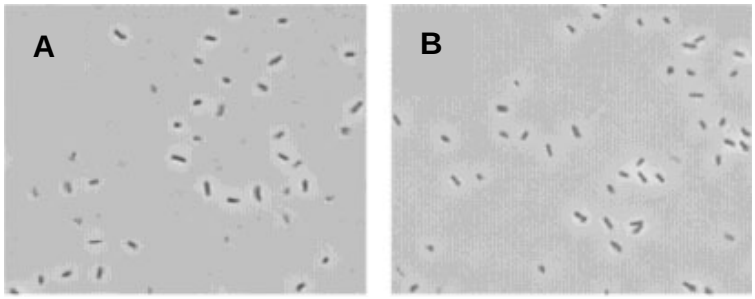

Fig. 2.2. Phase contrast microscopic images of untreated (A) and proteinase K-treated (B) cells of *Geobacter sulfurreducens* (x 100 magnification).

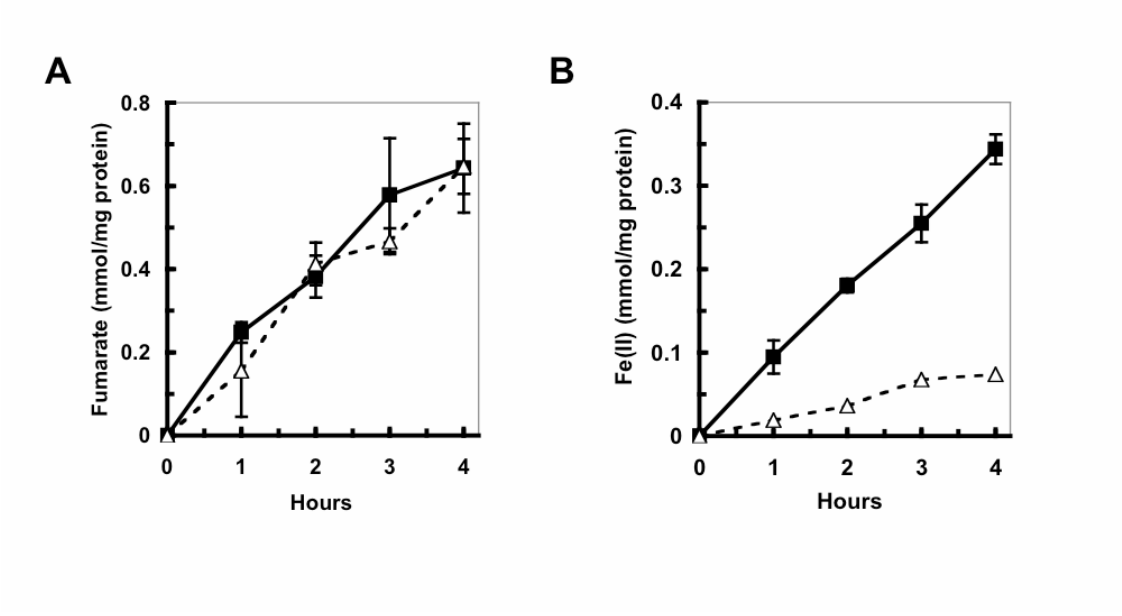

Fig. 2.3. Time-course of fumarate (A) and Fe(III) (B) reduction by proteinase K-treated (dashed line) or untreated (solid line) cell suspensions of *G. sulfurreducens*. Fumarate reduction was measured as a function of fumarate disappearance and Fe(III) reduction as a function of Fe(II) formation. Error bars are standard deviations from the mean of triplicate samples.

Exposure of the *c*-type cytochrome OmcB on the outer cell surface

Although *G. sulfurreducens* is predicted to have a multitude of outer membrane *c*-type cytochromes, only one, OmcB, has been definitely shown to be necessary for optimal reduction of soluble, chelated Fe(III) (Leang *et al.,* 2003, Kim *et al.,* 2005). As previously discussed (Leang *et al.,* 2003), topology prediction programs such as SIGNALP (http://www.cbs.dtu.dk/services/SignalP/), HMMTOP (http://www.enzim.hu/hmmtop) and SOSUI (http://www.proteome.bio.tuat.ac.jp/sosuiframe0.html) indicate that OmcB is likely to be associated with the outer membrane of *G. sulfurreducens* because it contains a signal

peptide homologous to those of lipoproteins, which is followed by a cysteine residue after the putative cleavage site that is thought to serve as the specific lipid attachment site of the protein to the membrane.

Associated with the loss of the capability to reduce Fe(III) citrate in the proteinase K-treated cells was an apparent protease-catalyzed digestion of OmcB (Fig. 2.5A). When the proteins of cells treated with proteinase K for different periods of time were separated on SDSPAGE gels and detected with an antibody specific for OmcB, there was a progressive loss over time of the 85 kDa band associated with OmcB. There was no loss in untreated controls. The loss of OmcB from the protease-treated cells was accompanied by the appearance of an additional band with a lower molecular mass (ca. 40 kDa) that reacted with the OmcB antibody (Fig. 2.5A). This suggested that only a portion of the OmcB in intact cells was accessible to proteinase K.

In order to evaluate further the localization of OmcB, whole cells were treated with OmcB antibodies and gold-conjugated secondary antibodies and examined with TEM (Fig. 2.6). OmcB was not detected even though other surface-exposed proteins can be detected with this same technique (see below). However, OmcB appeared to be primarily localized in the outer membrane because when the cell was fractionated, the OmcB antibodies detected OmcB in the outer membrane fraction with only traces detected in the soluble cell fraction and in culture supernatant fluids (Fig. 2.7A). OmcB was absent in the cytoplasmic membrane fraction. These results suggest that although OmcB is localized in the outer membrane, only a portion of OmcB is exposed outside the cell. The OmcB antibodies were developed with a peptide of 281 amino acids from the central section of the OmcB sequence (Kim, 2005), which apparently is not

accessible to the antibody when OmcB is localized in the intact outer membrane *in vivo*.

Localization of the putative multicopper protein, OmpB

In order to evaluate further the approaches used to localize OmcB, the putative multicopper protein, OmpB, was studied with similar techniques. A study in which the gene for OmpB was deleted demonstrated that OmpB is required for the reduction of Fe(III) oxide, but not Fe(III) citrate (Mehta, 2006). OmpB is predicted to be localized on the outer surface of *G. sulfurreducens* because when *oxpG*, a gene necessary for proper functioning of a type II secretion system, is deleted, OmpB accumulates in the periplasm (Mehta, 2006).

Detection of OmpB with polyclonal antibodies raised against OmpB suggested that OmpB is loosely associated with the outer surface of *G. sulfurreducens*. OmpB was primarily detected in culture supernatant fluids (Fig. 2.7B). OmpB was also detected in the outer membrane but only in small amounts even after loading four times more protein than the amount used to detect OmcB in outer membrane fractions (Fig. 2.7B). OmpB was only weakly present in the soluble cell fraction, and was absent in the cytoplasmic membrane fraction.

TEM-immunogold analysis revealed that the OmpB antibodies could access OmpB on the cell surface and that OmpB was uniformly distributed on the cell (Fig. 2.6C). In these studies, culture samples were directly applied and fixed to the TEM copper grids; thus, supernatant proteins also were present in the cell surroundings and OmpB was detected in the culture supernatant fluids of wild-type cells, in agreement with cell fractionation studies. When a strain in which the gene for OmpB had been

deleted was treated with the antibody, the signal was very weak, demonstrating low levels of antibody cross-reactivity (Fig. 2.6D). If the wild-type cells were washed prior to adsorption and fixation to the copper grids, the signal for OmpB was absent (Fig. 2.6E), demonstrating that OmpB is very loosely associated with the cell surface.

Proteinase K treatment of whole cells resulted in progressive loss of OmpB over time without the production of a secondary band (Fig. 2.5B). This is consistent with the results from the localization studies, which suggest that OmpB is primarily exposed outside the cell.

Topological and structural analyses with the SIGNALP, HMMTOP, and SOSUI programs predicted that OmpB is a soluble protein with a single transmembrane domain spanning amino acids 6 to 28. This transmembrane motif also includes the predicted cleavage site for OmpB's signal peptide (between the alanine and phenylalanine at positions 26 and 27, respectively), but, unlike OmcB, no cysteine residue that may function as membrane anchor was found. This is consistent with the experimental data that OmpB is loosely bound to the outer membrane.

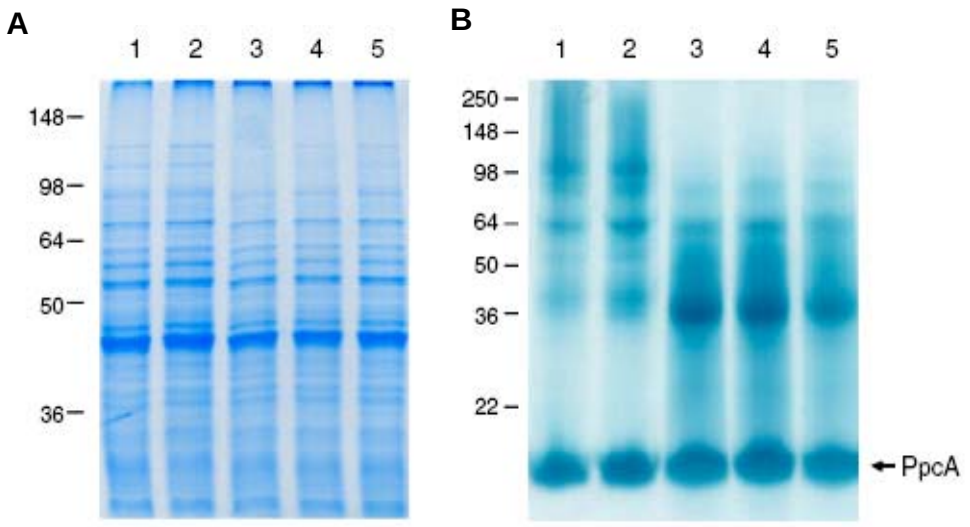

Fig. 2.4. Total protein (A) and heme-stained protein (B) profiles of whole cells treated with proteinase K. Lane 1, cells before protease treatment; lane 2, untreated control cells; lanes 3–5, whole cells treated with proteinase K (1 U mL^{-1}) for, respectively, 10, 20 and 30min. Each lane contained 5 mg of protein.

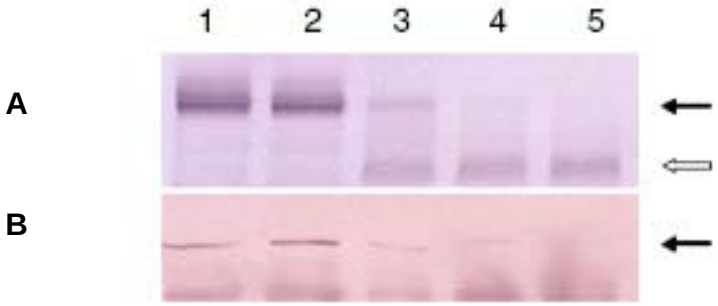

Fig. 2.5. Western blot analysis of OmcB (A) and OmpB (B) after the treatment of whole cells with proteinase K. Lane 1, cells before protease treatment; lane 2, control cells after 30 min of treatment without protease; lanes 3–5, whole cells treated with protease K (1 U mL^{-1}) for 10 min (Lane 3), 20 min (lane 4), and 30 min (lane 5). In each lane, 5 μg of protein were loaded. OmcB and OmpB are indicated with solid

arrows. The appearance of a new protein band upon protease digestion of OmcB is indicated with a clear arrow in (A).

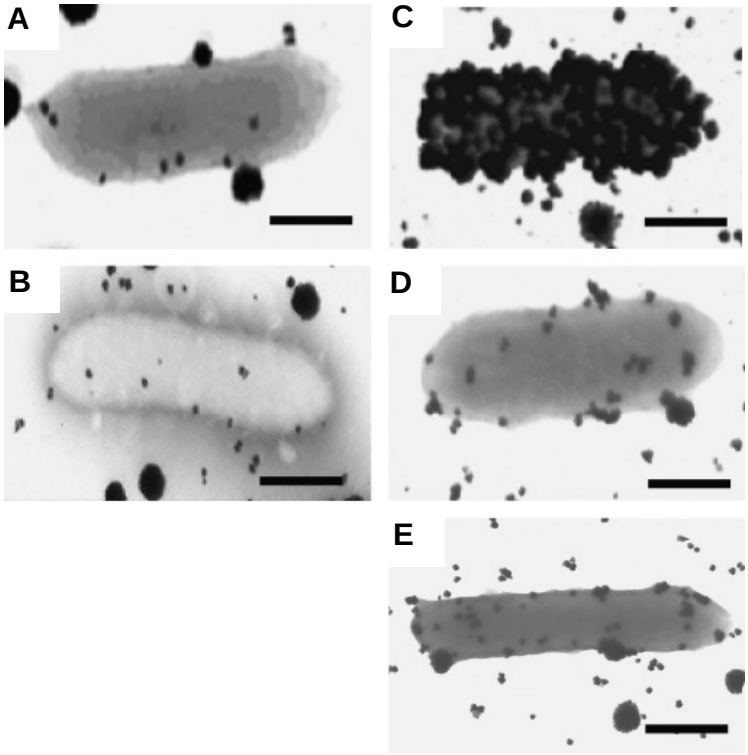

Fig. 2.6. TEM images of *Geobacter sulfurreducens* immunolabeled for OmcB (A, B) or OmpB (C–E). Cells of the wild type (A and C) were immobilized onto the copper grid support before immunolabeling. The *omcB* (B) and *ompB* (D) disruption mutant strains served as controls for nonspecific antibody binding. Wild type cells in panel (E) were immunolabeled before immobilization on the copper grid. Scale bars represent 0.5 μm.

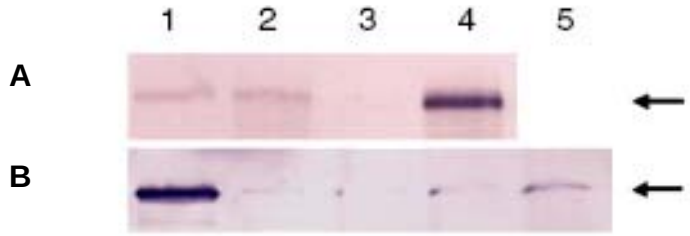

Fig. 2.7. Western blot analysis of OmcB (A) and OmpB (B) in the culture supernatant and different cell fractions. Lane 1, culture supernatant; lane 2, soluble fractions; lane 3, cytoplasmic membrane fraction; lane 4 and 5, outer membrane fraction. The amount of protein in each lane is 5 μg for lanes 1-4 and 10 μg for lane 5. OmcB and OmpB are indicated with arrows.

Implications

The results demonstrate for the first time that *G. sulfurreducens* requires protein(s) exposed on the outer surface of the cell in order to reduce soluble Fe(III) citrate. Previous studies have demonstrated that several proteins specifically required for the reduction of Fe(III) oxide are localized on the outer cell surface, but none of these have been required for the reduction of Fe(III) citrate. For example, pili are required for Fe(III) oxide reduction but not Fe(III) citrate reduction and, because of their electrical conductivity and specific binding of Fe(III) oxides, may be the final conduit for electron transfer from the cell to Fe(III) oxides (Reguera, 2005). Deletion of the genes for either of the outer membrane *c*-type cytochromes, OmcS or OmcE, inhibits Fe(III) oxide reduction, but has no impact on Fe(III) citrate reduction (Mehta, 2005). Both of these cytochromes are readily sheared off the outer cell surface, suggesting that they are

exposed on the outside of the cell (Mehta, 2005). In a similar manner, deletion of the gene for OmpB inhibits Fe(III) oxide reduction (Mehta, 2006), but not the reduction of Fe(III) citrate, and the studies described here demonstrate that OmpB is on the outside of the cell and so loosely associated with the cell surface that it is often primarily recovered in the culture supernatant. The OmpB that is associated with the cell surface is evenly distributed, unlike the conductive pili that are also required for Fe(III) oxide reduction, but localized to one side of the cell (Reguera, 2005).

Like OmcS, OmcE, and OmpB, OmcB can be considered an outer surface protein, but with some important differences. OmcB is required for optimal Fe(III) citrate reduction as well as Fe(III) oxide reduction (Leang, 2003). Furthermore, OmcB appears to be much more tightly associated with the outer membrane than OmcS, OmcE, or OmpB. The results presented here demonstrate that although a portion of OmcB is exposed on the outer surface of the cell, a significant portion is likely to be embedded within the outer membrane.

These considerations are consistent with the different properties of insoluble Fe(III) oxides and soluble, chelated Fe(III). Access of redox proteins to Fe(III) oxides is expected to be much more sterically hindered than access to soluble Fe(III). Therefore, in order for proteins to have the potential to transfer electrons directly to Fe(III) oxide, they must be significantly displayed outside the cell. In contrast, as long as a redox-active portion of a protein such as OmcB is exposed on the outer cell surface it is likely to have the possibility of transferring electrons to soluble Fe(III). Further analysis of the localization of other proteins predicted to be in the outer membrane of *G. sulfurreducens* is warranted in order to understand better their potential roles in

Extracellular electron transfer.

CHAPTER 3

PROTEIN-PROTEIN INTERACTION STUDIES OF MEMBRANE-ASSOCIATED COMPONENTS INVOLVED IN FE(III) REDUCTION IN *GEOBACTER SULFURREDUCENS*

Abstract

Previous studies revealed that several outer membrane-associated proteins, including heme-containing *c*-type cytochrome and non-heme proteins, are involved in Fe(III) reduction and electricity production in *Geobacter sulfurreducens*. However, the precise roles of different proteins in the mechanisms of Fe(III) reduction still remain unclear. A protein-protein interaction study of these protein components was performed to assess whether these proteins or others interact in the outer membrane or on the surface on the cell, in order to understand further their roles in Fe(III) reduction in *G. sulfurreducens*.

Two different methods were tried. The method of two-dimensional blue native/SDS polyacrylamide gel electrophoresis was not very effective in separation of outer membrane protein complexes despite the fact that it was able to separate inner membrane protein complexes. This was mainly due to the fact that the outer membrane proteins were less soluble than the inner membrane complexes.

Co-immunoprecipitation using purified antibody against a loosely bound outer surface cytochrome, OmcS, which is involved in the reduction of insoluble Fe(III),

successfully detected several proteins that interact with OmcS. Proteins that were identified as interacting with OmcS include two *c*-type cytochromes (OmcZ and GSU2887), the multicopper protein OmpB, the pilin monomer (PilA) of conductive pili, a putative protease, and two hypothetical proteins with unknown functions. Interestingly, OmcZ is implicated in electricity generation and not in Fe(III) reduction. PilA most likely has involvement in electricity generation, and has an indirect effect on Fe(III) reduction by facilitating the secretion of surface cytochromes.

The results of co-immunoprecipitation show that proteins involved in Fe(III) reduction interact. New proteins that may be important in Fe(III) respiration can be discovered by this method, although the significance of the proteins for either Fe(III) reduction or electricity generation requires further verification. This method is thus proven to provide valuable insight into the understanding of Fe(III) reduction in *G. sulfurreducens*.

Introduction

Geobacter species are the most abundant Fe(III)-reducing microorganisms in the subsurface environment where Fe(III) is the most abundant electron acceptor (Anderson, 2003; Holmes, 2005; Holmes, 2002; North, 2004; Ortiz-Bernad, 2004; Röling, 2001; Rooney-Varga, 1999; Snoeyenbos-West, 2000; Vrionis, 2005). They play important roles in degradation of natural and contaminant organic compounds (Coates, 2005; Lin, 2005; Lovley, 2004; Rooney-Varga, 1999; Sleep, 2006; Winderl, 2007) and in the immobilization of metal contaminations (Anderson, 2003; Chang, 2005; Istok, 2004; North, 2004; Petrie, 2003). It is of great importance to study the mechanism of Fe(III) reduction because Fe(III) oxide, the primary form of Fe(III) in subsurface

environments, is poorly accessible for microorganisms to reduce it due to its insoluble nature. *Geobacter sulfurreducens* has become the model organism to study in the genus *Geobacter* because of the availability of its genome sequence (Methe, 2003), a genetic manipulation system (Coppi, 2001) and an *in silico* genome-based metabolic model (Mahadevan, 2006). Previous studies suggested that *G. sulfurreducens* needs to establish direct contact in order to reduce insoluble Fe(III) (Nevin, 2000). Recent genetic studies revealed that a few outer membrane-associated proteins are involved in Fe(III) reduction (Afkar, 2005; Inoue, manuscript in preparation; Kim, 2006; Kim, 2005; Leang, 2003; Mehta, 2005; Mehta, 2006; Reguera, 2005), but no further information about the mechanisms of how these individual components interact has been revealed. This study was performed to characterize the interaction of outer membrane-associated proteins that are involved in Fe(III) reduction.

Two-dimensional blue native/SDS polyacrylamide gel electrophoresis (2-D BN/SDSPAGE), co-immunoprecipitation (co-IP) and other techniques were successfully used for the separation and identification of electron transport complexes of the mitochondrion and chloroplast membranes (Schägger, 2001). Protein-protein interaction may also be important for electron transport from the inner membrane via periplasmic space and outer membrane to an extracellular electron acceptor such as Fe(III) oxides in respiratory Fe(III) reducers. Although prior genetic studies indicated the involvement of different proteins in Fe(III) reduction or electron transport, such as *c*-type cytochromes (PpcA, OmcS, OmcE) (Lloyd, 2003; Mehta, 2005), a multicopper oxidase (OmpB) (Mehta, 2006), a porin-like protein (OmpJ) (Afkar, 2005), and pilin protein (PilA) (Reguera, 2005), these experiments were not designed for the assessment

of their interactions with other proteins.

The goal of this study was to investigate further the roles of these proteins in electron transport by studying protein-protein interactions among those proteins that are important for Fe(III) reduction. A further goal was to find other components of the Fe(III)-reducing system that have not been studied. The first step was to find suitable method(s) that can be adapted to the *Geobacter* system. First, 2-D BN/SDSPAGE was attempted. The first dimension is BN PAGE where individual complexes are separated by size. In order to keep the components of the protein complexes together, SDS was replaced by CBB G-250, which coats the entire complex and gives negative charges proportional to the complex's surface area (Schägger, 2001). The second dimension separates the components of the individual complexes by the addition of SDS.

The advantage of 2-D BN/SDSPAGE is that it does not require antibodies to detect protein-protein interaction. Moreover, this method is efficiently capable of identifying several complexes and their components in the same gel without antibodies. The availability of an antibody to a component of a protein complex would further help to confirm the interaction of proteins with the target protein by co-IP.

Materials and methods

Bacterial strains and culture conditions

Wild type (DL1) and *omcS* (DLTM1, *Δomcs::kan*) (Mehta, 2005) mutant strains of *G. sulfurreducens* are routinely maintained in our laboratory. These pure cultures were grown under strict anaerobic conditions as previously described (Coppi, 2001). Briefly, the growth medium consisted of a carbonate buffered minimal medium with 20

mM acetate as the electron donor and 40 mM fumarate as the electron acceptor. Cell growth was monitored by measuring the optical density at 600 nm (Genesys 2, Spectronic Instruments, Rochester, NY). Cultures were harvested at late exponential growth phase.

Membrane protein preparation by detergent solubilization

Wild type and mutant *G. sulfurreducens* cells in their late exponential growth phase were harvested by centrifugation (4000 x *g* for 15 minutes at 4˚C). The supernatants were concentrated 10-fold with a centrifugal filtration system equipped with a 10 kDa-cutoff membrane. Cells from the cultures were disrupted by sonication (Sonic dismembrator F550; Fisher Scientific, PA) and the soluble and insoluble fractions were collected by centrifugation at 257000 x *g* for 60 minutes at 4˚C. The soluble fraction of disrupted cells contains cytosolic and periplasmic proteins, whereas the insoluble fraction contains membrane proteins. Membrane proteins were further fractionated into cytoplasmic membrane and outer membrane proteins by solubilizing the first in 1% (wt/vol) sodium laurylsarcosine, as described elsewhere (Kaufmann, 2001; Nikaido, 1994).

Outer membrane protein fraction prepared by sucrose gradient centrifugation

The membrane protein fraction was resuspended in 50 mM Tris, pH 7.5, and subjected to sucrose gradient centrifugation (Ding, 2008). Membrane proteins were loaded on a sucrose gradient (30%, 50%, and 70%) in the same buffer and centrifuged at 82500 x *g* for 17 h at 4 °C in a Beckman SW28 rotor. Outer membrane protein layers were collected, diluted in 50 mM Tris, pH 7.5, and subjected to ultracentrifugation at

257000 x *g* for 60 min. The outer membrane protein fraction separated by ultracentrifugation was collected and resuspended in Blue Native solubilization buffer (50 mM NaCl, 5 mM 6-aminohexanoic acid, 50 mM imidazole HCl, pH 7.0).

Outer surface protein fraction preparation

Outer surface protein fractions from DL1 and *omcS* disruption mutant cells from late log phase culture were sheared using a blender at low speed for 2 min. Supernatants, separated from pellets by centrifugation of sheared cell culture at 5000 x *g* for 10 min, were concentrated with Amicon stirred cells with membrane of 10 kDa cutoff size (Millipore, MA), and washed with WB buffer. Protein concentration was determined with the BCA (bicinchoninic acid) protein analysis kit (Pierce, IL) as 0.7 mg m L^{-1}. Before co-immunoprecipitation, outer surface proteins were extracted by adding 25 μL of detergent dodecyl-β-D-maltoside from a 10% stock solution into 1 mL of protein and incubation at room temperature for 20 min. Solubilized outer surface protein fractions were diluted to 0.35 mg mL^{-1} with WB buffer and used for co-immunoprecipitation by OmcS antibody crosslinked to Dynabeads protein G.

Antibody production and purification

OmcB polyclonal antibodies were raised against a peptide of OmcB (Kim, 2005). Cross-reacting antibodies were removed by immunoabsorption using proteins extracted with acetone from an OmcB-deficient mutant as described by Sambrook *et al.* (Sambrook, 1989), except that cells were disrupted by sonication and cell debris and unbroken cells were removed by centrifugation at 10000 x *g* for 10 min.

Purified OmcS (3 mg) was used for OmcS polyclonal antibody generation in

rabbits at New England Peptide, MA.

OmcS antibodies were affinity purified using purified OmcS following the protocol from http://130.15.90.245/antibody_purification.htm. Purified OmcS was run on a 10% acrylamide SDSPAGE gel and electroblotted onto Immunoblot PVDF membranes (BioRad, CA). Transfer of OmcS from SDS gel to the PVDF membrane was confirmed by Ponceau S stain. After blocking with 5% fat-free milk, the PVDF membrane was incubated with the crude serum. Washing with TBS buffer removed the weakly binding antibodies. OmcS-specific antibodies were eluted with 0.15 M glycine buffer (pH 2.5). After elution, buffer was exchanged to neutral PBS with dialysis and purified antibody solution was stored at –20°C.

OmcZ polyclonal antibodies were raised against purified OmcZ in rabbits at New England Peptide, MA (Inoue, manuscript in preparation).

Cross-reactivity of OmcZ polyclonal antibodies was removed by affinity purification using purified OmcZ as described for purification of OmcS antibodies.

The hydrophilic portion of PilA (**AIPQFSAYRVKAYNSAASSDLRNLKTALESAFADDQTYPPES)** has been overexpressed in *E. coli* (Y. Londer, unpublished data). The purified peptide was used for polyclonal antibody production by immunizing two rabbits (Sigma, Genosys). Cross-reacting antibodies were removed by immunoabsorption using proteins extracted with acetone from a PilA-deficient mutant as described by Sambrook *et al.* (Sambrook, 1989), except that cells were disrupted by sonication and cell debris and unbroken cells were removed by centrifugation at 10000 x *g* for 10 min.

Western blot analysis

Proteins were separated by SDSPAGE in 10% acrylamide gels. Western blot analysis was performed by transferring the proteins to PVDF membranes. The membranes were probed with primary polyclonal antibodies followed with a secondary polyclonal alkaline phosphatase-conjugated anti-rabbit antibody (Sigma, MO). Western blot signals were visualized by staining with SigmaFast^{TM} 5-bromo-4-chloro-3-indolyl phosphatase/nitroblue tetrazolium (Sigma, MO).

Protein complex separation and identification by 2-D BN/SDSPAGE

First dimension BN PAGE was carried out as described (Schägger, 2001). The membrane protein fraction was resuspended in Blue Native solubilization buffer. Protein concentration was determined with the BCA kit (Pierce, IL). Detergent dodecyl-β-D-maltoside (Sigma, MO) was added at a ratio of 1 mg detergent to 1 mg protein from a 10% stock solution. After incubation on ice for 30 min, the membrane protein fraction was centrifuged at 16100 x *g* for 15 min at 4°C to separate the solubilized membrane proteins. Before loading protein samples on BN PAGE, CBB G-250 from a stock of 2 mg m L^{-1} was added to membrane proteins at a ratio of 0.5 mg CBB to 1 mg proteins. Seventy-five µg of membrane proteins were loaded on a 10-well 0.75 cm thick mini gel, run at 100 V and 4°C. When the sample had run to half the height of the gel, the cathode buffer was changed to light blue cathode buffer, which contains 1/10th the concentration of CBB of the previous deep blue cathode buffer.

A single lane was cut from the first-dimension BN PAGE, soaked in Tricine-SDSPAGE sample buffer with no reducing agent for 15 min, and inserted into

and laid on top of an 1 cm thick mini Tricine-SDSPAGE 10% acrylamide gel. Protein components of complexes were separated by the second dimension. CBB staining or silver staining (Invitrogen, CA), heme staining and Western blot analysis were carried out.

Conjugation and crosslinking of antibody and Dynabeads Protein G

Affinity-purified OmcS was conjugated and crosslinked to Dynabeads® Protein G (Invitrogen, Norway) using Bis(sulfosuccinimidyl)suberate (BS^3) (Sigma, MO) following the manufacturer's instructions. Briefly, antibody was incubated with Dynabeads protein G in WB buffer (0.1 M sodium phosphate, 0.01% Tween 20, pH 8.2) for 10 min at room temperature. After removal of supernatant, Dynabeads protein G was washed with PBS ($BupH^{TM}$ phosphate buffer saline, Pierce, IL) buffer. Antibody coupled Dynabeads protein G then were washed with conjugation buffer (20 mM sodium phosphate, 0.15 M NaCl, pH 7.2) and incubated in 5 mM BS^3 conjugation buffer at room temperature for 30 min for crosslinking. The reaction was stopped by adding Quenching buffer (1 M Tris HCl, pH 7.5). Antibody-crosslinked beads were washed and kept in WB buffer.

Co-immunoprecipitation using OmcS-specific antibodies

Co-immunoprecipitation was performed by following the manufacturer's instructions except that after incubation of protein fractions with antibody-crosslinked Dynabeads protein G, extensive washing with PBS buffer was performed to reduce the nonspecific binding as much as possible. After removal of most nonspecifically bound proteins, proteins that bound to Dynabeads were eluted with elution buffer (50 mM

glycine, pH 2.5). Non-specific binding of proteins to antibody and beads was detected by incubation of a sheared protein fraction from the *omcS* disruption mutant with antibody-crosslinked Dynabeads and a sheared fraction from wild type DL1 with non-antibody-conjugated Dynabeads. Eluted fractions were neutralized by adding 1 M Tris, pH 7.5, and analyzed by Tricine-SDSPAGE on a 10% acrylamide gel followed with silver staining (Invitrogen, CA), heme staining and Western blot analysis. Protein bands were cut out and sent for MALDI/MS analysis (Proteomic Mass Spectrometry Lab, UMASS Medical School).

Results and discussion

Detection of membrane protein complexes from *G. sulfurreducens* by 2-D BN/SDSPAGE

Membrane proteins were separated with ultracentrifugation from the soluble proteins of wild type cells cultured with acetate and fumarate as electron donor and acceptor, respectively. For the first dimension, a 3-15% acrylamide gradient blue native gel was used to separate the protein complexes by size after gentle solubilization with a nonionic detergent in order to keep the protein complexes intact (Fig. 3.1A, top gel). A CBB-stained blue native gel showed that there are multiple bands with large sizes ranging between 700 and 200 kDa, which suggests that they may contain multiple protein components. Individual complex components were then separated by SDSPAGE on a 10% acrylamide gel as the second dimension followed by CBB staining (Fig. 3.1A, lower gel). Several well-separated protein spots were observed, indicating that the electrophoresis in the second dimension was able to separate the

individual components of the complexes. The proteins were excised from the gel and subjected to tryptic digestion, and peptides were identified by MALDI/MS. As shown in Table 3.1 and Table 3.2, the identified proteins were all inner membrane-related with few exceptions such as OmpJ, a porin-like protein, which is the most abundant outer membrane protein.

In order to assess whether other outer membrane proteins are present in the second dimension, Western blot analysis was also carried out using the antibody generated against the outer membrane *c*-type cytochrome, OmcB (Fig. 3.1B, lower gel). A distinct OmcB spot was detected in the second dimension, which originated from the top of the native gel, indicating that some OmcB was unable to enter the first-dimension gel, the native, 3-15% acrylamide gradient gel (Fig. 3.1B). The rest of the OmcB signal was detected from the area ranging from 440 to 140 kDa as a streaking line, suggesting that the resolution of outer membrane proteins were extremely poor (Fig. 3.1B).

Separation of other cytochromes by 2D BN PAGE was further analyzed by using heme-specific staining in the 2^{nd} dimension. A few cytochromes were separated by the two-dimensional BN/SDSPAGE, but the resolution was as poor as that of OmcB (data not shown).

An attempt was made to improve the method, especially the quality of the protein sample. The outer membrane fraction was separated from the inner membrane proteins by either ultracentrifugation with a sucrose gradient or with the sarcosyl extraction method (Ding, 2006; Kaufmann, 2001). Although the proportion of inner membrane proteins was reduced in the sample, this was not reflected in the results after the 2-D

blue native gel separation. The most dominant and best-separated proteins were still the inner membrane proteins (Fig. 3.2 and Table 3.1; Fig. 3.3 and Table 3.2).

The failure to detect outer membrane protein complexes by 2-D BN/SDSPAGE could result from the poor solubility of the outer membrane proteins. Outer membrane proteins are difficult to solubilize with nonionic detergents and they tend to be retained in the top of the native gel. After entering the first dimension, they migrate through the gel with variable velocity, resulting in streaking lines instead of well-defined spots, as was demonstrated in the case of OmcB. The solubility of outer membrane proteins could not be improved by increasing the ratio of the nonionic detergent, dodecyl-β-D-maltoside, to proteins or by replacing dodecyl-β-D-maltoside with other nonionic detergents such as Triton X-100. Subsequent studies showed that separation and solubilization of outer membrane-associated proteins of *G. sulfurreducens* remain very poor unless harsh treatments of heat and strong ionic detergents are used. This poor solubility may be caused by outer membrane-associated lipopolysaccharides and/or extracellular polysaccharides. This could be the reason for the enrichment of more soluble inner membrane proteins from prepared membrane protein fractions in 2 D BN/SDSPAGE. However, the results clearly indicate that this method is suitable for the separation of inner membrane complexes. The identification of inner membrane complexes is also of interest, since inner membrane electron transport complexes involved in Fe(III) reduction have not been fully identified.

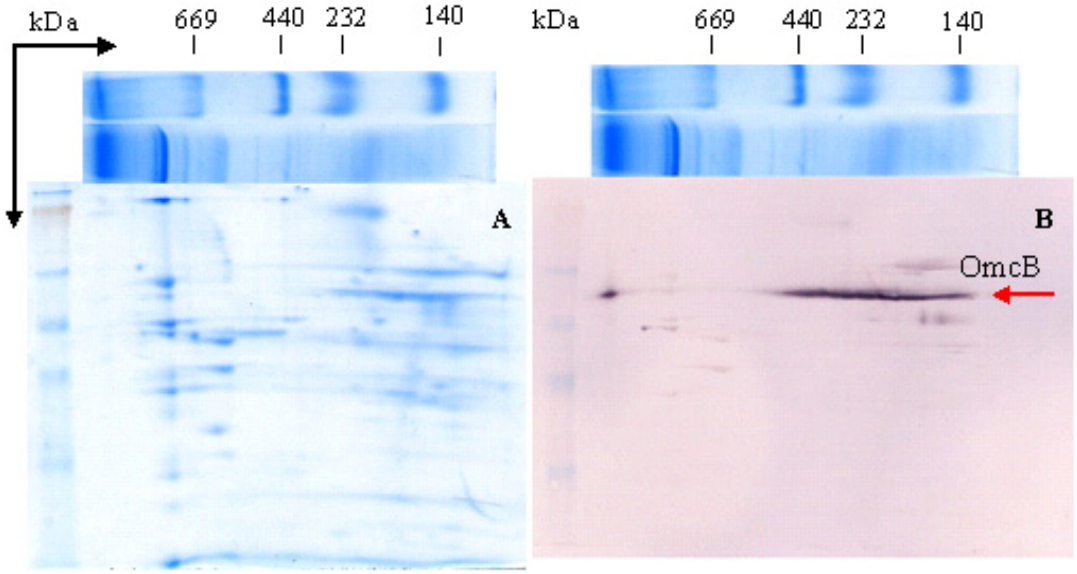

Fig. 3.1. Membrane protein complex components separated by 2-D BN/SDSPAGE. Two identical 2nd dimension SDS gels were run. One was followed with CBB staining for proteins (A) and the other was transferred to a nitrocellulose membrane and blotted with OmcB polyclonal antibodies (B). Separation of protein complexes in the 1st dimension of BN PAGE was shown on the top gel. Separation of complex components was shown on the lower gel. Black arrows indicate the direction of protein migration in the first (top) and second (lower) dimension, respectively. The red arrow indicates OmcB.

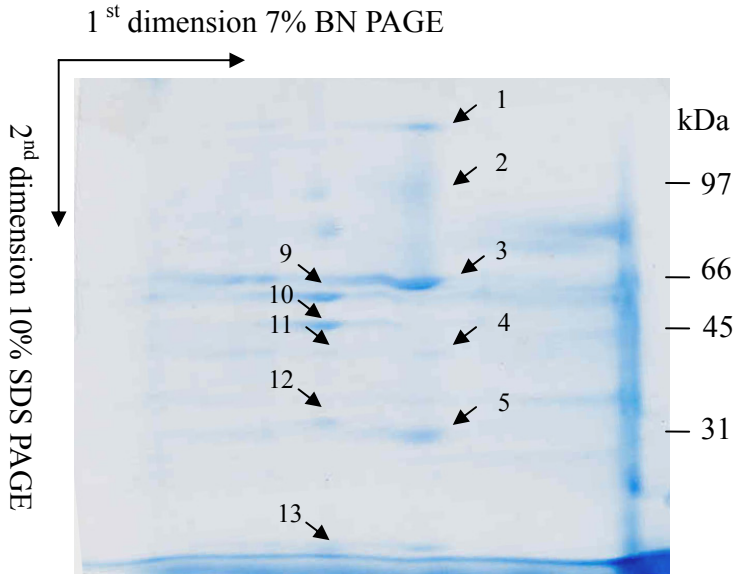

Fig. 3.2. Separation of components of wild type outer membrane protein complexes obtained from sucrose gradient centrifugation. The numbered protein spots were identified by MALDI/MS. Arrows indicate the migration of proteins in the first and second dimensions, respectively. Protein sample IDs are shown in the table.

Table 3.1. Proteins identified by MALDI/MS from 2-D BN/SDSPAGE from Fig. 3.2.

1	GSU1177 *frdA*, fumarate reductase, flavoprotein subunit
2	GSU1177 *frdA*, fumarate reductase, flavoprotein subunit
3	GSU1177 *frdA*, fumarate reductase, flavoprotein subunit
4	GSU0341, *nouD*, NADH dehydrogenase I D subunit
5	Gsu1178 *frdB*, fumarate reductase iron-sulfur protein
9	GSU0111 *atpA*, ATP synthase I
10	GSU 0113, *atpD*, ATPsynthase F_1 gamma subunit
11	GSU0341, *nouD*, NADH dehydrogenase I D subunit
12	GSU0112 *atpG*, ATP synthase F_1 gamma subunit
13	GSU0109 *atpF*, ATPsynthase F_0, B subunit

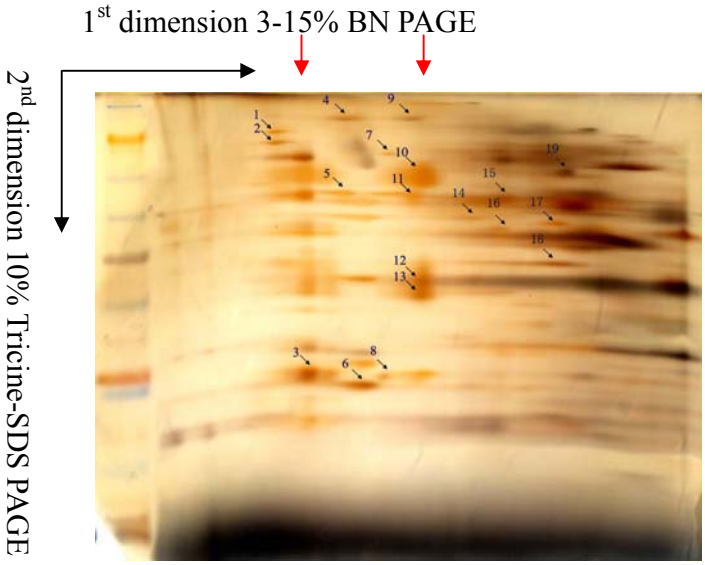

Fig. 3.3. The membrane protein complex components separated by 2nd dimension (SDSPAGE) and visualized by silver staining. The numbered protein spots are identified by MALDI/MS. Protein sample IDs are shown in the table. Typical protein complexes are indicated by red arrows. Black arrows indicate the migration of proteins in the first and second dimensions, respectively.

Table 3.2. Proteins identified by MALDI/MS from 2-D BN/SDSPAGE from Fig. 3.3.

1	carboxyl transferase domain protein
2	biotin-requiring enzyme subunit
3	NADH dehydrogenase I, B subunit
4	DNA-directed RNA polymerase beta
5	60 kDa chaperonin
6	ATP synthase F_0, B subunit
7	ATP-dependent protease
8	riboflavin synthase, beta
9	succinate dehydrogenase 70 kDa, and evidence of DNA-directed RNA polymerase
10	succinate dehydrogenase 70 kDa, and hypothetical protein GSU2090
11	glutamine synthetase type I
12	succinate dehydrogenase 27 kDa
13	succinate dehydrogenase 27 kDa
14	lamB porin family protein
15	bovine Serum Albumin, and *Geobacter* LamB porin family protein
16	enolase, and hypothetical GSU3403
17	outer membrane efflux protein
18	PPIC-type PPIASE domain protein
19	polyribonucleotide nucleotidyltransferase

Detection of proteins interacting with OmcS by co-immunoprecipitation

Since the application of 2-D BN/SDSPAGE has not been successful in separation of outer membrane complexes, another widely used method was tried: co-immunoprecipitation to determine protein-protein interaction. First, antib**o**dies were applied against OmcB and OmpB, the outer membrane cytochrome and multicopper protein, respectively. However, OmcB and OmpB antibodies were not raised against the properly folded holoproteins but against peptides, and showed relatively weak affinity for the native OmcB and OmpB as demonstrated by an enzyme-linked immunosorbent assay (ELISA) (data not shown). Consequently, the co-immunoprecipitation using these antibodies did not give any meaningful results.

Co-immunoprecipitation was tried again when antibodies raised against the purified outer membrane cytochrome, OmcS, were available, because the ELISA and TEM with immunogold labeling indicated a good affinity of this antibody for OmcS protein. Previous evidence (Mehta, 2005) and recent TEM studies (C. Leang, unpublished data) showed that OmcS is localized at the cell surface and/or in the cell surroundings and it can be easily sheared off from the cell surface. OmcS and proteins that interact with it are of great interest since OmcS is one of the few proteins found to be important in Fe(III) oxide reduction. Identification of the proteins that are interacting with OmcS on the outer surface of the cell would help to understand electron transfer to Fe(III). Therefore, the loosely bound cell surface protein fraction was used in a first attempt to identify proteins interacting with OmcS.

Probably due to the presence of lipo- and/or extracellular polysaccharides, the loosely bound cell surface protein fraction is very viscous, therefore separations using

spin columns or gravity flow columns are not feasible. However, protein G-coupled magnetic beads (Dynabead protein G, Invitrogen) provided effective separation conditions for the isolation of proteins interacting with OmcS.

As the first step, purified OmcS antibodies were crosslinked to Dynabeads protein G. Analysis of the antibody solution before and after incubation with beads did not reveal much difference on the gel in the amount of IgG (Fig. 3.4A, arrow A). After conjugation, antibodies were crosslinked to beads using BS^3. Crosslinking was confirmed by boiling the same volume of beads in buffer with reducing agent (dithiothreitol) before and after crosslinking and comparing the amounts of heavy and light chain protein released from beads. In Fig. 3.4, arrows B and C, corresponding to heavy and light chains, respectively, both showed a decrease in band intensity in the after-crosslinking fraction, which suggests successful crosslinking.

As a control, protein G Dynabeads without OmcS antibody crosslinking were incubated with the loosely bound cell surface protein fractions in the same way as OmcS-crosslinked Dynabeads protein G (results in Fig. 3.5A). The loosely bound surface protein fraction of the *omcS* deletion mutant strain was also incubated with OmcS antibody crosslinked to protein G Dynabeads under the same conditions as proteins from the wild type strain (results in Fig. 3.5B). No proteins from either control bound strongly enough to the beads or antibodies. No proteins were detected in the elution fractions by SDSPAGE with silver staining.

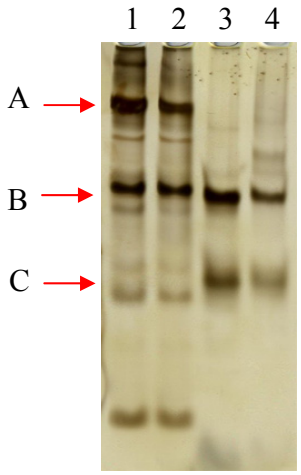

Fig. 3.4. Construction of antibody-crosslinked Dynabeads protein G. Lane 1, 10 µL of antibody diluted in WB buffer and lane 2, 10 µL of antibody diluted in WB buffer after incubation with Dynabeads were loaded. Lane 3 and 4, 10 µL of antibody-conjugated Dynabeads protein G before and after crosslinking were boiled with sample buffer containing reducing agent, and the supernatant, separated from beads by centrifugation, was loaded. Red arrows A, B and C indicate IgG, heavy chain and light chain, respectively.

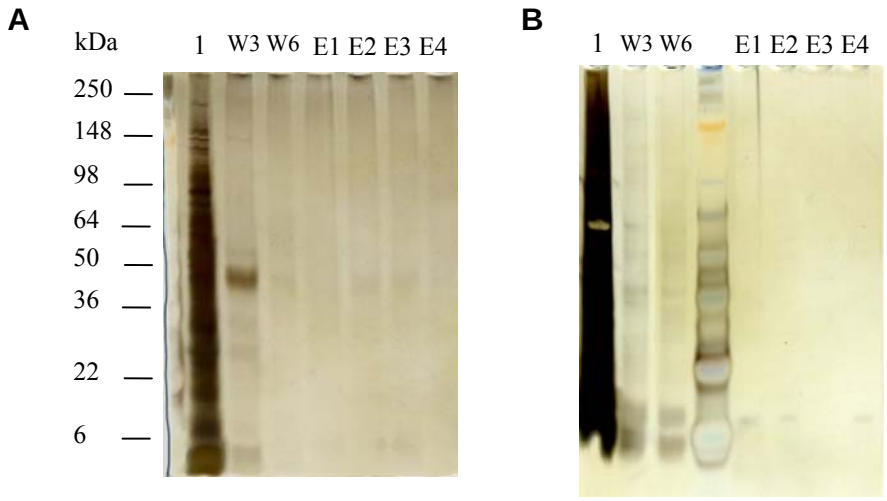

Fig. 3.5. Detection of nonspecific binding between sheared proteins from DL1 and non-antibody-conjugated Dynabeads protein (A), and sheared proteins from the *omcS* disruption mutant and antibody-crosslinked Dynabeads protein G (B). Lane 1, proteins not bound after incubation. W3 and W6, the 3rd and 6th wash with 200 µL PBS buffer after incubation. E1, 2, 3 and 4, the 1st to 4th elution with 20 µL elution buffer. Washed fractions were concentrated by centrifugation using Amicon spin columns with a 10 kDa cutoff membrane. Fractions were analyzed by SDSPAGE followed with silver staining. Volumes of washed and eluted fractions loaded on the gel were normalized to the fraction volume.

Co-immunoprecipitation with outer surface proteins of the wild type strain using OmcS antibody-crosslinked Dynabeads detected several proteins that interact with OmcS as shown in Fig. 3.12A. There are protein bands that appear only when the low pH elution buffer was applied, which may suggest a tighter interaction with OmcS (Fig. 3.6 band 1 and band 4). Only OmcS was observed in the last elution, indicating good specificity of the crosslinked antibody to its antigen. On the other hand, some protein bands were found in the mild washing buffer as well as in the elution buffer, such as bands 2, 5, 6, and 7 in Fig. 3.6, which may indicate a weaker association with OmcS. However, the intensity of all these bands increased in the elution fractions compared to those in the washing fraction, indicating that these proteins had true protein-protein interaction with OmcS. The proteins were identified with MALDI/MS and the results are summarized in Table 3.3. The identity and abundance of interacting proteins with available antibodies were further confirmed with Western blot analysis (Fig. 3.6C and D).

Among the identified proteins there are three *c*-type cytochromes including OmcS (Fig. 3.6B). One of the cytochromes identified is OmcZ (Fig. 3.6C), an extracellular matrix-associated cytochrome (Inoue, manuscript in preparation; Nevin, 2009). It is a very interesting finding that OmcZ interacts with OmcS, since OmcZ is the only cytochrome *c* that is necessary for electricity production but not for reduction of Fe(III) citrate or Fe(III) oxide (Nevin, 2009). Previous studies also suggested that OmcS is only required for Fe(III) oxide reduction (Mehta, 2005) but not for the reduction of soluble Fe(III) forms. Furthermore, the deletion of OmcS has an initial negative effect on electricity production, but cells adopt soon thereafter (Nevin, 2009). Recent results

from immunogold labeling of OmcZ and OmcS revealed that both *c*-type cytochromes are abundant in the biofilm structure (K. Inoue, unpublished data). Based on all these results, it is tempting to speculate that OmcS and OmcZ may function as individual electron sinks but are also connected in order to transfer electrons to different terminal electron acceptors. The dynamic in expression and function between these two cytochromes and the nature of their interaction require further investigation to understand their role in Fe(III) reduction and electricity production.

The other *c*-type cytochrome, GSU2887, identified from band 3 (Fig. 3.6B), was predicted to be a 92 kDa protein with 27 heme-binding motifs and extracellular localization. The deletion mutant of GSU2887 does not have a phenotype on soluble Fe(III) citrate (B. C. Kim, unpublished data) but further phenotype testing on insoluble Fe(III) oxide and electrode is recommended in order to elucidate further the role of this cytochrome.

Proteins other than *c*-type cytochromes were also found to interact with OmcS. One of the most interesting non-heme proteins is PilA (Fig.3.6D), the structural building block of the conductive pili of *G. sulfurreducens*, which has an important role in electricity production (Reguera, 2005). Recently it was discovered that deletion of the *pilA* gene inhibits the proper localization of outer surface cytochromes such as OmcS and OmcZ (Izallalen, 2008). While the total heme content of the cells and the mRNA levels of outer surface cytochromes are unchanged, the abundance of *c*-type cytochromes on the cell surface is decreased in the *pilA* deletion mutant. Izallalen *et al*. demonstrated that it is due to the failure to localize these cytochromes properly, as heme proteins were discovered to accumulate in the periplasmic space. This suggests

that PilA is part of a secretion system and may be required to transport cytochromes to their designated location. The relationship of PilA to the secretion systems of *G. sulfurreducens* and its role in outer surface cytochrome secretion require further studies.

Immunogold labeling TEM using OmcS-specific antibodies suggested that the OmcS protein attached to filaments and was localized along the length of the filaments (C. Leang, unpublished data). This localization can be observed best when an OmcS-overproducing strain (DL27, a GSU1240 gene deletion mutant strain) was used. The real identity of the filaments that were observed on the *G. sulfurreducens* cell surface by TEM is still unknown. PilA-specific antibodies do not bind to this filament; instead, PilA antibodies with immunogold labeling are observed on the cell surface. Further studies are necessary to investigate whether the PilA antibodies have a strong enough affinity to detect polymerized PilA. It is not yet clear whether PilA is capable of forming filaments under the circumstances tested, and whether the filaments to which OmcS is attached are made of PilA. A plausible hypothesis is that PilA may be involved in export of OmcS, and at the same time may assemble to form filament structures (C. Leang, personal communication). The fact that co-immunoprecipitation with OmcS-specific antibodies detected PilA makes this hypothesis more plausible (Fig. 3.6).

There are other non-heme proteins identified such as OmpB, the putative multicopper protein (Fig. 3.6A, band 2). Localization studies showed that OmpB is loosely attached to the outer surface (Mehta, 2006; Qian, 2007). Previous genetic studies showed that OmpB is involved in reduction of Fe(III) oxide (Mehta, 2006), but there is no further biochemical evidence to describe the nature of the involvement for

this copper protein. Other multicopper proteins with similar structures are redox proteins using oxygen as electron acceptor and oxidizing phenols and metals such as Fe(II) and Mn(II) (Claus, 2004). Therefore it is difficult to predict the role of OmpB in Fe(III) reduction and the mode of interaction of OmpB with OmcS or other cytochromes.

OmpJ, one of the most abundant proteins of the cell membrane (Afkar, 2005) was identified in the co-immunoprecipitate (Fig. 3.6 band 5). OmpJ is an outer membrane porin-like protein, which has no homologs outside the *Geobacteraceae* family. A deletion mutant lacking functional OmpJ had no ability to reduce Fe(III) oxides (Afkar, 2005). It is suggested that OmpJ is required to maintain the integrity of the periplasmic space to ensure proper folding and function of periplasmic and outer membrane electron transfer components (Afkar, 2005).

GSU0331, identified from band 5 (Fig. 3.6) was annotated as a protease containing a PDZ domain. It is predicted to be most likely a periplasmic protein. It is possible that this protease is responsible for the posttranslational modification of OmcZ. About one-third of the original length of OmcZ is removed from the C-terminus at the interface of periplasm and outer membrane, and the shorter version of OmcZ is found only on the outer surface of the cells (Inoue, manuscript in preparation). The reason and the significance of this posttranslational modification of OmcZ are unknown. The PDZ domain is a multifaceted protein binding domain. PDZ proteins bind sequence-specifically to C-terminal peptides, sometimes to internal peptides, and even to lipids (Fanning, 1996). PDZ domain proteins are often found to be cytoskeleton-associated and typically involved in the assembly of supramolecular

complexes that perform localized signaling functions at particular subcellular locations (Fanning, 1996; Sheng, 2001). Organization around a PDZ-based scaffold allows the stable localization of interacting proteins and enhances the rate and fidelity of signal transduction within the complex (Sheng, 2001). The identification of whether this protein is a true protease involved in the processing of OmcZ, or rather facilitates the assembly of OmcS containing protein complexes, would further help an understanding of extracellular electron transport.

GSU1855.4 (Fig 3.6. band 7), a protein of unknown function, also showed physical contact with OmcS. It has been found to be abundant in the culture medium, indicating that it is loosely bound to the cell surface. In spite of its abundance, its disruption mutant does not show any phenotype (H. Tran, unpublished data).

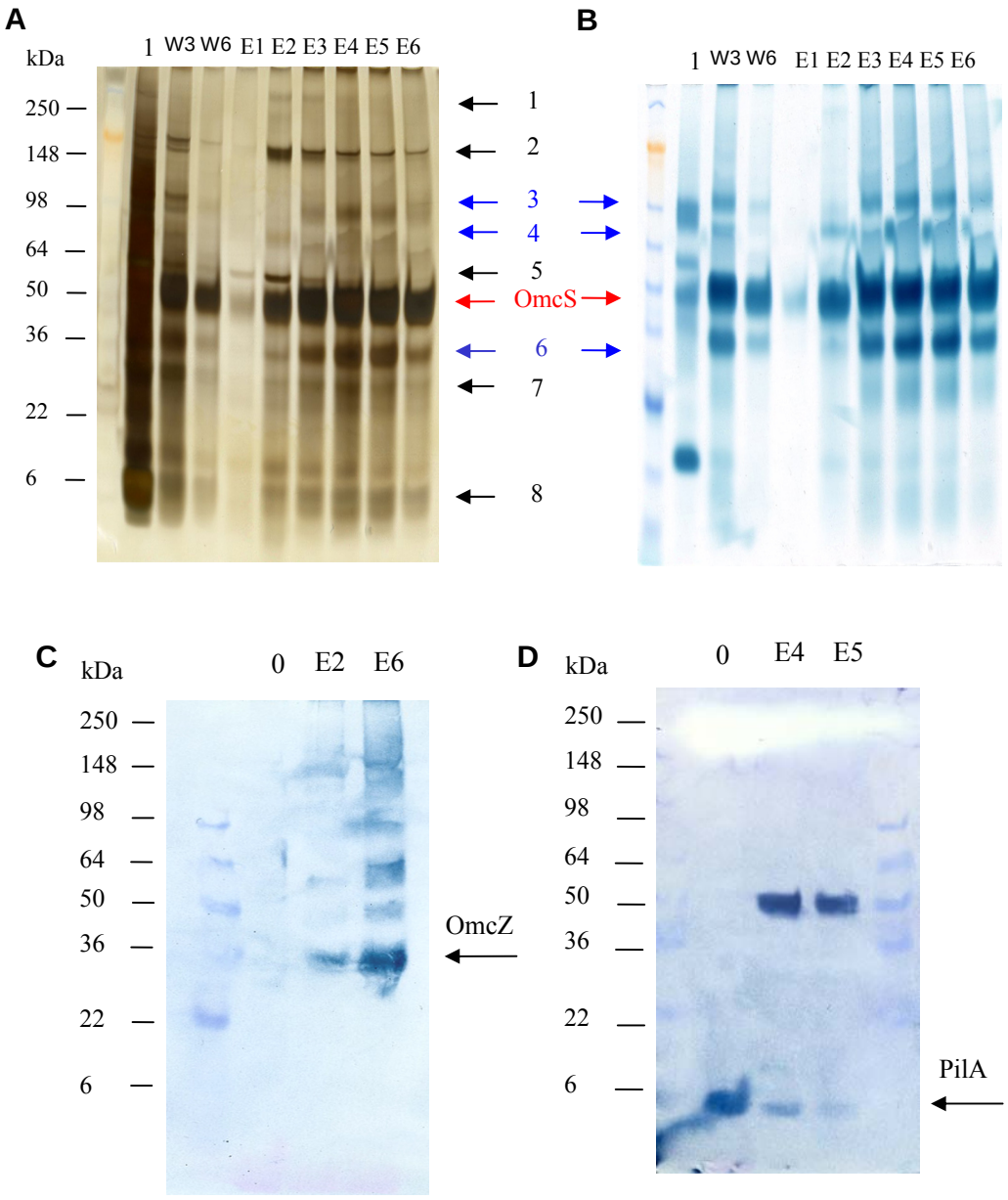

Fig. 3.6. Immunodetection of proteins interacting with OmcS. Proteins sheared from DL1 (lane 0) were incubated with antibody-crosslinked Dynabeads protein G. Unbound (lane 1) and nonspecifically bound proteins were washed from Dynabeads protein G by 200 µL of PBS buffer (lane W3, W6: the 3rd and 6th wash); specific bound proteins were eluted with 20 µL of elution buffer (lane E1-6, the 1st - 6th elution). Washed fractions

were concentrated by centrifugation using Amicon spin columns with a 10 kDa cutoff membrane. Fractions were analyzed by Tricine SDSPAGE followed with silver staining (A) and heme staining (B). Volumes of washed and eluted fractions loaded on the gel (A) and (B) were normalized to the fraction volume. Eluted fractions E2, E6 and E4, E5 were analyzed with sheared proteins from DL1 (lane 0 in panel C and D) by SDSPAGE followed with Western blot analysis using OmcZ (C) and PilA antibodies (D). The red arrow indicates OmcS. Blue and black arrows indicate cytochromes and non-cytochrome proteins that interact with OmcS, respectively. OmcZ and PilA were indicated by arrows in panels C and D, respectively.

Table 3.3. Proteins identified by MALDI/MS from OmcS co-IP from Fig. 3.6.

	GSU	Annotation	Size on gel (Da)	MW (Da)
1	NA[#]	NA	250,000	NA
2	GSU1394	OmpB, spore coat protein-related protein	150,000	139,476
3	GSU2504 GSU2887	OmcS, cytochrome c cytochrome c	100,000	45,360 92,184
4	NA	NA	70,000	NA
5	GSU0331 GSU3304	trypsin domain-PDZ domain protein OmpJ, LamB porin family protein	50,000	49,560 48,852
7	GSU1855.4 GSU0039	conserved hypothetical protein hypothetical protein	30,000	24,318 3,920
8	GSU1855.4	conserved hypothetical protein	6,000	24,318

NA[#]: not available. No significant signal was detected.

Implications

The attempts to separate membrane protein complexes by 2D BN/SDSPAGE showed that it is a method more suitable for separation of inner membrane protein complexes due to its milder separation conditions. Outer membrane proteins of *G. sulfurreducens* are more insoluble, tightly associated with the membrane structure, and require stronger treatment to be solubilized in order to be separated.

Co-IP using OmcS-specific antibodies is the first successful attempt to describe protein-protein interaction in *G. sulfurreducens*. It has shown the interaction of several proteins with known roles in Fe(III) reduction or electricity production. The discovery of OmcZ, the only *c*-type cytochrome that is required for electricity production, as one of the proteins that interacts with OmcS is the first evidence showing the possible interaction of two cytochromes with different functions. Further studies on their manner of interaction and of their biochemical differences may help us to understand better the reasons why these two cytochromes have different functions in *G. sulfurreducens*, and the significance of this interaction.

It was recently proposed that PilA may be part of a secretion system instead of functioning as structural component of pili. The finding that PilA interacts with OmcS and other evidence that PilA may be involved in outer membrane protein transportation makes this hypothesis more plausible.

The interaction of OmpB with OmcS furthers interest in the characterization of the involvement of OmpB in Fe(III) reduction, which could make this multicopper protein distinct from its homologs.

Furthermore, co-immunoprecipitation revealed the interaction with OmcS of

proteins that have not been studied yet and may be the targets of future studies.

CHAPTER 4

PURIFICATION AND CHARACTERIZATION OF OMCB, A *C*-TYPE CYTOCHROME INVOLVED IN FE(III) REDUCTION IN *GEOBACTER SULFURREDUCENS*

Abstract

Previous studies showed that OmcB is the only *c*-type cytochrome that is involved in the reduction of both soluble and insoluble Fe(III) in *Geobacter sulfurreducens*. Localization studies also confirmed that OmcB is embedded in the outer membrane but partially exposed to the cell surface. OmcB and potentially other surface exposed proteins are essential not only for the reduction of insoluble Fe(III) but for soluble Fe(III) reduction, indicating that OmcB may connect the periplasmic space and the cell surface in the extracellular electron transfer process of dissimilatory Fe(III) reduction. To understand better the distinct role that OmcB plays in Fe(III) reduction, purification and characterization of OmcB was performed. OmcB was purified from a gene deletion mutant of *omcC*, which shares 79% similarity of gene sequence. A two-step purification scheme has been developed, including the first separation of OmcB from other membrane proteins using preparative continuous SDSPAGE by size. This is followed by a purification step of anion exchange chromatography. Purified OmcB showed molecular mass and heme content consistent with the prediction from amino acid sequence without signal peptide and the numbers of putative heme-binding motifs, respectively. Purified OmcB showed typical UV-visible spectra of a reduced and oxidized *c*-type cytochrome. OmcB remained redox-active after the purification

procedure. It was readily reduced with dithionite and reoxidized by either Fe(III) citrate or Fe(III) oxide, which is consistent with its physiological role. The reaction of OmcB with the soluble Fe(III) citrate is much faster than that with the insoluble Fe(III) oxide. In order to characterize OmcB further for better understanding of its role in Fe(III) reduction, a different purification strategy, which will result in higher yield of pure OmcB, is needed.

Introduction

Microorganisms in the family *Geobacteraceae* are the most abundant Fe(III) reducers in many different subsurface environments, and they play an important role in degradation of organic compounds and bioremediation of toxic metals (Anderson, 2003; Ortiz-Bernad, 2004; Röling, 2001; Rooney-Varga, 1999; Sung, 2006). *Geobacter sulfurreducens* has been extensively studied as the first *Geobacter* species with a sequenced genome (Methe, 2003), a genetic manipulation system (Coppi, 2001) and an *in silico* genome-based metabolic model (Mahadevan, 2006). Progress is being made to understand dissimilatory Fe(III) reduction, an environmentally important process, but knowledge of its biochemistry remains limited.

Due to their electron transfer capability, *c*-type cytochromes are generally believed to play an important role in Fe(III) reduction in *G. sulfurreducens*. A search of the genome of *G. sulfurreducens* revealed that it contains more than 100 *c*-type cytochromes (Methe, 2003), and many of them are predicted to be membrane-associated. Previous studies revealed that there are several *c*-type cytochromes involved in Fe(III) reduction, such as OmcB (Leang, 2003), OmcE (Mehta, 2005), and OmcS (Mehta, 2005).

Genetic (Leang, 2003) and localization (Qian, 2007) studies demonstrated that OmcB is probably at the center of respiratory Fe(III) reduction as part of the electron transport network from the inner membrane to the cell surface in *G. sulfurreducens*. It is implicated that OmcB is involved in the reduction of soluble and insoluble Fe(III) by testing the growth of an *omcB* disruption mutant in cultures supplemented with sources of either soluble or insoluble Fe(III) (Leang, 2003). OmcB has been the only cytochrome so far to be implicated in the reduction of both forms of Fe(III). Moreover, localization studies showed that OmcB is embedded in the outer membrane, but a portion of it is surface-exposed (Qian, 2007), indicating the possibility that OmcB reacts with a periplasmic electron carrier such as PpcA and donates the received electron directly to Fe(III) or other surface *c*-type cytochromes such as OmcS.

Before the genome sequence was available, an outer membrane cytochrome *c* was purified and tested for *in vitro* Fe(III) reduction (Magnuson, 2001), of which characteristics showed similarities to those of OmcB. However, the genome sequence revealed the existence of a paralog, OmcC, which indicates that the purified outer membrane protein was a mixture of OmcB and OmcC (Leang, 2003). The disruption mutants of *omcB* and *omcC* were tested for Fe(III) reduction (Leang, 2003) and it was found that only the *omcB* mutant showed slower growth on either soluble or insoluble Fe(III).

The goal of this study was to purify and characterize the OmcC-free OmcB, which was made possible by using an *omcC* disruption mutant, and to (re)test its characteristics in order to understand better its role in the reduction of soluble and insoluble Fe(III).

Materials and methods

Bacterial strains and culture conditions

Wild type (DL1) and *omcC* mutant (DL5, *omcC*::*kan*) (Leang, 2003) strains of *G. sulfurreducens* are routinely maintained in our laboratory. These pure cultures were grown under strict anaerobic conditions as described previously (Coppi, 2001). Briefly, the growth medium consisted of a carbonate-buffered minimal medium with 20 mM acetate as the electron donor and 40 mM fumarate as the electron acceptor. Cultures were started with inocula that were 10% of the final volume. Cell growth was monitored by measuring the optical density spectrophotometrically at the wavelength of 600 nm (Genesys 2, Spectronic Instruments, Rochester, NY). Cultures were harvested at late exponential growth phase.

Membrane protein fraction preparation

OmcC deletion mutant (Leang, 2003) cells in their late exponential growth phase were harvested by centrifugation (4000 x *g* for 15 min at 4°C). The supernatants were concentrated 10-fold with a centrifugal filtration system equipped with a 10 kDa cutoff membrane (Millipore, MA). Cells from the cultures were disrupted by sonication (Sonic dismembrator F550; Fisher Scientific, PA) and cell debris was separated from cell lysate by centrifugation (8000 x *g* for 15 min at 4°C). The membrane proteins, cytoplasmic and periplasmic fractions were separated by ultracentrifugation at 257000 x *g* for 60 min at 4°C. Membrane proteins were resuspended in 50 mM Tris, pH 7.5, and kept at -20°C before purification.

Antibody production and purification

OmcB-specific polyclonal antibodies were raised against a peptide of OmcB (Kim, 2005). Cross-reacting antibodies were removed by immunoabsorption using proteins extracted with acetone from an OmcB-deficient mutant as described by Sambrook *et al*. (Sambrook, 1989), except that cells were disrupted by sonication and cell debris and unbroken cells were removed by centrifugation at 10000 x *g* for 10 min.

Western blot analysis

Proteins were separated by SDSPAGE on 10% acrylamide gels. Western blot analysis was performed by transferring the proteins to PVDF membranes. The membranes were probed with primary polyclonal antibodies followed with a secondary polyclonal alkaline phosphatase-conjugated anti-rabbit antibody (Sigma, MO). Western blot signals were visualized by staining with a SigmaFast^{TM} 5-bromo-4-chloro-3-indolyl phosphatase/nitroblue tetrazolium tablet (Sigma, MO).

Purification of OmcB

For purification of OmcB, *omcC* deletion mutant cells were cultured with acetate serving as the electron donor and fumarate as the electron acceptor. Cells were harvested at the late exponential growth phase where the cell density and OmcB production reached the highest level. Cells were separated by centrifugation at 6000 x *g* for 10 min and disrupted by sonication (Sonic dismembrator F550; Fisher Scientific, PA). Cell debris was removed by centrifugation at 8000 x *g* for 10 min at 4°C. Membrane protein fraction was prepared by separating the membrane proteins from soluble proteins with ultracentrifugation as described previously. As the starting

material for purification, membrane proteins were separated by size using continuous elution from a Tricine-SDS 7.5% acrylamide gel (28 mm diameter x 70 mm long) at 350 V constant voltage in a preparative PAGE cell equipped with a continuous cooling system. Protein was eluted at 1 mL min^{-1} and the fraction collection size was 4.0 mL. Fractions (one out of every ten) were concentrated and analyzed on a Tricine-SDS 10% acrylamide gel for protein and cytochrome content. Fractions containing a cytochrome *c* of the same size as OmcB were pooled and concentrated with an Amicon stir cell with a 30 kDa cutoff membrane (Millipore, MA). Further separation of OmcB was achieved by anion exchange chromatography (Q-sepharose, 1.5 cm diameter x 11 cm long), Amersham Bioscience, Switzerland) using fast protein liquid chromatography (FPLC) (Amersham Bioscience, Switzerland). Protein elution was achieved by step-wise increasing concentration of sodium chloride from 0 to 1 mM in 50 mM Tris, pH 8.0. The flow rate was 1 mL min^{-1} and fraction size was 2 mL. Collected fractions were analyzed by SDSPAGE followed by CBB staining and heme staining. Fractions containing OmcB were pooled together, concentrated and desalted with Amicon stir cells equipped with a 30 kDa cutoff membrane. Protein concentration was determined with the BCA protein analysis kit (Pierce, IL).The identity of the cytochrome was further tested with Western blot analysis using OmcB-specific antibodies.

Characterization of purified OmcB

Spectrometric analysis

UV-visible absorption spectra were acquired on a Cary 50 Bio UV-visible spectrophotometer (Australia) using a 1 mL quartz optical cell designed for anaerobic

reaction. Reduction of the sample was achieved by adding controlled amounts (in small increments) of a 10 mM solution of sodium dithionite until maximum reduction was achieved.

Redox-activity assay

OmcB was reduced with sodium dithionite prior to the assay. Changes in the spectrum of OmcB at wavelengths between 500 and 600 nm were recorded at intervals of 12 seconds after the addition of 1 mM Fe(III) citrate or Fe(III) oxide.

Molecular mass

The molecular mass of OmcB was determined by Sephadex 200 (1.8 x 92 cm) calibrated with protein standards (Sigma, MO) (cytochrome *c*, 12400; carbonic anhydrase, 29000; albumin, 66000; alcohol dehydrogenase, 150000; β-amylase, 200000) using FPLC (Amersham bioscience). The column was equilibrated and protein was eluted with 50 mM Tris, pH 7.5, containing 100 mM NaCl.

Heme quantification

Purified cytochromes were incubated with pyridine (2.1 M) and NaOH (75 mM) in aqueous solution at room temperature for 15 min. The reducing agent sodium dithionite and the oxidizing agent potassium ferricyanide were separately added in excess to half of the cytochrome pyridine solution, resulting in pyridine ferrohemochrome and pyridine ferrihemochrome. Heme content was determined using the absorption coefficient of 11.3 mM^{-1} cm^{-1} for the absorbance of pyridine ferrohemochrome minus the absorbance of pyridine ferrihemochrome at 550 nm (Field,

2000). Protein concentration was determined with the BCA protein analysis kit (Pierce, IL).

Results and discussion

Purification of OmcB

The purification of OmcB started from culturing of the *omcC* deletion mutant (Leang, 2003) in order to avoid the copurification of OmcB and OmcC, because OmcC has a similar predicted molecular mass and 79% gene sequence identity to OmcB (see Material and Methods Fig. 2.1). The membrane fraction was separated from whole cells as starting material for purification of OmcB based on the localization results indicating that OmcB is embedded in the outer membrane. FPLC was tried as a first step of purification to separate OmcB from other membrane proteins, but little enrichment of OmcB was achieved with any of the different chromatography methods tried, such as ion exchange, chromatofocusing, hydrophobic interaction and size exclusion (data not shown). The best result was obtained when OmcB was first separated from proteins with large size differences by continuous elution in preparative SDSPAGE. Fractions collected from preparative SDSPAGE were analyzed by analytical SDSPAGE followed with CBB and heme-specific staining for appropriate protein size and heme content (Fig. 4.1A and B). The presence of OmcB in the combined fractions was confirmed by Western blot analysis using affinity purified OmcB antibodies (data not shown). The OmcB-containing fractions were further purified by anion exchange chromatography. SDSPAGE analysis showed that OmcB was further separated from other proteins (Fig. 4.2). The identity of OmcB was again confirmed by Western blot analysis using affinity

purified OmcB antibodies (Fig. 4.2C). Fractions from multiple runs containing the purest OmcB were combined and desalted, and kept in 50 mM Tris, pH 7.5, for further characterization. The absorbance of purified OmcB at the wavelengths of 410 nm and 280 nm showed a ratio of 4.6, which represents the ratio between the peak absorbances of heme groups and protein, respectively. The purification procedure yielded very little purified OmcB (10 μg/L), which limited efforts for further characterization of OmcB.

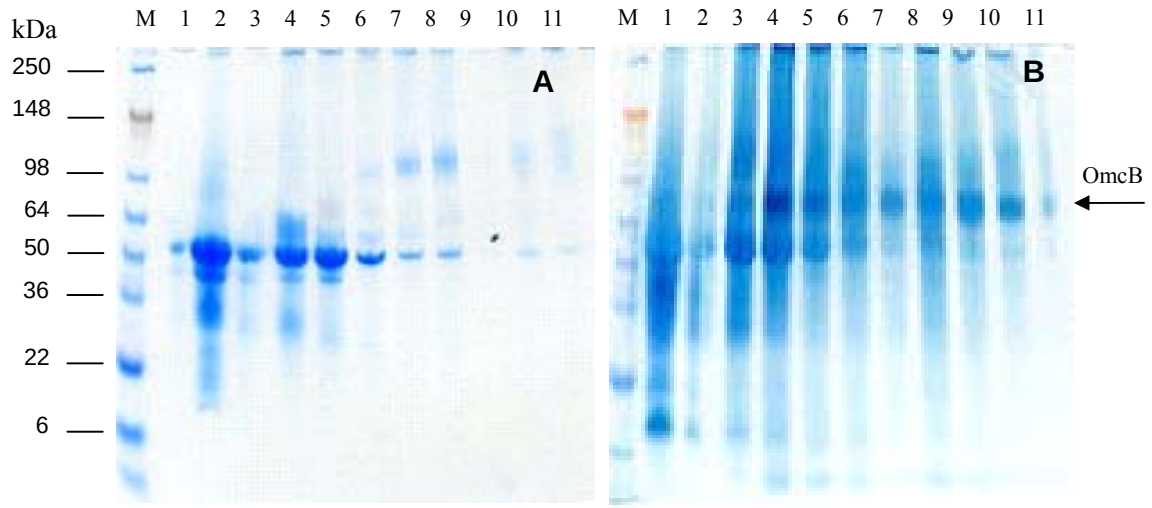

Fig. 4.1. Protein (**A**), and *c*-type cytochrome (**B**) analysis of preparative SDSPAGE fractions collected from a 7.5% acrylamide gel. The membrane fraction (20 mg) was applied to the gel. The separation conditions were as follows: Tricine-SDS 7.5 % acrylamide gel (28 mm x 70 mm), 350 V constant voltage under continuous cooling, 1 mL min^{-1} protein elution rate and 4.0 mL fraction volume. Fractions (one out of every ten) were concentrated and analyzed on a Tricine-SDS 10% acrylamide gel for protein and cytochrome content. The position of OmcB is indicated by the arrow.

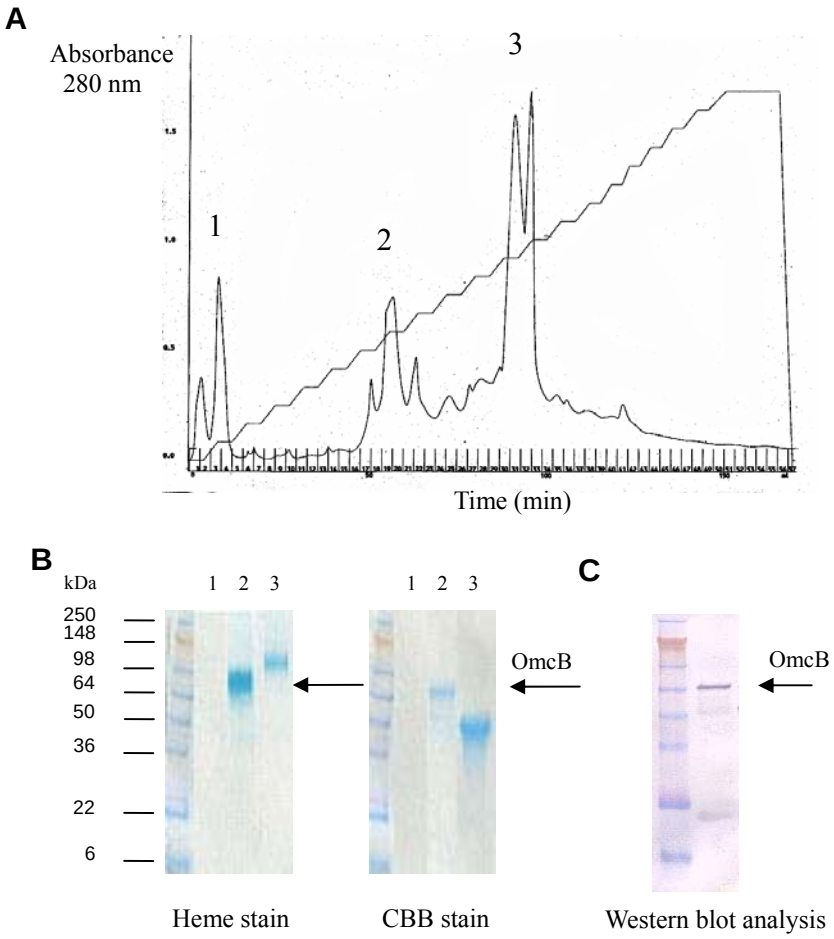

Fig. 4.2. FPLC profile (A), protein/*c*-type cytochrome profile (B) and Western blot analysis (C) of fractions from the anion exchange chromatography. Fractions from the previous Prep Cell run containing OmcB were concentrated and applied. The position of OmcB is indicated by the arrow.

Characterization of OmcB

Amino acid sequence of OmcS and predicted features

The *omcB* gene encodes a protein of 744 amino acids with a predicted signal

peptide of 23 amino acids (Leang, 2003). The first cysteine residue in the matured protein is a predicted lipid attachment site. The lack of aspartate residues downstream in the vicinity of that cysteine suggested that OmcB is an outer membrane protein. This prediction based on the amino acid sequence is in agreement with the result of the localization study (Qian, 2007).

MSRKVTKYSAVLAVSLFAAALAGCGSENKEGTVGTGPGGVATVGDSACVQCHSAVTEALTGESLIAQYQK
SSPHNTAGLGCESCHGGGAQHNGVGPIPFAQPDASRCADCHDGTTAVATNSDTAFAESRHNIQTIRSGAT
CRRCHTHEGAVLSNIAGYTGDLATLEDTVNQNKVPLVSSYSQISCATCHEHGGGLRTIKATNGAAGPVVN
WDPNNNRTVDQFDLCTSCHNMYSYNGSTLLTNGVPVNGVATGTVGHHETTWYRIIATTHFDNYSTGPQAG
AGASGTNAKVEGYVLRRTGANPCFDCHGHEAKTNTRPGRDATIHTDWAKSAHAGGLLTAKYNAVGALTGA
AAVNAAMNAYVDDTTAIAWTHYNWDASSRGSCQRCHTATGAANFMSNPAGYDPTGAGNSFSHLQGWSAAN
GSKQNELLYCWGCHTNAGTGELRNPGAITENYAGVNSTSTGTTGTAVTISYPDIAGSNVCMTCHLGREAG
ENIKAITDADGILGFVNSHYLAAGGQLFGKTGYEYATRSYAKPTFFAHDKIGTAAAPGTGTNGPCAGCHM
TTPNSHSFLPVTKDGTGAVTAITSTACATCHAGAYALTPEALTAEEEEYVASLEALKAALAGKGILFFNA
HPYFYRDTNANGIGDPGELVSSNAFTNWAGVYGLALWKDVMGAAFNANLLIHDPGGYAHNRFYVKRLIWD
SIDFIYDGVLNNDVTAAIDAQVTATRLDSATATAAKAYLGTTRP

Fig. 4.3. The amino acid sequence of OmcB (GSU2737). The predicted signal peptide is underlined. Predicted heme-binding motifs (CXXCH) are in red. The lipid attachment cysteine residue is in white.

Molecular mass and heme content

The predicted molecular mass of OmcB apoprotein is 77177.14 Da, while it is 74840.32 Da without the signal peptide. (http://ca.expasy.org/tools/pi_tool.html). When the molecular mass of twelve putative heme groups (616.5 Da each) is added (Zhu, 1996), the predicted size of OmcB without signal peptide is 82241.32 Da.

Experimental determination of the molecular mass of OmcB was first attempted by gel filtration using a Sephadex 200 column with comparison to standards of

appropriate molecular mass. The molecular mass of OmcB was calculated to be 380.2 kDa, which is most likely the result of the aggregation of purified OmcB, as CBB and heme-specific staining after SDSPAGE does not show the presence of other proteins. The addition of 0.05% zwittergent did not prevent the aggregation of OmcB. The molecular mass was calculated to be 82 kDa from the SDSPAGE when the relative motility of OmcB was compared to those of molecular mass standards. This calculated molecular mass is in agreement with the theoretical molecular mass of holoprotein without signal peptide.

The heme content of OmcB was determined using the pyridine hemochrome method. According to the measurements, one mole of OmcB contains 11.45 moles of heme. The heme content was somewhat lower than that predicted, probably due to some impurities in the preparation or the lack of precise determination of molecular mass.

UV-visible spectrum of purified OmcB

The optical absorption of the oxidized and reduced OmcB is shown in Fig. 4.4. During the purification procedure, OmcB was air-oxidized. However, it was readily reduced by the addition of dithionite and remained reduced under anaerobic conditions, indicating that OmcB preserved its redox-activity during purification. The oxidized OmcB showed the Soret (γ) peak at 409 nm. When reduced, the spectrum shows a shift resulting in a sharper and more intense Soret maximum at 419 nm. The oxidized OmcB had a wide peak at around 530 nm. When it was reduced, the α and β peaks appeared at 551 and 523 nm, respectively. The spectral profiles of the oxidized and reduced OmcB show the characteristics of a typical low-spin *c*-type cytochrome. However, EPR and

NMR spectroscopic studies are necessary to confirm the exact heme coordinations.

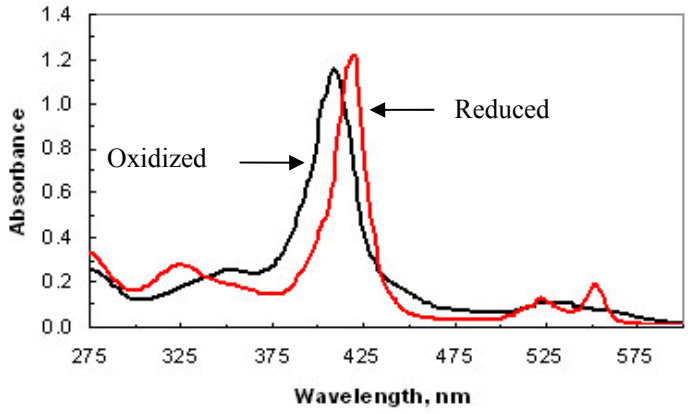

Fig. 4.4. UV-visible absorption spectra of purified OmcB in 50 mM Tris HCl, pH 7.5. The spectrum of air-oxidized OmcB is in black. Red traces correspond to the dithionite-reduced OmcB.

Redox-activity of OmcB

The redox-activity of OmcB was tested *in vitro* with Fe(III) citrate and Fe(III) oxide. OmcB was reduced by dithionite under anaerobic conditions by replacing air with nitrogen gas in an airtight cuvette. The reoxidation of OmcB was monitored at wavelengths between 500 and 600 nm. The addition of both substrates resulted in the oxidation of OmcB. However, Fe(III) citrate oxidized OmcB much faster and the oxidation was complete in a short period of time. Fe(III) oxide oxidized OmcB much more slowly and the oxidation never reached completion under the experimental conditions.

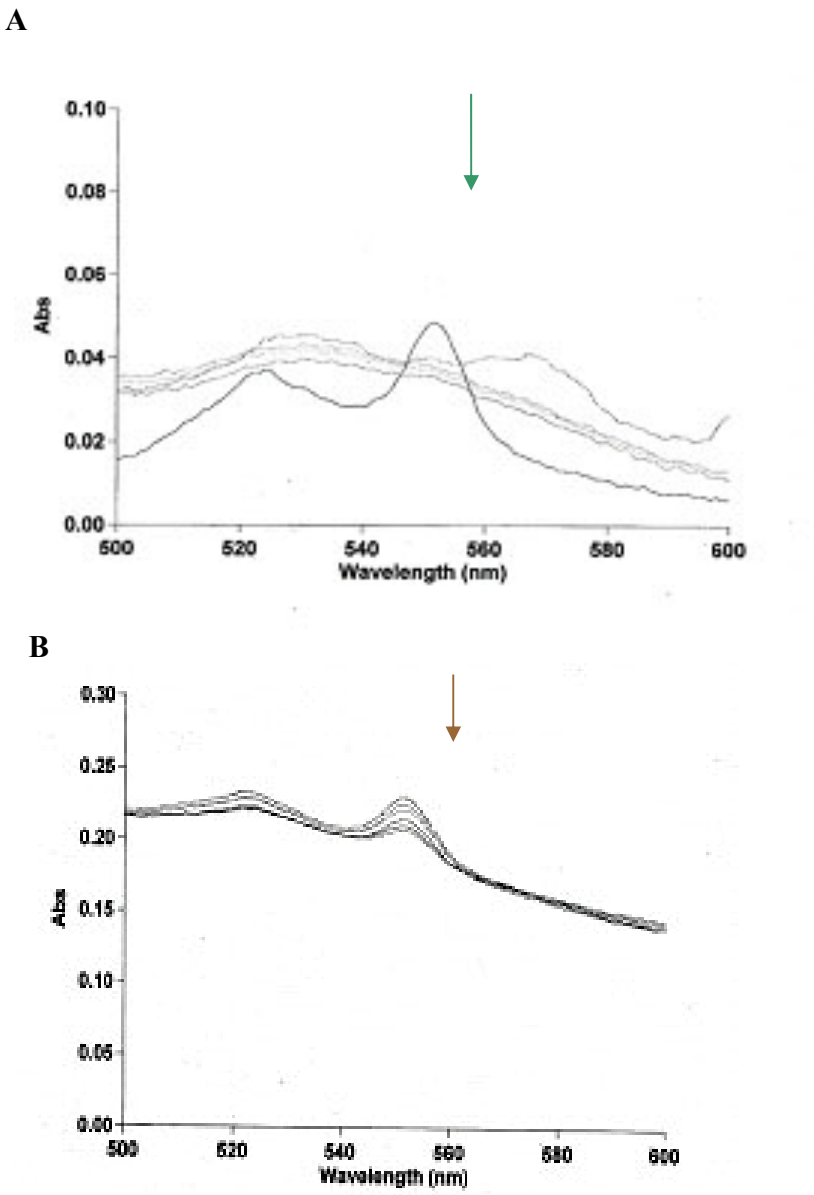

Fig. 4.5. Redox-activity of purified OmcB with potential electron acceptors. OmcB was reduced with dithionite prior to the reaction. Changes in the spectra of OmcB were recorded at intervals of 12 seconds after the addition of 1 mM Fe(III) citrate (A) and Fe(III) oxide (B). The arrow indicates the direction of the changes in the spectra.

Implications

In this study, it was possible to identify the molecular mass, heme content, and UV-visible spectroscopic profile of oxidized and reduced OmcB. Furthermore, it was possible to confirm that the purified OmcB is capable to reduce Fe(III) citrate and Fe(III) oxide *in vitro*. Further studies are necessary to yield more information on the biochemical characteristics of OmcB. However, the purification procedure is very inefficient for OmcB. Consequently, this strategy has not resulted in enough purified protein for further studies. Since an attempt has failed for heterologous overexpression of the holoprotein in *E. coli* (data not shown), an alternative strategy may be the construction of a homologous overexpression strain, as was done for another *c*-type cytochrome, OmcZ (Inoue, manuscript in preparation) or to search in our mutant collection for a strain which produces a higher amount of OmcB, as was done for the purification of OmcS.

CHAPTER 5

BIOCHEMICAL CHARACTERIZATION OF PURIFIED OMCS, A *C*-TYPE CYTOCHROME REQUIRED FOR INSOLUBLE FE(III) REDUCTION IN *GEOBACTER SULFURREDUCENS*

Abstract

Previous studies with *Geobacter sulfurreducens* demonstrated that deletion of the gene for OmcS, a loosely bound outer surface *c*-type cytochrome, inhibits Fe(III) oxide reduction and delays maximal current production in microbial fuel cells. These results and the outer surface localization of OmcS suggest that it could be involved in extracellular electron transfer to Fe(III) oxide and the electrode. Furthermore, the relatively high abundance of this cytochrome in the outer cell surface suggests that it could serve as a capacitor, accepting electrons and permitting continued respiration during periods when G. sulfurreducens is not in direct contact with electron acceptors.

In order to investigate these functions further, OmcS was purified from a GSU2215 gene deletion mutant, which overproduces OmcS. OmcS was purified from the loosely bound protein fraction and solubilized by detergent. Purified OmcS showed typical reduced and oxidized spectra of a *c*-type cytochrome and remains redox-active. Dithionite-reduced OmcS was able to transfer electrons to a variety of substrates of environmental importance. Purified OmcS was characterized to have a molecular mass of 47015 Da, and six low-spin *bis*-histidyl hexacoordinated heme groups. OmcS has a

low midpoint redox potential of -212 mV. A thermal stability test showed that the melting point of purified OmcS is in the range of 65-82°C. Circular dichroism spectroscopy showed that the secondary structure of purified OmcS was retained. The reduced OmcS was able to transfer electrons to several soluble and insoluble electron acceptors, including Fe(III) citrate and Fe(III) oxide. Stopped flow analysis revealed that OmcS has a ten-fold faster reaction rate with anthraquinone-2, 6-disulfonate (AQDS) (25.2 s^{-1}) than with Fe(III) citrate (2.9 s^{-1}).

Introduction

Members of the *Geobacteraceae* family are the predominant dissimilatory Fe(III) reducers in a diversity of subsurface environments where Fe(III) reduction is coupled with the metabolism of organic compounds and bioremediation of organic pollutants, radionuclides and toxic metals (Anderson, 2003; Bond, 2003 ; Bond, 2002; Lloyd, 2001; Ortiz-Bernad, 2004; Rooney-Varga, 1999; Sung, 2006). Previous studies have demonstrated that *Geobacter* species have to establish direct contact with insoluble Fe(III) oxide for dissimilatory Fe(III) reduction (Childers, 2002; Nevin, 2000; Nevin, 2002), in contrast to other species such as *Shewanella* and *Geothrix* species (Nevin, 2000; Nevin, 2002) that release compounds that act as electron shuttles between the cell surface and the Fe(III) oxides, as well as compounds that can solubilize Fe(III).

The role of *c*-type cytochromes in electron transfer to Fe(III) in *Geobacter* species has been proposed based on their well-established function as electron carrier proteins in general, on the number of genes encoding putative *c*-type cytochromes in *Geobacter* species (e.g. *Geobacter sulfurreducens* (Methe, 2003)) and genetic studies of *G. sulfurreducens* that have demonstrated their involvement in Fe(III) reduction (Butler,

2004; Kim, 2006; Kim, 2008; Kim, 2005; Leang, 2003; Lloyd, 2003; Mehta, 2005; Nevin, 2009).

The insolubility of Fe(III) oxide requires that electrons be transferred outside the cell and consequently cytochromes that are the most important proteins in electron transfer to Fe(III) oxides are located on the outer surface of the cell. There are two cytochromes, OmcE and OmcS, that were found to be loosely attached to the cell surface (Mehta, 2005). Genetic studies confirmed that they are involved in the reduction of insoluble Fe(III) but not soluble Fe(III) citrate (Mehta, 2005). Recently, OmcS was found to be one of the most abundant cytochromes when the proteome of Fe(III) oxide-grown cultures was compared to that of Fe(III) citrate-grown cultures, further supporting the importance of OmcS in Fe(III) oxide reduction (Ding, 2008).

In this study, OmcS was purified and characterized in order to shed light on its function in Fe(III) reduction. The selection of this cytochrome for further characterization was based on its localization, abundance, and exclusive function in the reduction of insoluble Fe(III), which indicates its potential significance in the last step(s) of electron transfer from *G. sulfurreducens* cells to Fe(III) oxide.

Materials and methods

Bacterial strains and culture conditions

The DLHT2215(Δ*GSU2215::kan*) (Tran, manuscript in preparation) mutant strain of *G. sulfurreducens* is routinely maintained in our laboratory. These pure cultures were grown under strict anaerobic conditions as described previously (Coppi, 2001). Briefly, the growth medium consisted of a carbonate-buffered minimal medium with 20 mM

acetate as the electron donor and 40 mM fumarate as the electron acceptor. Cultures of the DLHT2215 mutant strain were started with inoculation to 3% of final volume and cultured with 500 mL medium in 2 L bottles sitting horizontally. Cells were harvested after 5 days. The shallow cultures with larger glass surface promoted biofilm formation. OmcS production reached the maximum under these conditions.

Purification of OmcS

DLHT2215 mutant cells were harvested by centrifugation at 6000 x *g* and 4°C for 5 min, resuspended in 50 mM Tris, pH 7.5, and subjected to a shearing force for 2 min at a low setting in a commercially available blender (Mehta, 2005). Sheared outer surface proteins were separated from cell debris by centrifugation at 8000 x *g* for 10 min, and concentrated using Amicon stirred cells with a 30 kDa cutoff membrane (Millipore, MA). The sheared-off fraction was twice extracted with detergent by incubating with 5% SDS with stirring at room temperature for 20 min. The undissolved fraction was pelleted by centrifugation at 12000 x *g* for 20 min at 15°C, resuspended in 50 mM Tris, pH 7.5, and incubated in a 100°C water bath for 1 min followed with a 10 min centrifugation at 16100 x *g* and 4°C. Supernatant containing solubilized OmcS was collected. Excess SDS in the collected supernatant was removed using a Detergent-OUT SDS-300 spin column (GE Biosciences, MO). Buffer was exchanged using a Zeba desalt spin column (Pierce, IL). Purified protein was stored at -20°C.

OmcS quantification and extinction coefficient

The concentration of purified OmcS (OmcS standard) was determined with the BCA protein analysis kit (Pierce, IL). The absorbances of its absorption maxima were

recorded for both reduced and oxidized OmcS standards in a series of different concentrations. The value of the molar extinction coefficient was calculated as the slope of a straight line fitted to a graph of absorbance *vs*. protein concentration. The reduction of OmcS with dithionite was performed under anaerobic conditions in a cuvette sealed with rubber stopper. Concentrations of unknown samples were determined from spectrometric analysis using the extinction coefficient at 550 nm.

Molecular mass

The theoretical molecular mass of OmcS was calculated according to the amino acid composition (http://ca.expasy.org/tools/pi_tool.html). The molecular mass of OmcS was determined by ESI under denaturing conditions (Bruker Daltonics Esquire-LC Ion trap mass spectrometer, UMass Amherst Mass Spectrometry Center).

Heme quantification

Purified cytochromes were incubated with pyridine (2.1 M) and NaOH (75 mM) in aqueous solution at room temperature for 15 min. The reducing agent sodium dithionite and the oxidizing agent potassium ferricyanide were separately added in excess to half of the cytochrome pyridine solution, resulting in pyridine ferrohemochrome and pyridine ferrihemochrome. Heme content was determined using the absorption coefficient of 11.3 mM^{-1} cm^{-1} for the absorbance of pyridine ferrohemochrome minus the absorbance of pyridine ferrihemochrome at 550 nm (Field, 2000).

UV-visible spectroscopy

UV-visible absorption spectra were acquired on a Cary 50 Bio UV-visible spectrophotometer (Australia) or an Amersham Biosciences Ultrospec 2100pro spectrophotometer (Switzerland) using a quartz optical cell. Reduction of the sample was achieved by adding controlled amounts (small excess) of a solution of sodium dithionite.

Circular dichroism analysis

CD spectrum in far UV, near UV and visible region was carried out on 1 mg/ml sample at room temperature using a 0.01, 0.05 and 0.05 cm cell, respectively. The subtracted spectrum was converted to the mean residue ellipticity using the protein concentration (1 mg/ml), the path-length of the cell (0.01/0.05 cm) and the mean residue weight (105.5).

Thermal melting was done on a Jasco J-715 spectropolarimeter and a PTC-348WI temperature programmer. Temperature of the sample was controlled in a Peltier cell holder. The sample in 50 mM Tris, pH 7.5, was diluted to 0.2 mg mL^{-1} for thermal scanning at 220 nm. The 0.2 mg mL^{-1} sample was scanned at 30°C h^{-1}. The sample was also diluted to 0.5 mg mL^{-1} for a thermal scan at 401 nm. The scan rate was set at 20°C h^{-1}.

Stopped flow kinetics

Oxygen in all solutions was replaced with nitrogen. A solution of 2.6 μM purified OmcS in 50 mM Tris, pH 7.5, was fully reduced by adding sodium dithionite in small increments from a 2 M stock solution until full reduction was achieved. The reaction of

reduced OmcS in 50 mM Tris, pH 7.5, with substrates anthroquinone-2,6-disulphonate (AQDS) and Fe(III) citrate was monitored in a rapid-scanning monochromator (Olis, Inc, GA) with a 2 cm path length cell at 25°C with an interval of 0.016 s. The stopped flow apparatus was intensively washed with oxygen-free 50 mM Tris (pH 7.5) before each run in order to maintain anaerobic conditions. Oxidation of OmcS by substrates such as AQDS and Fe(III) citrate was studied by monitoring the absorbance change at 550 nm. Traces obtained were fitted to an analytic expression containing one exponential term by application of non-linear iterative regression based on a least squares criterion using the Sigma plot program. Theoretical curves were fitted to the experimental data with the Sigma plot program.

EPR and NMR spectroscopies

For the EPR and NMR studies, OmcS solutions were prepared in 32 mM sodium phosphate buffer with NaCl (100 mM final ionic strength) at pH 7. Reduction of the samples was achieved by first flushing out the air from the oxidized sample with argon and then adding controlled amounts (small excess) of a sodium dithionite solution to the EPR or NMR tube with a gas-tight syringe through the rubber cap. The EPR spectra were recorded with a Bruker EMX 6/1 spectrometer equipped with an Oxford Instruments ESR-900 continuous-flow helium cryostat in the following conditions: sample temperature, 4 K; microwave frequency, 9.65 GHz; microwave power, 0.6 mW; modulation amplitude, 5 G. All ^{1}H-1D NMR spectra were recorded at 400 MHz in a Bruker Avance III 400. Chemical shifts are reported in parts per million (ppm), relative to tetramethylsilane, and the proton spectra were calibrated using the water signal as internal reference. All spectra were acquired at 25°C, by collecting 64K data points to

cover a sweep width of 60 kHz, with 48k scans.

Determination of redox potential

Redox titrations of the purified form of OmcS were followed by visible spectroscopy inside an anaerobic glove box kept at < 1 ppm oxygen. Following the previously described procedure (Louro, 2001), protein solutions in 32 mM sodium phosphate buffer with NaCl (100 mM final ionic strength) at pH 7 and 298 K were used. Each redox titration was performed in both reductive and oxidative directions, using sodium dithionite and potassium ferricyanide solutions as reductant and oxidant, respectively. To ensure a good equilibrium between the redox centers and the working electrode, a mixture of the following redox mediators was added to the solution, all at approximately 1.5 μM final concentration: phenasine methosulphate, phenasine ethosulphate, gallocyanine, methylene blue, indigo tetrasulfonate, indigo trisulfonate, indigo disulfonate, 2-hydroxy-1,4-naphthoquinone, anthraquinone-2,6-disulfonate, anthraquinone-2-sulfonate, safranine 0, neutral red, benzyl viologen, diquat and methyl viologen. These mediators covered the potential range of -440 to +80 mV. The OmcS reduced fraction was determined by integrating the area of the α-band above the line connecting the flanking isosbestic points (543 and 562 nm in the reductive direction and 545 and 559 nm in the oxidative direction) to subtract the optical contribution of the redox mediators, as described previously (Paquetea, 2007).

Redox-activity assays

Various substrates were prepared in anaerobic 50 mM Tris (pH 7.5). An OmcS solution in the same buffer was also prepared, reaching the concentration of 0.3 μM.

OmcS was reduced by adding sodium dithionite in small increments from a 2 M stock solution until full reduction was achieved. The reduction and oxidation of OmcS were monitored by recording the change of absorbance spectra at wavelengths between 250 nm and 600 nm.

Results and discussion

Purification of OmcS

Purification of OmcS was started from strain DLHT2215, in which OmcS production is considerably higher than that of the wild type strain (Tran, manuscript in preparation). A previous study showed that OmcS was loosely attached to the outer surface and it can be sheared off from the cell surface by treating the cells with mild mechanical force in a Waring blender (Mehta, 2005). In the sheared fraction, OmcS was the major protein (Fig. 5.1A, lane 2) and the major *c*-type cytochrome (Fig. 5.1B, lane 2). At this point in the purification OmcS and other proteins were considerably insoluble in 50 mM Tris (pH 7.5) resulting in the precipitation of the proteins by centrifugation. The high insolubility made it impossible to purify OmcS by any column chromatography (data not shown). Even the addition of detergents such as zwittergent (1%) did not prevent precipitation of OmcS in the columns. As an alternative purification method, detergent extraction was used successfully. First, the addition of 5% SDS solubilized all the impurities, leaving purified OmcS in the precipitate. However, OmcS itself was not easily solubilized. Different strategies such as the use of different buffer systems, changing the pH of the buffers, and different detergents have been tried to improve the efficacy of solubilization. Solubilization of OmcS was only

achieved by submerging it into boiling water for 1 minute in the presence of a trace amount of SDS. This procedure resulted in the separation of a non-soluble clear or brownish viscous material, of which the chemical composition is uncertain, and the soluble OmcS. Solubilized OmcS was further purified from detergent and salt (Fig. 5.1, lane 3) by using a de-SDS and desalt column in order to avoid the interference of any detergent with further characterization studies. After removing the detergent in the final step of purification, additional protein bands have occurred in SDSPAGE gels, which can be stained by CBB and heme specific staining. The sizes of these bands were approximately equal to two- or three-fold that of OmcS. When reducing agent DTT was added to sample buffer, these bands either disappeared or their intensity greatly decreased (data not shown) indicating a slight polymerization of OmcS in the absence of a detergent.

Highly purified OmcS reached the absorbance ratio of 6.7 measured at the wavelengths of 410 nm and 280 nm for heme groups and protein, respectively. The typical yield of OmcS obtained from 1 L culture was 0.6 mg. Until further use, purified OmcS was kept in 50 mM Tris (pH 7.5) at –20°C. The cycle(s) of freezing and thawing did not affect the quality of OmcS.

In order to confirm that the purified cytochrome is OmcS, the protein band shown by CBB staining was cut and digested with trypsin for matrix-assisted laser desorption ionization (MALDI) mass spectrometry. The analysis confirmed its identity as OmcS (GSU2504) (data not shown).

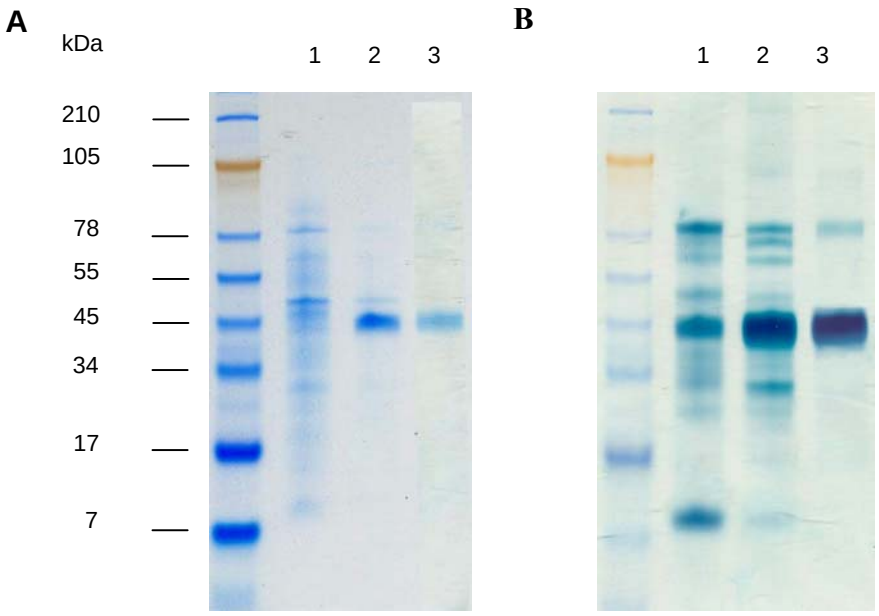

Fig. 5.1. Protein (A) and *c*-type cytochrome (B) profiles of samples from different purification steps. Lane 1, cell lysate of the DLHT2215 mutant; Lane 2, sheared-off fraction of the DLHT2215 mutant; Lane 3, purified OmcS. Protein amount of 3, 1.5 and 1 µg were loaded in lanes 1, 2, and 3, respectively.

Characterization of OmcS

Amino acid sequence of OmcS, and predicted features

The *omcS* gene (GSU2504) encodes a protein consisting of 432 amino acids. Various prediction programs such as SignalP and PSORT predict the presence of a signal peptide, which is 26 amino acids long, indicating that OmcS is secreted. There are also 6 CXXCH sequences, which is the typical heme-binding motif in *c*-type cytochromes. There are no predicted transmembrane helices in the amino acid system, indicating that OmcS is not an integral part of the cell membrane. The PSORT algorithm predicts that OmcS is an outer membrane protein.

MKKGMKVSLSVAAAALLMSAPAAFAFHSGGVAECEGCHTMHNSLGGAVMNSATAQFTTGPMLLQGATQSS
SCLNCHQHAGDTGPSSYHISTAEADMPAGTAPLQMTPGGDFGWVKKTYTWNVRGLNTSEGERKGHNIVAG
DYNYVADTTLTTAPGGTYPANQLHCSSCHDPHGKYRRFVDGSIATTGLPIKNSGSYQNSNDPTAWGAVGA
YRILGGTGYQPKSLSGSYAFANQVPAAVAPSTYNRTEATTQTRVAYGQGMSEWCANCHTDIHNSAYPTNL
RHPAGNGAKFGATIAGLYNSYKKSGDLTGTQASAYLSLAPFEEGTADYTVLKGHAKIDDTALTGADATSN
VNCLSCHRAHASGFDSMTRFNLAYEFTTIADASGNSIYGTDPNTSSLQGRSVNEMTAAYYGRTADKFAPY
QRALCNKCHAKD

Fig. 5.2. Amino acid sequence of OmcS (GSU2504). The predicted signal peptide is indicated by underlining. Predicted heme binding motifs (CXXCH) are marked red.

Molecular mass and heme content

The precise determination of the molecular mass of OmcS was not feasible by gel filtration because the protein tends to aggregate when any column chromatography is used, even in the presence of detergent. Gel filtration produced two not well-separated peaks with a molecular mass of 38 kDa and greater than 60 kDa (Table 5.1). For precise molecular mass determination, OmcS was subjected to electrospray ionization mass spectrometry (ESI-MS) under denaturing conditions. The molecular mass was determined as 47015 Da (Table 5.1). This number is very close to the predicted molecular mass of OmcS without signal peptide and with the addition of the molecular mass of six heme groups (3699 Da, 616.5 Da each) (Zhu, 1996). Under denaturing conditions during ESI-MS, heme groups are expected to remain attached to the apoproteins with their covalent bonds. This molecular mass determination does not support the hypothesis that OmcS is anchored by its signal peptide to the outer membrane (Mehta, 2005).

The similarity between the predicted and experimental molecular masses of holoprotein indicates that OmcS has six heme groups. To confirm further the number of

hemes per molecule of protein, the pyridine hemochrome assay was performed. The heme content was determined as 5.7 moles of heme per mole of protein, which is consistent with the predicted heme content.

Table 5.1. Molecular mass of OmcS determined by various methods

	Apoprotein (Da)	Holoprotein (Da)
Theoretical with signal peptide	45,389	49,088*
Theoretical without signal peptide	43,160	46,859*
Gel filtration	NA[#]	38,000
ESI-MS	NA	47,015

* The molecular weights masses of hemes (616.5 Da per heme) were added

Not available

UV-visible spectroscopy

The optical absorption spectra of OmcS are shown in Fig. 5.3. The oxidized form of OmcS has the Soret band at 406 nm and a band at 528 nm. Upon reduction with an excess of sodium dithionite, the reduced protein shows the Soret, β, and α bands at 417 nm, 520 nm and 550 nm, respectively. (The molar extinction coefficients of these peaks are summarized in Table 5.2.) This spectral pattern is typical of hexacoordinated low-spin hemes. In low-spin *c*-type cytochromes containing hemes with His-Met axial coordination, a small band at 695 nm can be detected in the oxidized form (Moore, 1990). Analysis of spectra of the ferricytochrome OmcS provided no evidence for the presence of a methionine as an axial ligand (see inset in Fig. 5.3).

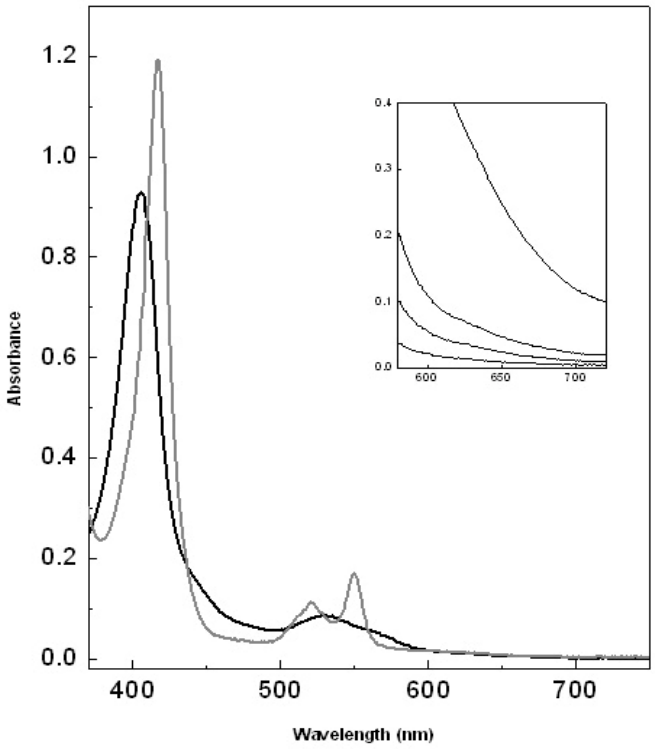

Fig. 5.3. UV-visible absorption spectra of OmcS. Black and gray lines correspond to the OmcS oxidized and reduced forms, respectively. In the inset are represented expansions of the region 580-720 nm of the oxidized spectrum of OmcS recorded with increased concentrations.

Table. 5.2. Molar extinction coefficient of OmcS at its absorption maxima

	(nm)	(M^{-1} cm^{-1})
Oxidized form	528	46000
	406	424400
	353	111200
Reduced form	550	107800
	520	67200
	417	487800

EPR and NMR spectroscopies

The combined use of EPR and NMR spectroscopies on OmcS samples aimed to elucidate the spin state of the hemes and their axial coordination. The EPR spectrum of OmcS in the oxidized form shows very intense signals with *g*-values of 2.94 and 2.25, which are characteristic of low-spin hexacoordinated heme groups with S=1/2 (Fig. 5.4). A very small signal at *g*-value 6.02, typical of high-spin hemes (S=5/2), was also detected. However, the intensity of this signal is extremely low, representing less than 1% of the total EPR heme signal intensity. This signal is in general observable even for low-spin heme proteins and represents a vestigial denaturation that occurs in the freezing of the EPR tube. The EPR spectrum of the reduced OmcS (data not shown) indicates that the spin state of the hemes is integer, however the distinction between spin-states S=0 or S=2 cannot be obtained from EPR. To elucidate this, ^{1}H-1D-NMR

spectra of both oxidized and reduced forms of OmcS were acquired (Fig. 5.5). High-spin heme groups typically have NMR signals above 40 ppm in the oxidized spectrum and above 15 ppm in the reduced spectrum (Bertini, 1986) This is clearly not the case for OmcS, for which signals are confined to the regions -3 to 35 ppm and -5 to 11 ppm, respectively, in the oxidized and reduced ^{1}H-NMR spectra (Fig. 5.5). Thus, from the NMR studies it can be concluded that all the OmcS heme groups are low-spin in both the oxidized (S=1/2) and reduced (S=0) forms. From the ^{1}H-1D-NMR OmcS reduced spectrum it can also be concluded that none of the heme groups is axially coordinated by a methionine residue. Indeed, axially methionine-coordinated hemes display a very well-defined pattern in the low-frequency region of the reduced ^{1}H-NMR spectrum that includes a three-proton intensity peak at approximately -3 ppm, and up to four resolved one-proton intensity peaks (McDonald, 1969; Moore, 1990). In the reduced spectrum of OmcS this pattern is clearly absent, which unequivocally shows that OmcS heme groups are not axially coordinated by a methionine residue.

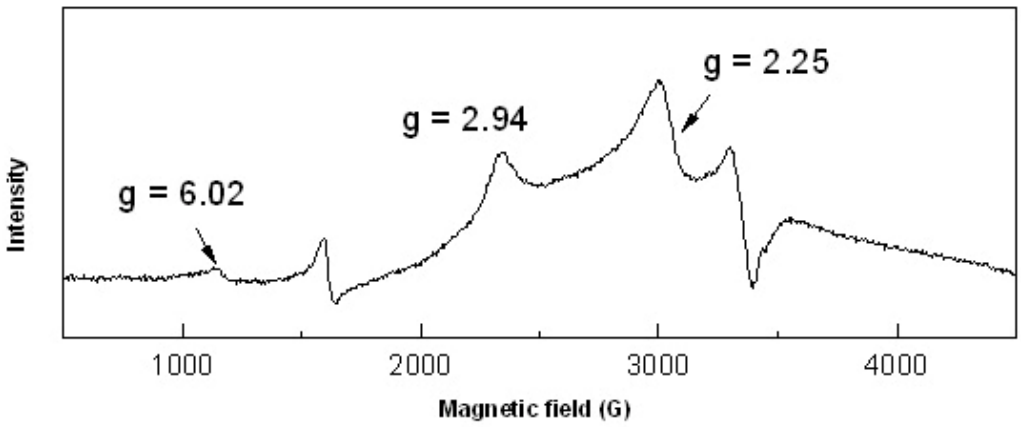

Fig. 5.4. EPR spectrum of the oxidized OmcS. The *g*-values for the heme signals are indicated by arrows.

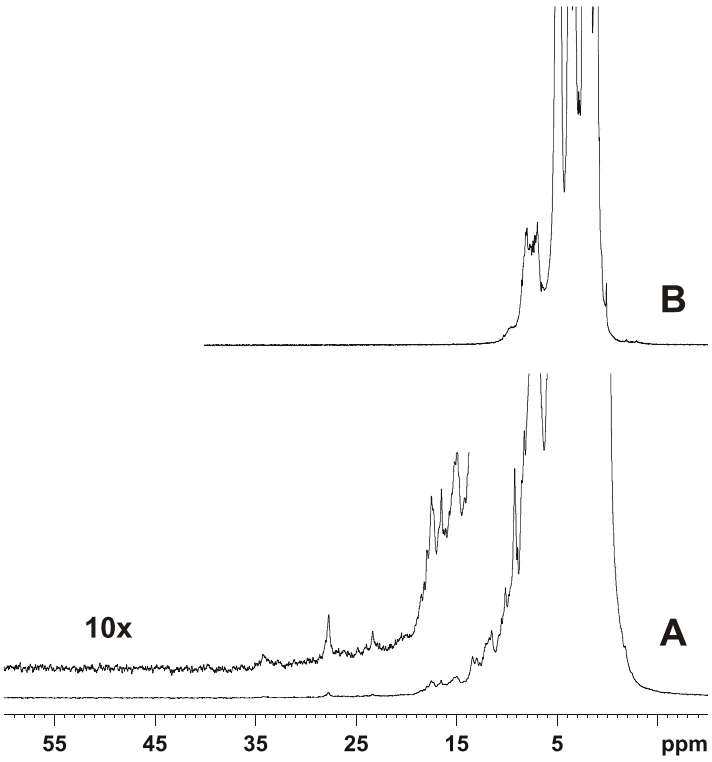

Fig. 5.5. Oxidized (A) and reduced (B) OmcS ^{1}H-1D NMR spectra. Expansion of the lower field region of the oxidized spectrum is shown in the inset.

Circular dichroism analysis

In order to elucidate further the structural features of OmcS, circular dichroism analysis was performed. The spectrum in the far UV region shows that OmcS contains~11 % helix, ~26 % anti-parallel and ~5 % parallel beta-sheet (Fig. 5.8). While the absorbance spectrum shows a single peak at 408 nm (Fig. 5.6), the CD spectrum is split into two peaks (400 and 426 nm), indicating that the chromophore is in two different structures. As shown in the HT[V] spectrum, the sample has one absorbance peak, indicating that the CD comes from chromophores of identical chemical structure. Thus, the split into two peaks implies that the chromophore is in different

environments.

The thermal stability of purified OmcS was also estimated from the CD spectra as a function of temperature at 220 nm and 401 nm to monitor secondary structure and heme environments. It appears that the CD signal at 220 nm first decreases at 52°C and then increases at 65°C. The HT[V] data show a gradual increase at 40°C, suggesting aggregation even before significant melting. Due to this aggregation, it is difficult to determine the end temperature of melting. In addition, aggregation makes the melting irreversible. As shown in Fig. 5.9, the CD intensity starts to decrease at ~65°C and ends at ~82°C, although the end temperature is difficult to determine because of aggregation for the same reason. Aggregation starts to occur around 45°C. By comparing the thermal scan of OmcS at 401 nm and 220 nm, a similar melting temperature can be observed, which indicates that secondary structure and heme environments undergo conformational changes simultaneously at 65-82°C (Fig. 5.10).

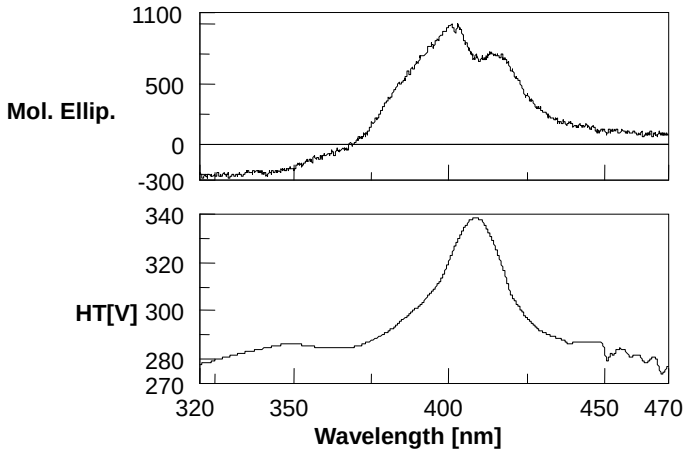

Fig. 5.6. Visible CD spectrum of OmcS.

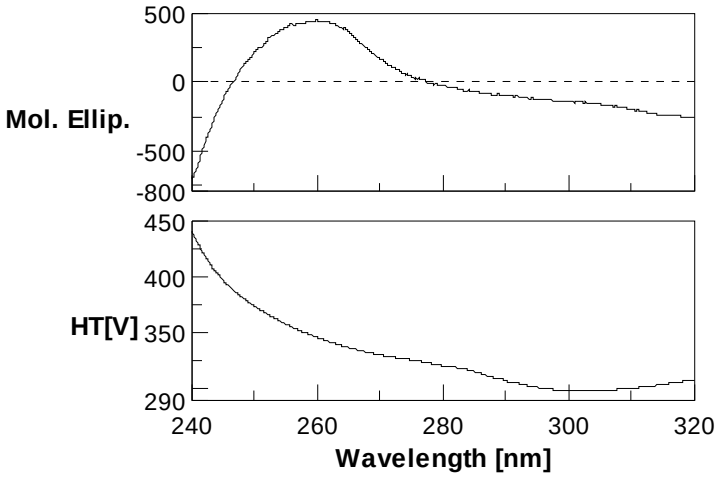

Fig. 5.7. Near UV CD spectrum of OmcS.

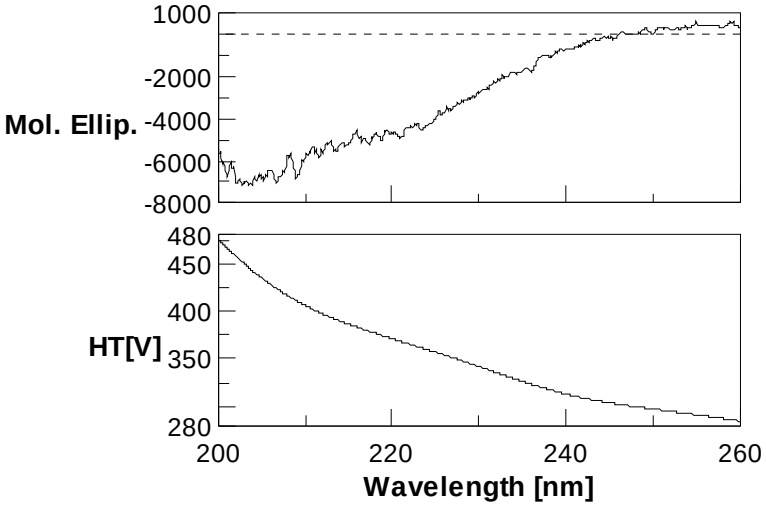

Fig. 5.8. Far UV CD spectrum of OmcS.

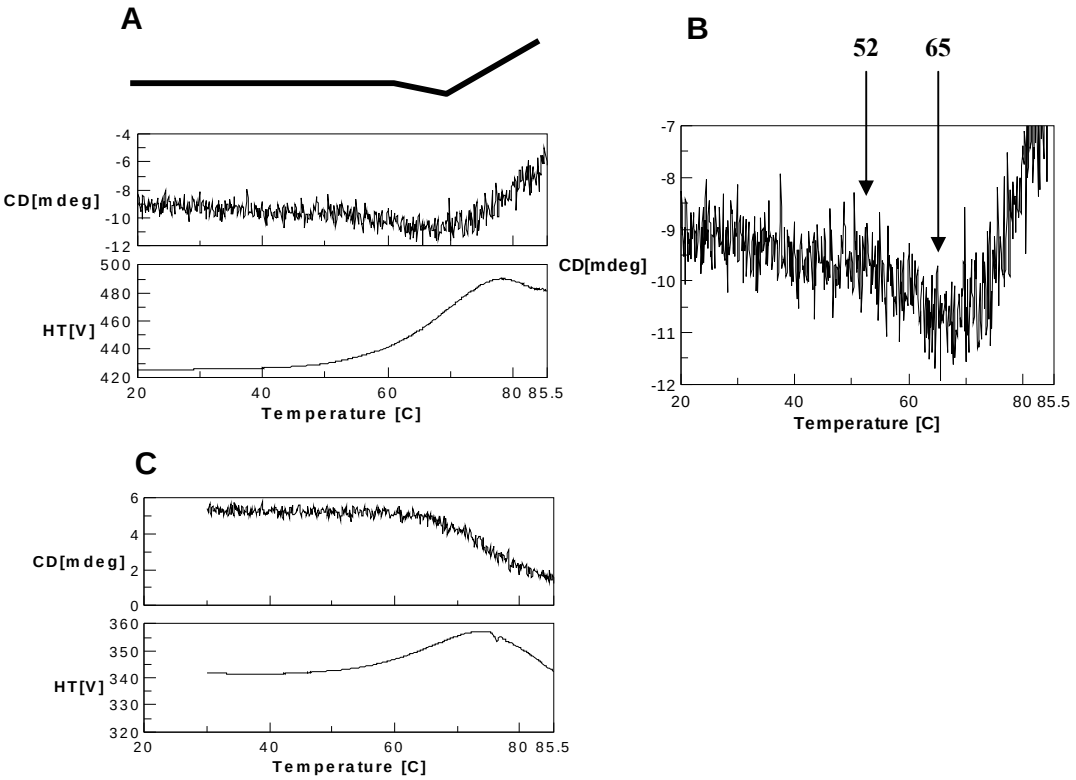

Fig. 5.9. Thermal melting of reduced OmcS. OmcS was diluted to 0.2 mg mL^{-1} for thermal scanning at 220 nm, 30°C h^{-1} (A). OmcS diluted to 0.5 mg m L^{-1} was scanned at 401 nm, 20°C h^{-1} (C). CD data of the scan at 220 nm were expanded in B.

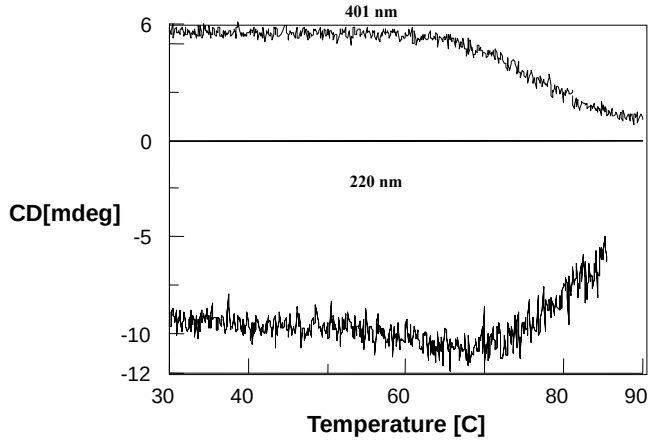

Fig. 5.10. Comparison of thermal melting of reduced OmcS at 0.5 mg mL^{-1} in Tris, pH 7.5, scanned at 401 nm and 220 nm, respectively.

Redox potential determination

The redox potential of OmcS was determined by electrochemical redox titration (Fig. 5.11). The reductive and oxidative curves are superimposable, indicating that under these experimental conditions the protein can cycle between the fully reduced and fully oxidized states reversibly. The E_{app} value (i.e., the point at which the oxidized and reduced fractions are equal) at pH 7 was determined to be -212 mV. The redox curve spans over a large range of reduction potentials (-360 to -40 mV) and the experimental points deviate from the n=1 Nernst curve shown in Fig. 5.11 (the dashed line). This observation points to a non-equivalence of the redox centers, which is expected for a multiredox center with six heme groups. The low reduction potential values covered by the OmcS redox curve are also compatible with *bis*-His axially coordinated heme groups (Moore, 1990).

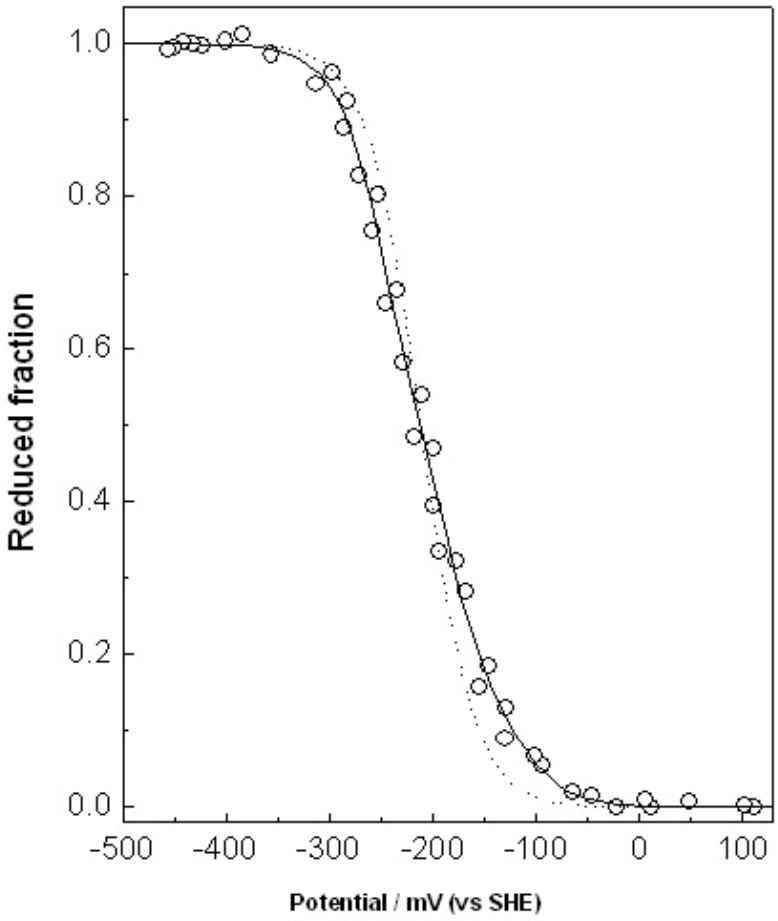

Fig. 5.11. Redox titrations followed by visible spectroscopy for OmcS at 298 K and pH 7. Experimental points are represented by open symbols and the continuous line indicates the fitting to a model considering six sequential one-electron Nernst equations. The dashed line represents a Nernst curve for one-electron reduction with -212 mV.

Redox-activity of OmcS

Geobacter sulfurreducens is able to reduce various metals and humic substances, which have relevance in biogeochemical redox cycles and environmental

bioremediation of toxic organic compounds and metals. The low midpoint redox potential of OmcS suggests that it can react with a wide range of substrates. The reducing capability of the purified OmcS was tested with a variety of soluble and insoluble electron acceptors, which may be the natural substrates of OmcS or have relevance to environmental bioremediation. The purified OmcS was reduced with dithionite in an airtight quartz cuvette under anaerobic conditions. The reduced state of OmcS was maintained for hours without adding any oxidizing agent. Various substrates (Table 5.3) were added under anaerobic conditions and the oxidation of OmcS was monitored at wavelengths between 500 and 600 nm by the disappearance of α and β bands, characteristics of reduced cytochromes (Fig. 5.12). All of the substrates tested were able to oxidize OmcS (Table 5.3). This experiment was only designed to test various substrates and was not suitable to assess the reactivity between substrates and OmcS. However, it was obvious that reactions with soluble substrates, with the exception of gold, were instantaneous while reactions with insoluble substrates were much slower. The permanent attachment of OmcS to Fe(III) oxide and gold was also observed. After the redox reaction, a portion of substrate and OmcS precipitated together to the bottom of the cuvette, significantly lowering the intensities of the absorbance of the Soret, α and β bands of OmcS. To identify whether this phenomenon is an artifact of the purification process or demonstrates the capability of OmcS to strongly bind to certain substrates requires further studies.

Table 5.3. List of substrates that can be reduced by OmcS

Soluble substrates	**Significance**	**References**
Fe(III) citrate	Model substrate for chelated Fe(III)	Coccavo, 1994
U(VI)	Environmental bioremediation biological uranium ore formation	Lovley, 1991 Lovley, 1992
Cr(VI)	Environmental bioremediation	Lovley, 1993
Au(VI)	Biological gold ore formation	Lovley, 1993 Lovley, 1993 Kashefi, 2001
AQDS	Model compound for humics	Lovley, 1996
Insoluble substrates	**Significance**	**References**
Fe(III) Oxide	Most abundant Fe(III) source in subsurface environment, biological magnetite formation, geochemical iron redox cycle	Coccavo, 1994 Lovley, 1987 Lovley, 2004
Mn(IV) Oxides	Geochemical manganese redox cycle	Lovely, 1988 Lovley, 1995 Lovley, 2004
Humic substances	Natural substrate and redox mediator	Lovley, 1996

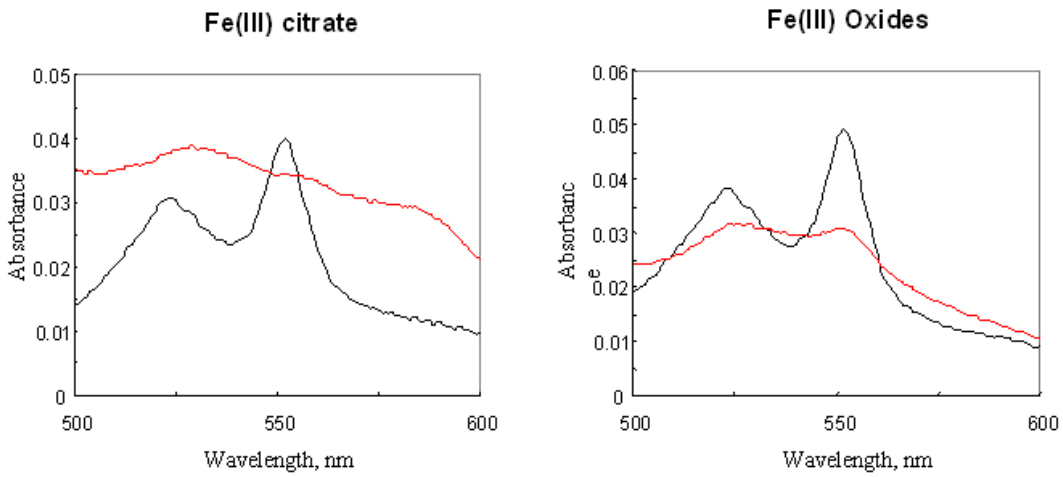

Fig. 5.12. Typical examples for the reoxidation of OmcS by a soluble [(Fe(III) citrate] and an insoluble [Fe(III) oxide] substrate monitored at wavelengths between 500 and 600 nm. Reduced and oxidized OmcS were represented by black and red line, respectively.

Stopped flow kinetics

Because the reducing substrate of OmcS is yet unknown, native kinetic reactions could not be studied. However, to shed light on the possible redox reactions in which it may be involved, OmcS was reacted with potential physiological substrates and monitored using stopped flow techniques. Fe(III) citrate and anthraquinone-2,6-disulfonate (AQDS) were used in these experiments as models for chelated metals and humic substances, respectively. These compounds were demonstrated to be terminal electron acceptors in the respiration of *G. sulfurreducens* (Caccavo, 1994; Lovley, 1996). OmcS was reduced prior to the stopped flow experiment and showed high stability. Series of concentrations of Fe(III) citrate and

AQDS were selected to be consistent with pseudo-first-order conditions. All the stopped flow experiments were performed under anaerobic conditions.

After rapid mixing of reduced OmcS and the substrate, a rapid equilibrium is assumed to be reached due to the large excess amount of substrate, and the electron transfer to substrate is irreversible:

$$OmcS_{red} + substrate_{ox} \overset{K_d}{\rightleftharpoons} OmcS_{red} \cdots substrate_{ox} \overset{k}{\longrightarrow} OmcS_{ox} + substrate_{red}$$

The oxidation of OmcS was monitored through itsα-band absorption, between 500 and 600 nm (Fig. 5.13). There was no substrate interference in the absorbance with OmcS oxidation in this interval. The reaction rates were calculated based on the rate of disappearance of the band at 550 nm, attributed to $OmcS_{red}$, (Fig. 5.13 insets). The traces obtained were fitted with a single exponential equation ($A=A_0e^{(-kt)}$) in order to obtain the observed reaction rate k_{obs}.

When the observed rate constants were plotted as the function of the substrate concentration, hyperbolic dependence of rate constants was observed for both substrates (Fig. 5.14). This indicates that the reduction of these substrates is the result of a reaction that consists of more than one step. The kinetic parameters were calculated by fitting the plotted k_{obs} data versus the corresponding substrate concentrations in Fig. 5.14 with the Michaelis-Menten equation (Table 5.4). The rate constant k for AQDS reduction is ten-fold higher than that of Fe(III) citrate reduction. The dissociation constants (K_d) for both substrates showed much less difference.

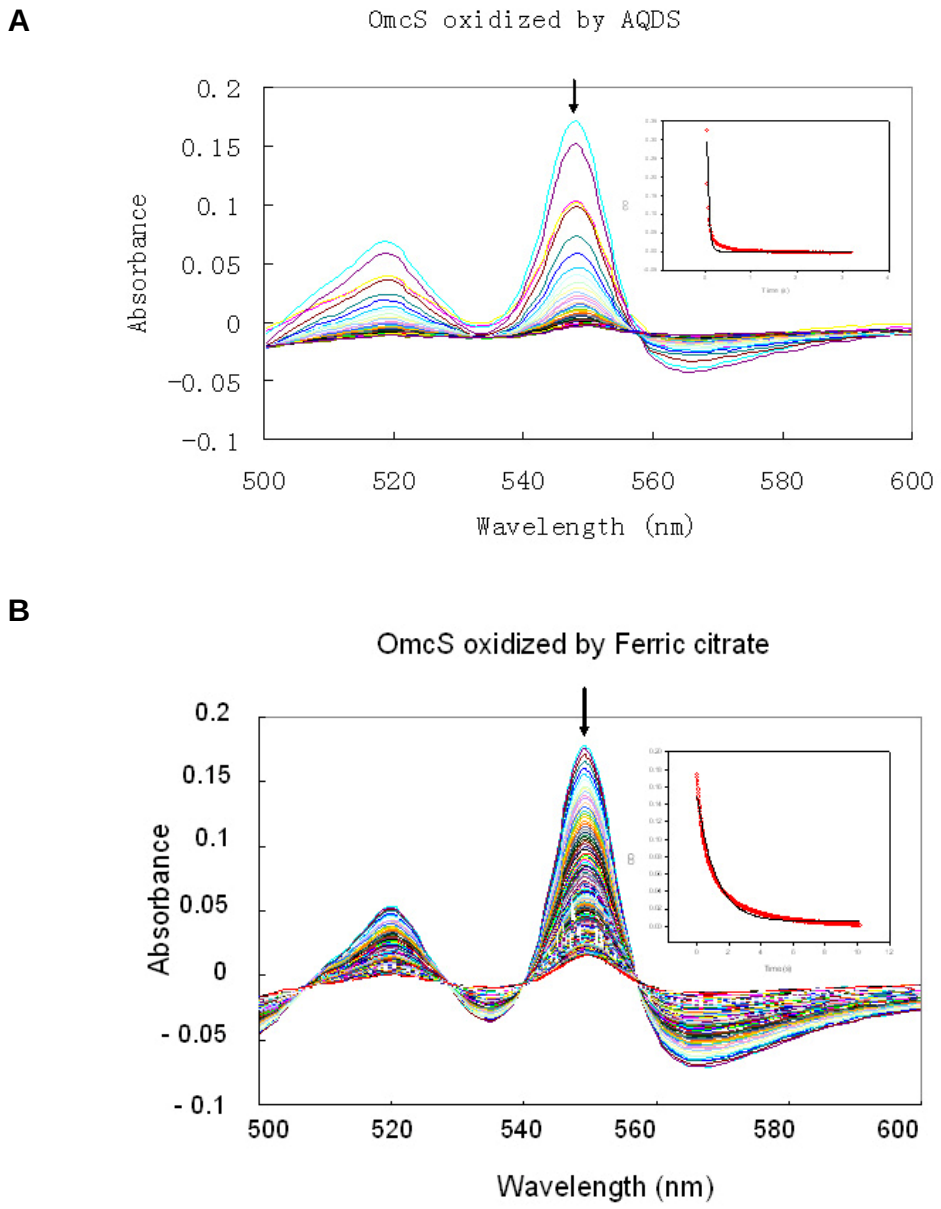

Fig. 5.13. Representative visible absorption spectra of OmcS after rapid mixing with substrates AQDS (A) and ferric citrate (B). Arrows indicate the direction of the changes in the spectra. Traces obtained at 550 nm were fitted with a single exponential decay equation $A=A_0e^{(-kt)}$ by Sigma plot as shown in insets (traces are in red, black continuous lines are fitted curves).

When the observed rate constants were plotted as the function of the substrate concentration, hyperbolic dependence of rate constants was observed for both substrates (Fig. 5.14). This indicates that the reduction of these substrates is the result of a reaction that consists of more than one step. The kinetic parameters were calculated by fitting the plotted k_{obs} data versus the corresponding substrate concentrations in Fig. 5.14 with the Michaelis-Menten equation $k_{obs}=k/(1+K_d/[S])$ (Table 5.4). The rate constant k for AQDS reduction is ten-fold higher than that of Fe(III) citrate reduction. The dissociation constants (K_d) for both substrates showed much less difference.

Table 5.4. Pre-steady state kinetic parameters for oxidization of reduced OmcS by substrates

substrate	V_{max} (s^{-1})(SD)	K_d (μM)(SD)
AQDS	25.2 (2.0)	194 (44.4)
Fe^{3+}	2.9 (0.2)	246 (43.0)

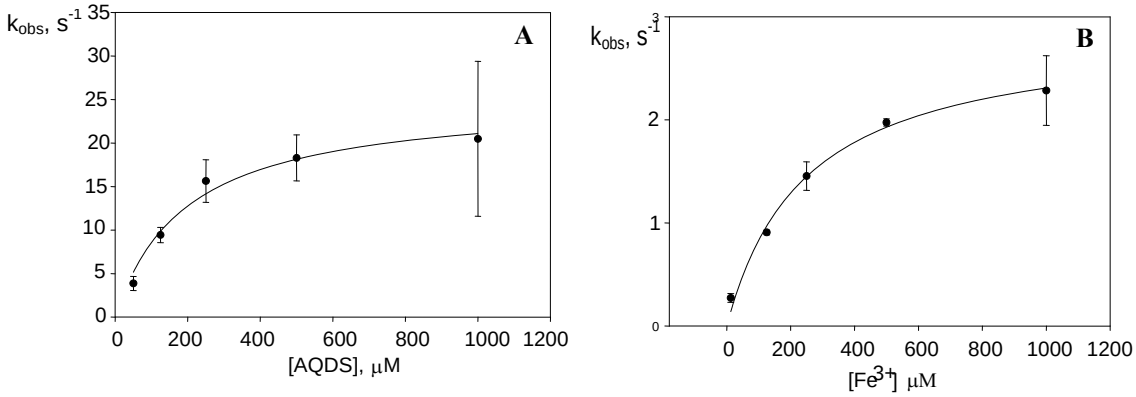

Fig. 5.14. Dependence of the pseudo-first-order rate constants of oxidization of reduced OmcS on the concentration of AQDS (A) and Ferric citrate (B). Each data point represents the mean value of at least three determinations in a single experiment. The continuous line represents the fitting of experimental data using the equation of $k_{obs}=k/(1+K_d/[S])$.

Bacterial multiheme cytochromes have a relatively low redox potential (Moore, 1990), which is required for the reduction of a wide range of redox partners. The reducing capability of OmcS has been confirmed by testing substrates such as Fe(III), Mn(IV), U(IV), and AQDS. When OmcS was incubated with various soluble or insoluble potential physiological redox partners, soluble substrates were reduced significantly faster than insoluble substrates. This transient state kinetic study demonstrated that the rate of soluble substrate reduction could also differ and show as high as ten-fold difference. If this difference in rate constants is attributed to the difference in redox potentials of the two substrates, an opposite trend would have been observed, because Fe(III) citrate has a more positive redox potential (-14 mV) (Wang, 2008) than that of AQDS (- 184 mV) (Hernandez, 2001).

By examineing the traces of OmcS reduction with Fe(III) citrate or AQDS, it can be observed that the two traces are somewhat different (Fig. 5.13, insets). While the oxidation of OmcS by Fe(III) citrate occurs more gradually, the oxidation of OmcS by AQDS can be divided into two phases, starting with a faster initial phase and ending with a slower phase. This two-phase, pre-steady-state kinetic pattern was proposed for *Shewanella*'s outer membrane cytochromes, MtrC and OmcA, using Fe(III) chelated with citrate, EDTA, or NTA (Wang, 2008). Using the equation $A=A_0e^{-k_1t}+A_0e^{-k_2t}$, consistent with a two-phase reaction in order to fit the OmcS oxidation traces, the result is statistically equally good fitting for traces of OmcS oxidation by AQDS, but not for Fe(III) citrate, as those obtained with the single exponential fits. If the k_1 and k_2 obtained for AQDS were plotted versus substrate concentration, the fast and slow process also shows hyperbolic dependency of the concentration of the redox partner, resulting in the rate constants of 50.7 s^{-1} and 3.6 s^{-1}, respectively. The dissociation constants for the fast and slow phases were determined as 121 μM and 106 μM for AQDS, respectively.

The Physical, (electro)chemical, and kinetic characteristics of OmcS that were identified do not explain either the one-phase or two-phase model of OmcS oxidation by AQDS. OmcS contains six hemes, which might cluster into two or more distinct or overlapping groups separated by redox potentials or different amino acid environments, as observed in other cytochromes (Hartshorne, 2007; Wigginton, 2007). In this case, the redox partners could react with two groups of hemes with different redox potential, resulting in a slower and a faster reaction. The only indication of two potentially different clusters of heme groups present in OmcS comes from the CD spectrum at

visible wavelength by detecting a split peak, which may indicate different heme environments. In order to confirm this possibility, more structural studies are required.

The biphasic behavior may also be explained by the presence of two or multiple reaction sites with different accessibilities to the redox centers. The conformation of cytochromes may be altered by the degree of oxidation within one molecule (Leys, 2002), resulting in an initial fast and a subsequent slow reaction as the oxidation of cytochromes progresses, as was observed in the case of cytochrome P450 (Inouye, 2000). That explanation would be more consistent with the different transient state kinetic patterns of OmcS oxidation with the two very different redox partners such as Fe(III) citrate and AQDS, which may bind differently to the potential reaction sites. However, neither the monophasic nor the biphasic pre-steady-state kinetics of OmcS oxidation by AQDS should be endorsed at this stage of the study. Further structural and kinetic studies are necessary to understand better the reaction kinetics of OmcS with different redox partners.

Implications

This is the most comprehensive biochemical study of an outer surface cytochrome from *G. sulfurreducens*. The purification and characterization of OmcS resulted in valuable structural and redox kinetic information in order to understand better the role of OmcS in dissimilatory Fe(III) reduction. This study demonstrates that OmcS is a promiscuous redox protein, which is able to donate electrons to a wide variety of electron acceptors. This capability explains, at least in part, why *G. sulfurreducens* can use several metals, humics and humics-related compounds as terminal electron

acceptors. However, transient state kinetics studies showed that there are differences in the reaction rates of reduction of different substrates, which cannot be explained simply by the redox potentials of the substrate, indicating that perhaps structural features of the proteins result in preference for one substrate over the other. To elucidate further the kinetic features of OmcS, structural studies and further kinetic studies with other metals are proposed. The most significant kinetic study would be the use of an insoluble substrate such as Fe(III) oxide, which is the most significant Fe(III) form in subsurface environments. Moreover, when characteristics of OmcS are compared to those of other cytochromes, which have different functions in *G. sulfurreducens*, including OmcB which is involved in the reduction of soluble and insoluble Fe(III) or OmcZ which is important in electricity production, an explanation may be obtained for their functional differences.

CHAPTER 6

CONCLUSIONS AND FUTURE WORK

Conclusions

The results of this study further confirmed the significance of the cellular outer surface and its proteins in respiratory Fe(III) reduction. Previous studies suggested that outer surface proteins are involved in the reduction of insoluble Fe(III) (Mehta, 2005; Mehta, 2006). These studies further proved that removal of outer surface proteins inhibits the reduction of soluble Fe(III). They demonstrated that soluble Fe(III) citrate need not enter the cell in order to be reduced, contrary to earlier hypotheses which predicted that the periplasm and its proteins are responsible for the reduction of soluble Fe(III) (Butler, 2004; Lloyd, 2003). This finding is consistent with that of genetic studies which have found that the outer membrane *c*-type cytochrome OmcB is also involved in the reduction of soluble Fe(III) (Leang, 2003). OmcB is the only outer membrane cytochrome that has been found so far to be important for the reduction of soluble and insoluble Fe(III) (Leang, 2003). As a general trend, genetic studies showed that cell surface cytochromes and other proteins are only responsible for the reduction of insoluble Fe(III), and not for soluble Fe(III). It was observed, however, by using mild protease treatment on the cells, that OmcB is partially surface-exposed, in contrast to OmpB which is very loosely attached to the cell surface, and the removal of outer surface proteins including the portion of OmcB and whole protein of OmpB resulted in a significant decrease in soluble Fe(III) reduction. This investigation provided

convincing evidence that the reduction of soluble Fe(III) also takes place on the cell surface and surface exposure is not only required for the reduction of insoluble Fe(III) but also for soluble Fe(III).

Recent genetic studies have found several cell surface proteins to be involved in the reduction of insoluble Fe(III), including heme and non-heme proteins (Inoue, manuscript in preparation; Leang, 2003; Mehta, 2005; Mehta, 2006; Reguera, 2005). However, these studies did not provide evidence whether and how these proteins interact during Fe(III) reduction. The co-immunoprecipitation experiment using the antibody against the loosely bound *c*-type cytochrome OmcS provided the first evidence that proteins found to be involved in Fe(III) reduction interact. This interaction includes cytochromes and non-heme proteins such as OmpB, OmpJ, and PilA, which may provide further clues how these proteins participate in or support electron transfer and/or Fe(III) reduction. This study also identified proteins interacting with OmcS, of which the involvement in Fe(III) reduction is not yet known, which provides further targets for follow-up studies on this subject. This result is the first experimental evidence for *Geobacter* which supports the hypothesis that proteins involved in Fe(III) reduction create networks or protein complexes for efficient Fe(III) reduction.

The first part of this study established the importance of protein localization and protein-protein interaction in dissimilatory Fe(III) reduction, and the second part emphasizes the significance of biochemical characterization of individual components of Fe(III)-reducing networks in order to understand the mechanism better. For instance, multiheme cytochromes such as PpcA were found to be involved in the reduction of

soluble Fe(III), and others such as OmcS and OmcE were implicated in that of insoluble Fe(III), with OmcB implicated in both. More striking differences were found in function between two loosely bound outer surface cytochromes, OmcS and OmcZ, where the former is involved in the reduction of insoluble Fe(III) (Mehta, 2005) and the latter is exclusively implicated in electricity production (Nevin, 2009). Furthermore, the altered function of OmcS and OmcZ cannot be explained by localization, either. Therefore, the process of purification and characterization of outer surface cytochromes important for Fe(III) reduction was undertaken in order to understand their functional differences better.

The purification of OmcB resulted in confirmation of its size and heme content, as well as confirmation of its capability to reduce soluble and insoluble Fe(III) *in vitro*. However, in order to continue the characterization of OmcB, the improvement of protein yield is essential.

The discovery that the mutant strain 2215DLHT (Tran, manuscript in preparation) overproduces OmcS made a comprehensive characterization of OmcS possible. The molecular mass of purified OmcS is consistent with the cleavage of the signal peptide, contrary to what was proposed earlier (Mehta, 2005): that OmcS is anchored by it to the outer membrane. OmcS was also found to be a six-heme cytochrome with *bis*-His hexacoordination of its low-spin heme groups in both oxidized and reduced states. OmcS reduced a wide variety of substrates *in vitro*, which is due in part to its low redox potential ranging from -360 to -40 mV. Initial transient kinetic studies of oxidation of OmcS with AQDS and Fe(III) citrate showed the different electron transfer rates to the substrates by OmcS and a potential difference in the reaction of OmcS with the two

substrates, which require further investigation. This approach indicates that valuable information can be obtained by *in vitro* studies with purified cytochromes. Differences in their biochemical characteristics may account for their functional differences in the physiology of dissimilatory Fe(III) reduction.

Future work

In order to understand better the localization of extracellular Fe(III) reduction components in *Geobacter*, co-localization of known components is essential. With the availability of antibodies, combined with transmission electron microscopy (TEM), the relationship between the localization and function of the proteins can be established. Co-localization with multiple antibodies can also be achieved by TEM, which would provide further evidence of physical contact and probable electron transfer between various components. However, in order to find new proteins that may participate directly or indirectly in electron transfer, the use of the co-immunoprecipitation method is proposed. If antibodies against known components of dissimilatory Fe(III) reduction were more available, it would be possible to "walk through" and eventually identify an electron transport network from the inner membrane to the outer surface.

The results of this study show that 2-dimensional blue native/SDSPAGE is not suitable for identification of the outer membrane protein complexes, but it unintentionally demonstrated that this method could be used for isolation and identification of inner membrane protein complexes. This study is also of interest because very little is known about inner membrane complexes participating in dissimilatory Fe(III) reduction.

The purification of *c*-type cytochromes shows that valuable information can be

obtained by their biochemical characterization. The information gained for one cytochrome, however, is more valuable when compared to that of another cytochrome with different function. It is essential to find a method to overexpress these proteins to be available in large quantities for meaningful studies as is evident in the case of OmcB and OmcS. Since the attempt failed to overexpress OmcB heterologously in *E. coli*, alternative strategies to produce OmcB in large quantities must be proposed, such as the construction of a homologous overexpression strain, as was done for OmcZ (Inoue, manuscript in preparation), or screening for a strain that produces a higher amount of OmcB in our mutant collection, as was done for the purification of OmcS (Tran, manuscript in preparation). When purified OmcB is available in large quantities, further biochemical characterization and comparison of its biochemical features to those of OmcS can be achieved in order to understand the different roles they play in Fe(III) reduction.

The fact that OmcB is only partially exposed to the cell surface provides an opportunity to identify the reactive site(s) of this cytochrome with soluble and insoluble Fe(III). The availability of a better antibody would help to purify (by affinity purification) both the whole OmcB and the outer membrane-embedded part of protease-treated OmcB. Amino acid sequencing of both would result in the determination of the surface-exposed moiety of OmcB.

Apart from the major focus of this study on cytochromes, genetic studies (Mehta, 2006) and protein-protein interaction experiments showed the importance of a multicopper protein (OmpB) in Fe(III) reduction. It will be very interesting to study the mode of involvement of OmpB in Fe(III) reduction by purifying and characterizing this

protein. OmpB is one of the most abundant proteins in culture supernatant. Experience with purification of OmcS suggests a possible method to avoid difficulties which arose in previous attempts to purify OmpB by using detergent extraction to separate OmpB from impurities, which causes heavy clogging of the FPLC column and a low degree of separation from other proteins. Purified OmpB could be tested for its redox-activity and potential electron acceptors and donors, which have not been identified in any anaerobic organism.

Co-IP using OmcS-specific antibodies discovered several proteins that interact with OmcS. With the availability of OmcZ-specific antibodies, it is possible to do co-IP with OmcZ to confirm further its interaction with OmcS. For other proteins with unknown function, it is possible to start with genetic characterization to understand the interaction and their role in Fe(III) reduction.

The characterization of purified OmcS can be continued by testing its transient state kinetics behavior towards other substrates. The most significant experiment would be to test the capability to reduce insoluble Fe(III) and compare it to that of other cytochromes, especially to that of OmcZ, which may explain their roles in Fe(III) reduction and electricity production, respectively.

BIBLIOGRAPHY

Afkar, E., Reguera, G, Schiffer, M, and D. R. Lovley (2005). A novel *Geobacteraceae*-specific outer membrane protein J (OmpJ) is essential for electron transport to Fe (III) and Mn (IV) oxides in *Geobacter sulfurreducens*. *BMC Microbiol* **5**.

Anderson, R. T., H. A. Vrionis, I. Ortiz-Bernad, C. T. Resch, P. E. Long, R. Dayvault, K. Karp, S. Marutzky, D. R. Metzler, A. Peacock, D. C. White, M. Lowe, and D. R. Lovley (2003). Stimulating the *in situ* activity of *Geobacter* species to removeuranium from the groundwater of a uranium-contaminated aquifer. *Appl Environ Microbiol* **69**, 5884-5891.

Bertini, I., and C. Luchinat (1986). *NMR of Paramagnetic Molecules in Biological Systems*.

Bond, D. R., and D. R. Lovley (2003). Electricity production by *Geobacter sulfurreducens* attached to electrodes. *Appl Environ Microbiol* **69**, 1548-1555.

Bond, D. R., D. E. Holmes, L. M. Tender and D. R. Lovley (2002). Electrode-reducing microorganisms that harvest energy from marine sediments. *Science* **295**, 483-485.

Butler, J. E., F. Kaufmann, M.V. Coppi, C. Nunez and D. R. Lovley (2004). MacA, a diheme *c*-type cytochrome involved in Fe(III) reduction by *Geobacter sulfurreducens*. *J Bacteriol* **186**, 4042-4045.

Caccavo, F., D. J. Lonergan, D. R. Lovley, M. Davis, J. F. Stolz, and M. J. Mclnerney (1994). *Geobacter sulfurreducens* sp. nov., a hydrogen- and acetate-oxidizing dissimilatory metal-reducing microorganism. *Appl Environ Microbiol* **60**, 3752-3759.

Chang, Y. J., P. E. Long, R. Geyer, A. D. Peacock, C. T. Resch, K. Sublette, S. Pfiffner, A. Smithgall, R. T. Anderson, and other authors (2005). Microbial incorporation of ^{13}C-labeled acetate at the field scale: detection of microbes responsible for reduction of U(VI). *Environ Sci Technol* **39**, 9039-9048.

Childers, S. E., S. Ciufo, D. R. Lovley (2002). *Geobacter metallireducens* accesses insoluble Fe(III) oxide by chemotaxis. *Nature* **416**, 767-769.

Claus, H. (2004). Laccases: structure, reactions, distribution. *Micron* **35**, 93-96.

Coates, J. D., D. J. Lonergan, H. Jenter, and D. R. Lovley (1996). Isolation of *Geobacter* species from diverse sedimentary environments. *Appl Environ Microbiol* **62**,

1531-1536.

Coates, J. D., K. A. Cole, U. Michaelidou, J. Patrick, M. J. McInerney, and L. A. Achenbach (2005). Biological control of hog waste odor through stimulated microbial Fe(III) reduction. *Appl Environ Microbiol* **71**.

Coppi, M. V., C. Leang, S. J. Sandler, and D. R. Lovley (2001). Development of a genetic system for *Geobacter sulfurreducens*. *Appl Environ Microbiol* **67**, 3180-3187.

DiDonato, L. N., E. S. Shelobolina, S. A. Sullivan, K. P. Nevin, T. L. Woodard and D. R. Lovley (2004). Characterization of a family of small periplasmic *c*-type cytochromes in *Geobacter sulfurreducens* and their role in Fe(III) respiration. *Poster presented at the 104rd General ASM meeting, New Orlean, LA.*

Ding, Y. H., K. K. Hixson, C. S. Giometti, A. Stanley, A. Esteve-Núñez, T. Khare, S. L. Tollaksen, W. Zhu, J. N. Adkins, M. S. Lipton, R. D. Smith, T. Mester, and D. R. Lovley (2006). The proteome of dissimilatory metal-reducing microorganism *Geobacter sulfurreducens* under various growth conditions. *Biochim Biophys Acta* **1764**, 1198-1206.

Ding, Y. R., K. Hixson, S. Ciufo, A. Esteve-Nunez, A. Stanley, W. Lin, J. Burns and D. R. Lovley (2004). Proteomic investigation of *c*-type of cytochromes in *Geobacter sulfurreducens*. Poster presented at the 104rd General ASM meeting, New Orlean.

Ding, Y. R., K. K. Hixson, M. A. Aklujkara, M.S. Liptonc, R. D. Smith, D. R. Lovley and T. Mester (2008). Proteome of *Geobacter sulfurreducens* grown with Fe(III) oxide or Fe(III) citrate as the electron acceptor. *Biochimica et Biophysica Acta (BBA) - Proteins & Proteomics* **1784**, 1935-1941.

Druschel, G. K., D. Emerson, R. Sutka, B. G. Glazer, C. Kraiya, and G. W. Luther (2008). Low oxygen and chemical kinetic constraints on the geochemical niche of neutrophilic iron(II) oxidizing microorganisms. *Geochim Cosmochim Acta* **72**, 3358-3370.

Fanning, A. S., and J. M. Anderson (1996). Protein–protein interactions: PDZ domain networks. *Current Biology* **6**, 1385-1388

Field, S. J., P. S. Dobbin, M. R. Cheesman, N. J. Watmough, A. J. Thomson, and D. J. Richardson. (2000). Purification and magneto-optical spectroscopic characterization of cytoplasmic membrane and outer membrane multiheme *c*-type cytochromes from *Shewanella frigidimarina* NCIMB 400. *J Biol Chem* **275**.

Francis, J., R. T., and R. R. Becker (1984). Specific indication of hemoproteins in polyacrylamide gels using a double-staining process. *Anal Biochem* **136**, 509–514.

Gaspard, S., F. Vazquez, and C. Holliger (1998). Localization and solubilization of

the iron(III) reductase of *Geobacter sulfurreducens*. *App Environ Microbiol* **64**, 3188-3194.

Gorby, Y. A., and D. R. Lovley (1991). Electron transport in the dissimilatory iron reducer, GS-15. *Appl Environ Microbiol* **57**, 867-870.

Hartshorne, R. S., B. N. Jepson, T. A. Clarke, S. J. Field, J. Fredrickson, J. Zachara, L. Shi, J. N. Butt, and D. J. Richardson (2007). Characterization of *Shewanella oneidensis* MtrC: a cell-surface decaheme cytochrome involved in respiratory electron transport to extracellular electron acceptors. *J Biol Inorg Chem* **12**, 1083-1094.

Hernandez, M. E., and D. K. Newman (2001). Extracellular electron transfer. *Cell Mol Life Sci* **58** 1562-1571.

Holmes, D. E., K. P. Nevin, R. A. O'Neil, J. E. Ward, L. A. Adams, T. L. Woodard, H. A. Vrionis, and D. R. Lovley (2005). Potential for quantifying expression of the *Geobacteraceae* citrate synthase gene to assess the activity of *Geobacteraceae* in the subsurface and on current-harvesting electrodes. *Appl Environ Microbiol* **71**, 6870-6877.

Holmes, D. E., K. T. Finneran, R. A. O'Neil, and D. R. Lovley (2002). Enrichment of members of the family *Geobacteraceae* associated with stimulation of dissimilatory metal reduction in uranium-contaminated aquifer sediments. *Appl Environ Microbiol* **68**, 2300-2306.

Inoue, K., B. Kim, L. Morgado, T. Mester, X. Qian, M. Izallalen, C. A. Salgueiro, D. R. Lovley (manuscript in preparation). Isolation, characterization, and localization of the *c*-type cytochrome, OmcZ, required for optimal current production by *Geobacter sulfurreducens*.

Inouye, K., T. Mizokawa, A. Saito, B. Tonomura, and H. Ohkawa (2000). Biphasic kinetic behavior of rat cytochrome P-4501A1-dependent monooxygenation in recombinant yeast microsomes. *Biochim Biophys Acta* **1481**.

Istok, J. D., J. M. Senko, L. R. Krumholz, D. Watson, M. A. Bogle, A. Peacock, Y. J. Chang, and D. C. White (2004). In situ bioreduction of technetium and uranium in a nitrate-contaminated aquifer. *Environ Sci Technol* **38**, 468-475.

Izallalen, M., R. H. Glaven, T. Mester, K. P. Nevin, A. E. Franks, D. R. Lovley (2008). Going Wireless? Additional Phenotypes of a Pilin-Deficient Mutant Weaken the Genetic Evidence for the Role of Microbial Nanowires in extracellular Electron Transfer. In *108th ASM*. Boston, MA.

Kaufmann, F., and D. R. Lovley (2001). Isolation and characterization of a soluble NADPH-dependent Fe(III) reductase from *Geobacter sulfurreducens*. *J Bacteriol* **183**,

4468-4476.

Kim, B., X. Qian, C. Leang, M. V. Coppi, and D. R. Lovley (2006). Two putative *c*-type multiheme cytochromes required for the expression of OmcB, an outer membrane protein essential for optimal Fe(III) reduction in *Geobacter sulfurreducens*. *J Bacteriol* **188**, 3138-3142.

Kim, B. C., and D. R. Lovley (2008). Investigation of direct vs. indirect involvement of the *c*-type cytochrome MacA in Fe(III) reduction by *Geobacter sulfurreducens*. *FEMS Microbiology Letters* **286**, 39-44.

Kim, B. C., C. Leang , Y. H. Ding, R. H. Glaven, M. V. Coppi, and D. R. Lovley (2005). OmcF, a Putative *c*-Type Monoheme Outer Membrane Cytochrome Required for the Expression of Other Outer Membrane Cytochromes in *Geobacter sulfurreducens*. *J Bacteriol* **187**, 4505-4513.

Klimes, A., K. P. Nevin, M. Izallalen, R. H. Glaven and D. R. Lovley (2008). Characterization of Pilin Function through Heterologous Complementation of the *Geobacter sulfurreducens* PilA-deficient Mutant. In *108th ASM*. Boston, MA.

Leang, C., L. A. Adams, K. J. Chin, K. P. Nevin, B. A. Methé, J. Webster, M. L. Sharma, and D. R. Lovley (2005). Adaptation to disruption of the electron transfer pathway for Fe(III) reduction in *Geobacter sulfurreducens*. *J Bacteriol* **187**, 5918-5926.

Leang, C., M. V. Coppi, and D. R. Lovley (2003). OmcB, a *c*-Type Polyheme Cytochrome, Involved in Fe(III) Reduction in *Geobacter sulfurreducens*. *J Bacteriol* **185**, 2096–2103.

Leys, D., T. E. Meyer, A. S. Tsapin, K. H. Nealson, M. A. Cusanovich, and J. J. Van Beeumen (2002). Crystal structures at atomic resolution reveal the novel concept of "Electron-harvesting" as a role for the small tetraheme cytochrome *c*. *J Biol Chem* **277**.

Lin, B., M. Braster, B. M. van Breukelen, H. W. van Verseveld, H. V. Westerhoff, and W. F. Roling (2005). *Geobacteraceae* community composition is related to hydrochemistry and biodegradation in an iron-reducing aquifer polluted by a neighboring landfill. *Appl Environ Microbiol* **71**, 5983-5991.

Lloyd, J. R., and D. R. Lovley (2001). Microbial detoxification of metals and radionuclides. *Curr Opin Biotechnol* **12**, 248-253.

Lloyd, J. R., C. Leang, A. L. Hodges Myerson, M. V. Coppi, S. Ciufo, B. Methe, S. J. Sandler, and D. R. Lovley (2003). Biochemical and genetic characterization of PpcA, a periplasmic *c*-type cytochrome in *Geobacter sulfurreducens*. *Biochem J* **369**, 153-161.

Lloyd, J. R., V. A. Sole, C. Gaw, and D. R. Lovley (2000). Enzymatic and

Fe(II)-mediated reduction of technetium by Fe(III)-reducing bacteria. *Appl Environ Microbiol* **66**, 3743-3749.

Louro, R. O., T. Catarino, J. LeGall, D. L. Turner, and A. V. Xavier (2001). Cooperativity between electrons and protons in a monomeric cytochrome *c*3: the importance of mechano-chemical coupling for energy transduction. *Chem Bio Chem* **2** 831-837.

Lovley, D. R. (1991a). Dissimilatory Fe(III) and Mn(IV) reduction. *Microbiol Rev* **55**, 259-287.

Lovley, D. R. (1995). Bioremediation of organic and metal contaminants with dissimilatory metal reduction. *J Indurst Microbiol* **14**, 85-93.

Lovley, D. R. (2000). Chapter 1: Fe(III) and Mn(IV) Reduction. *Environmental Microbe-Metal Interactions*, 3-30.

Lovley, D. R. (2001). Reduction of iron and humics in subsurface environments, In J. K. F. Fredrickson, M. (ed.). *Subsurface Microbiology and Biogeochemistry Wiley-Liss, Inc, New York*, 193-217.

Lovley, D. R. (2006a). Microbial energizers: Fuel cells that keep on going. *Microbe* **1**, 323-329.

Lovley, D. R. (2006b). Bug juice: harvesting electricity with microorganisms. *Nat Rev Microbiol* **4**, 497-508.

Lovley, D. R., and E. J. P. Phillips (1988). Novel mode of microbial energy metabolism: organic carbon oxidation coupled to dissimilatory reduction of iron or manganese. *Appl Environ Microbiol* **54**, 1472-1480.

Lovley, D. R., D. E. Holmes, and K. P. Nevin (2004). Dissimilatory Fe(III) and Mn(IV) reduction. *Adv Microb Physiol* **49**, 219-286.

Lovley, D. R., E. J. P. Phillips, Y. A. Gorby and E. R. Landa (1991b). Microbial reduction of uranium. *Nature* **350**, 413-416.

Lovley, D. R., J. D. Coates, E. L. Blunt-Harris, E. J. P. Phillips and J. C. Woodward (1996). Humic substances as electron acceptors for microbial respiration. *Nature* **382**, 445-447.

Lovley, D. R., S. J. Giovannoni, D. C. White, J. E. Champine, E. J. P. Phillips, Y. A. Gorby, and S. Goodwin (1993). *Geobacter metallireducens* gen. nov. sp. nov., a microorganism capable of coupling the complete oxidation of organic compounds to the reduction of iron and other metals. *Arch Microbiol* **159**, 336-344.

Magnuson, T. S., A. L. Hodges-Myerson, and D. R. Lovley (2000). Characterization of a membrane-bound NADH-dependent Fe^{3+} reductase from the dissimilatory Fe^{3+}-reducing bacterium *Geobacter sulfurreducens*. *FEMS Microbiol Lett* **185**, 205-211.

Magnuson, T. S., N. Isoyama, A. L. Hodges-Myerson, G. Davidson, M. J. Maroney, G. G. Geesey, and D. R. Lovley (2001). Isolation, characterization and gene sequence analysis of a membrane-associated 89 kDa Fe(III) reducing cytochrome *c* from *Geobacter sulfurreducens*. *Biochem J* **359**, 147-152.

Mahadevan, R., D. R. Bond , J. E. Butler , A. Esteve-Núñez , M. V. Coppi , B. O. Palsson , C. H. Schilling and D. R. Lovley (2006). Characterization of metabolism in the Fe(III)-reducing organism *Geobacter sulfurreducens* by constraint-based modeling. *Appl Environ Microbiol* **72**, 1558-1568.

McDonald, C. C., W. D. Phillips and S. N. Vinogradov (1969). Proton magnetic resonance evidence for methionine-iron coordination in mammalian-type ferrocytochrome *c*. *Biochemical and Biophysical Research Communications* **36**, 442-449.

Mehta, T., M. V. Coppi, S. E. Childers, D. R. Lovley (2005). Outer Membrane *c*-Type Cytochromes Required for Fe(III) and Mn(IV) Oxide Reduction in *Geobacter sulfurreducens*. *Appl Environ Microbiol* **71**, 8634–8641.

Mehta, T., S. E. Childers, R. Glaven, D. R. Lovley and T. Mester (2006). A putative multicopper protein secreted by an atypical type II secretion system involved in the reduction of insoluble electron acceptors in *Geobacter sulfurreducens*. *Microbiology* **152**, 2257–2264.

Methe, B. A., K. E. Nelson, J. A. Eisen, I. T. Paulsen, W. Nelson, J. F. Heidelberg, D. Wu, M. Wu, N. Ward, M. J. Beanan, R. J. Dodson, R. Madupu, L. M. Brinkac, S. C. Daugherty, R. T. Deboy, A. S. Durkin, M. Gwinn, J. F. Kolonay, S. A. Sullivan, D. H. Haft, J. Selengut, T. M. Davidsen, N. Zafar, O. White, B. Tran, C. Romero, H. A. Forberger, J. Weidman, H. Khouri, T. V. Feldblyum, T. R. Utterback, S. E. Van Aken, D. R. Lovley, and C. M. Fraser (2003). Genome of *Geobacter sulfurreducens*: metal reduction in subsurface environments. *Science* **302**, 1967-1969.

Moore, G. R., and G. W. Pettigrew (1990). Cytochromes *c*: Evolutionary, Structural and Physicochemical Aspects. *Berlin: Springer-Verlag*.

Murad, E., and W. R. Fischer (1998). *The geochemical cycle of iron. In: iron in soils and Clay Minerals. Rpoccedings of the NATO Advanced Study Institute on Iron in Soils and Clay Minerals (eds Stucki BAGJW, Schwertmann U)* Dorddrecht: Kluwer Academic Publishers.

Myers, C. R., and J. M. Myers (1993). Ferric reductase is associated with the

membrane of anaerobically grown *Shewanella putrefaciens* MR-1. *FEMS Microbiol Lett* **108**, 15-22.

Myers, C. R., and J. M. Myers (1997). Outer membrane cytochromes of *Shewanella putrefaciens* MR-1: spectral analysis, and purification of the 83-kDa *c*-type cytochrome *Biochim Biophys Acta* **1326**, 307-318.

Myers, C. R., and J. M. Myers (1992). Localization of cytochromes to the outer membrane of anaerobically grown *Shewanella putrefaciens* MR-1. *J Bacteriol* **174**, 3429-3438.

Nevin, K. P., and D. R. Lovley (2000). Lack of production of electron-shuttling compounds or solubilization of Fe(III) during reduction of insoluble Fe(III) oxide by *Geobacter metallireducens*. *Appl Environ Microbiol* **66**, 2248-2251.

Nevin, K. P., and D. R. Lovley (2002). Mechanisms for accessing insoluble Fe(III) oxide during dissimilatory Fe(III) reduction by *Geothrix fermentans*. *Appl Environ Microbiol* **68**, 2294-2299.

Nevin, K. P., B. Kim., R. H. Glaven, J. P. Johnson, T. L. Woodard, B. A. Methe, R. J. DiDonato, Jr., S. F. Covalla, A. E. Franks, A. Liu, D. R. Lovley (2009). Anode biofilm transcriptomics reveals outer surface components essential for high density current production in *Geobacter sulfurreducens* fuel cells. *PLoS ONE* **4**, e5608.

Nikaido, H. (1994). Isolation of outer membranes. *Methods Enzymol* **235**, 225-234.

North, N. N., S. L. Dollhopf, L. Petrie, J. D. Istok, D. L. Balkwill, and J. E. Kostka (2004). Change in bacterial community structure during in situ biostimulation of subsurface sediment cocontaminated with uranium and nitrate. *Appl Environ Microbiol* **70**, 4911-4920.

Ortiz-Bernad, I., R. T. Anderson, H. A. Vrionis, and D. R. Lovley (2004). Vanadium respiration by *Geobacter metallireducens*: novel strategy for *in situ* removal of vanadium from groundwater. *Appl Environ Microbiol* **70**, 3091-3095.

Paquetea, C. M., P. M. Pereiraa, T. Catarinoa, D. L. Turnera, R. O. Louroa and A. V. Xaviera (2007). Functional properties of type I and type II cytochromes *c*3 from *Desulfovibrio africanus*. *Biochimica et Biophysica Acta (BBA) - Bioenergetics* **1767**, 178-188

Petrie, L., N. N. North, S. L. Dollhopf, D. L. Balkwill, and J. E. Kostka (2003). Enumeration and characterization of iron(III)-reducing microbial communities from acidic subsurface sediments contaminated with uranium(VI). *Appl Environ Microbiol* **69**, 7467-7479.

Pokkuluri, P. R., Y. Y. Londer, S. J. Wood, N. E. Duke, L. Morgado, C. A.

Salgueiro, and M. Schiffer (2009). Outer membrane cytochrome *c*, OmcF, from *Geobacter sulfurreducens*: high structural similarity to an algal cytochrome *c*6. *Proteins* **74**, 266-270.

Qian, X., G. Reguera, T. Mester, and D. R. Lovley (2007). Evidence that OmcB and OmpB of *Geobacter sulfurreducens* are outer membrane surface proteins. *FEMS Microbiology Letters* **277**, 21-27.

Reguera, G., K. D. McCarthy, T. Mehta, J. S. Nicoll, M. T. Tuominen and D. R. Lovley (2005). Extracellular electron transfer via microbial nanowires. *Nature* **435**, 1098-1101.

Richter, H., K. P. Nevin, H. Jia, D. A. Lowy, D. R. Lovley and L. M. Tender (2009). Cyclic voltammetry of biofilms of wild type and mutant *Geobacter sulfurreducens* on fuel cell anodes indicates possible roles of OmcB, OmcZ, type IV pili, and protons in extracellular electron transfer. *Energy Environ Sci* **2**, 506-516.

Röling, W., B. M. van Breukelen, M. Braster, B. Lin, and H. W. van Verseveld (2001). Relationships between microbial community structure and hydrochemistry in a landfill leachate-polluted aquifer. *Appl Environ Microbiol* **67**, 4619 - 4619.

Rooney-Varga, J. N., R. T. Anderson, J. L. Fraga, D. Ringelberg, and D. R. Lovley (1999). Microbial communities associated with anaerobic benzene degradation in a petroleum-contaminated aquifer. *Appl Environ Microbiol* **65**, 3056 - 3063.

Sambrook, J., E. F. Fritsch, and T. Maniatis (1989). Molecular cloning a laboratory manual. *Cold spring harbor laboratory press NY*.

Schägger, H. (2001). Methods in cell biology. **65**, 231-244.

Schroder, I., E. Johnson, and S. de Vries (2003). Microbial ferric iron reductases. *FEMS Microbiol Rev* **27**, 427-447.

Seeliger, S., R. Cord-Ruwisch, and B. Schink (1998). A periplasmic and extracellular *c*-type cytochrome of *Geobacter sulfurreducens* acts as a ferric iron reductase and as an electron carrier to other acceptors or to partner bacteria. *J Bacteriol* **180**, 3686-3691.

Shelobolina, E. S., M. V. Coppi, A. A. Korenevsky, L. N. DiDonato, S. A. Sullivan, H. Konishi, H. Xu, C. Leang, J. E. Butler, B. C. Kim, and D. R. Lovley (2007). Importance of *c*-Type Cytochromes for U(VI) reduction by *Geobacter sulfurreducens*. *BMC Microbiol* **7**.

Sheng, M., and C. Sala (2001). PDZ domains and the organization of supramolecular complexes. *Annu Rev Neurosci* **24**, 1-29.

Sleep, B. E., D. J. Seepersad,M. O. Kaiguo, C. M. Heidorn, L. Hrapovic, P. L.

Morrill, M. L. McMaster, E. D. Hood, C. Lebron, and other authors (2006). Biological enhancement of tetrachloroethene dissolution and associated microbial community changes. *Environ Sci Technol* **40**, 3623-3633.

Smith, P. K., R. I. Krohm, G. T. Hermanson, A. K. Mallia, F. H. Gartner, M. D. Provenzano, E. K. Fujimoto, N. M. Goeke, B. J. Olson, and D. C. Klenk (1985). Measurement of protein using bicinchoninic acd. *Anal Biochem* **150**, 76-85.

Snoeyenbos-West, O. L., K. P. Nevin, and D. R. Lovley (2000). Stimulation of dissimilatory Fe(III) reduction results in a predominance of *Geobacter* species in a variety of sandy aquifers. *Microbial Ecol* **39**, 153-167.

Straub, K. L., M. Benz, B. Schink, and F. Widdel (1996). Anaerobic, nitrate-dependent microbial oxidation of ferrous iron. *Appl Environ Microbiol* **62**, 1458-1460.

Sung, Y., K. E. Fletcher, K. M. Ritalahti, R. P. Apkarian, N. Ramos-Hernandez, R.A. Sanford, N. M. Mesbah, and F. E. Loffler (2006). *Geobacter lovleyi* sp. nov. strain SZ, a novel metal-reducing and tetrachloroethene-dechlorinating bacterium *Appl Environ Microbiol* **72**, 2775-2782.

Tendera, L. M., S. A. Graya, E. Grovemanb, D. A. Lowyc, P. Kauffmand, J. Melhadoe, R. C. Tycef, D. Flynnf, R. Petreccag, and J. Dobarrog (2008). The first demonstration of a microbial fuel cell as a viable power supply: Powering a meteorological buoy. *J Power Sources* **179**, 571-575.

Thamdrup, B. (2000). Bacterial manganese and iron reduction in aquatic sediments. *Adv Microb Ecol* **16**, 41-84.

Thomas, P. E., D. Ryan, and W. Levin (1976). An improved staining procedure for the detection of the peroxidase activity of cytochrome P-450 on sodium dodecyl sulfate polyacrylamide gels. *Anal Biochem* **75**, 168–176.

Tran, H. T., D. R. Lovley, and R. M. Weis (manuscript in preparation). A chemotaxis-like signaling pathway/ /regulates the expression of extracellular materials in *Geobacter sulfurreducens*.

Vrionis, H., R. T. Anderson, I. Ortiz-Bernad, K. R. O'Neill, C. T. Resch, A. D. Peacock, R. Dayvault, D. C. White, P. E. Long and D. R. Lovley (2005). Microbiological and geochemical heterogeneity in an in situ uranium bioremediation field site. *Appl Environ Microbiol* **71**.

Wang, Z., C. Liu, X. Wang, M. J. Marshall, J. M. Zachara, K. M. Rosso, M. Dupuis, J. K. Fredrickson, S. Heald and S. Liang (2008). Kinetics of Reduction of Fe(III) Complexes by Outer Membrane Cytochromes MtrC and OmcA of *Shewanella oneidensis* MR-1. *Appl Environ Microbiol* **74**, 6746-6755.

White, D. (2000). The physiology and biochemistry of prokaryotes. *Oxford university press New York*.

Wigginton, N. S., K. M. Rosso, and M. F. Hochella Jr (2007). Mechanisms of Electron Transfer in Two Decaheme Cytochromes from a Metal-Reducing Bacterium. *J Phys Chem B* **111**, 12857-12864.

Winderl, C., S. Schaefer, and T. Lueders (2007). Detection of anaerobic toluene and hydrocarbon degraders in contaminated aquifers using benzylsuccinate synthase (*bssA*) genes as a functional marker. *Environ Microbiol* **9**, 1035-1046.

Zhu, H., M. Hargrove, Q. Xie, Y. Nozaki, K. Linse, S. S. Smith, J. S. Olson and A. F. Riggs (1996). Stoichiometry of Subunits and Heme Content of Hemoglobin from the Earthworm *Lumbricus terrestris*. *J Bio Chem* **271**, 29999-30006.